MITNE-147

SIMULATION AND OPTIMIZATION TECHNIQUES OF NUCLEAR IN-CORE FUEL MANAGEMENT DECISIONS

Joseph Patrick Kearney

Edward A. Mason

Work Sponsored by
Commonwealth Edison Company
Chicago, Illinois

Department of Nuclear Engineering
Massachusetts Institute of Technology
Cambridge, Massachusetts

MITNE-147

SIMULATION AND OPTIMIZATION TECHNIQUES OF NUCLEAR IN-CORE FUEL MANAGEMENT DECISIONS

by

Joseph Patrick Kearney

Supervisor

Edward A. Mason

DEPARTMENT OF NUCLEAR ENGINEERING
MASSACHUSETTS INSTITUTE OF TECHNOLOGY
CAMBRIDGE, MASSACHUSETTS

M.I.T. DSR PROJECT NO. 72107

Work Sponsored by

Commonwealth Edison Company
Chicago, Illinois

Issued: February 1973

SIMULATION AND OPTIMIZATION TECHNIQUES OF NUCLEAR IN-CORE FUEL MANAGEMENT DECISIONS

by

Joseph Patrick Kearney

Submitted to the Department of Nuclear Engineering on Jan. 17, 1973, in partial fulfillment of the requirement for the degree of Doctor of Philosophy.

ABSTRACT

This thesis presents a nuclear fuel simulation technique and an optimization procedure useful to utility system planners in making decisions on nuclear fuel reload enrichments, ε_i, and batch fractions, f_i (that fraction of the total fuel mass which is to be fresh fuel), for each cycle i over a mid-range planning period, five to ten years. The models presented were designed to permit their use with nuclear utility system optimization models.

This simulation and optimization approach uses a combination of on-line computer nuclear physics and nuclear fuel economics calculations as well as correlations to precalculated physics and economic data. The on-line nuclear computations use a two dimensional, modified two energy group diffusion code, CORCOST, to simulate all refueling decisions.

A Dynamic Programming, D.P., algorithm was developed to minimize the nuclear fuel revenue required to produce a set of cycle energies, E_i, over the planning period within specified constraint limits on power peaking and fuel burnup. The nuclear precalculations are used to aid the dynamic program in its economic evaluation of all feasible decisions ε_i and f_i at each cycle(or stage). This multi-stage dynamic optimization partially decouples all cycles by use of the book value of the nuclear fuel in the reactor at the end of each cycle. This decoupling permits the use of Belman's Principle of Optimality.

Use of this D.P. model to optimize a sample set of cycle energy demands, under various reactor conditions and under

various engineering constraint conditions, has demonstrated that:

1.) Significant economic gains, $2 million, for each reactor can be achieved in meeting a varying cycle energy demand (up to 35% variance in E_1) by optimizing the two variables fuel reload batch fraction and enrichment at a minimum computation cost of approximately $25.

2.) Consideration of the engineering constraints on power peaking and burnup requires that large cycle energy variations should be planned for two or three cycles in advance by the utility system optimization model.

3.) A sub-optimal set of five different strategies at each cycle was necessary and sufficient to contain the optimal refueling policy.

4.) The set of feasible batch fractions available to the optimization at each cycle should be a function of the energy demanded of the reactor in that cycle. An example of this function for a Zion-I type pressurized water reactor is presented.

Thesis Supervisor: Edward A. Mason
Professor of Nuclear Engineering

Thesis Reader: Manson Benedict
Professor of Nuclear Engineering

TABLE OF CONTENTS

LIST OF FIGURES

LIST OF TABLES

1. SUMMARY AND CONCLUSIONS

1.1 Utility System Mid-Range Planning

A method of optimization useful in the planning of fuel requirements for nuclear utility systems over a mid-range planning horizon of five to ten years is presented in this report. Operational and financial planning of utility systems which have a significant percentage (over about 30-40%) of their capacity in nuclear plants are sensitive to the impact of this nuclear capacity in the mid range.

In the short range, where daily or hourly dispatching decisions are made, the nuclear fuel for all of the available reactors in the system has already been inserted into the reactors. Consequently, the major decision remaining for the utility operator in the short run concerns the rate of energy extraction from each plant. The dispatching of this nuclear energy in the short term can be made on the basis of the incremental cost of energy from the nuclear plants in a fashion quite similar to the dispatching of fossil energy.

In the case of expansion planning, decisions on the timely purchase of additional electric power plants are made over a longer time horizon (from five to ten, through thirty years hence) than for mid-range planning. Expansion planning decisions are based on the anticipated average load factors

for the additional plants and reflect, but do not necessarily consider in detail, mid-range operating decisions. However, the decisions on all fuel purchases, all plant maintenance and nuclear plant refueling schedules in the mid range, out to five to ten years hence, are affected most directly by the presence of nuclear plants on the utility system. These decisions and their respective effects on meeting the electricity demanded of a utility system and the cost of producing that electricity are the concern of this report.

Before proceeding with the discussion of the simulation and optimization of a utility system's mid-range planning, a brief analysis of the nuclear fuel and plant decisions which are of paramount interest in the mid range will be presented.

1.2 Nuclear Reactor Plant and Nuclear Fuel Decisions

Since mid-range planning only covers a time period of up to five to ten years, all of the plants on the utility system are assumed to be operative or at least are being designed with a fixed start-up date. For the nuclear plants on the system this implies that their electricity capacity and their general reactor core designs are fixed. The reactor core design refers to the number and dimensions of fuel assemblies in the core, and the reactor coolant state, flow rate, pressure and temperature. Although the rated electric capacity, P, of the nuclear plants is fixed for mid-range considerations, the total amount of electric energy, E, from the plant over any period

of time, T, is a variable. The energy, E, produced by a reactor during T can be expressed by

$$E = P \cdot L \cdot T \qquad (1.1)$$

where L is the plant capacity factor, the ratio of the energy produced during any time period to the energy that would have been produced had the reactor operated at full power capacity during that time period, T.

There is a limit on the total energy that can be extracted from the nuclear plant which is determined by the uranium and plutonium enrichment in the fuel rods which are initially placed into the reactor. As energy is produced, the quantity of fissile isotopes in the core decreases and neutron absorbing fission products are produced until finally the neutron chain is no longer self-sustaining at the plant's rated power. Normally, at this point, the plant is shut down for refueling. The time period from one refueling to the next is referred to as a nuclear fuel cycle. The amount of energy, E_i, to be provided by each nuclear plant during cycle i and the duration of each cycle, T_i, are decisions which the mid-range planner must make. An over-all utility system simulation and optimization procedure (see Section 1.3) is used to indicate the cycle energy productions, $E_{r,i}$, and cycle durations, $T_{r,i}$, for all reactors, r, in the system for each cycle i over the mid-range planning period which result in the most economic energy production for the utility system. Part of this procedure requires the selection of the

optimal, i.e., minimum nuclear fuel cost, refueling strategy for each reactor to produce $E_{r,i}$ during $T_{r,i}$.

This optimization of nuclear refueling finds for each reactor for each cycle:

1. The number and location of irradiated fuel assemblies to be replaced
2. The pattern in which the remaining fuel assemblies are to be shuffled to new locations
3. The optimal fissile uranium and plutonium enrichment in each reload assembly
4. The optimal control poison policy for the entire reactor.

The optimization of fuel locations at the beginning of each cycle is a subject which has been investigated previously (35, 15). In this study a standardized procedure, generally typical of pressurized water reactors (PWRs) is used to select fuel for discharge and to shuffle the remaining and reload fuel. Likewise, since PWRs normally employ soluble neutron poison - usually boron dissolved at a uniform (but time-dependent) concentration - in the coolant through the reactor core, this control poison method is used in this study. As a result only the reload batch size and the fissile uranium and plutonium concentrations at the beginning of each cycle will be discussed in this report.

The fissile uranium and plutonium concentrations at the beginning of each cycle are affected by two decisions:

the number of assemblies presently in the reactor which are to be removed and replaced with fresh fuel and the uranium-235 enrichment of this fresh fuel (plutonium recycle is not considered in this study). These decisions must be made between fifteen and twenty-two months (22) prior to the refueling for each cycle in order that the uranium fuel can be purchased, enriched in U-235, and fabricated into assemblies. Usually, between 20 and 40% of the fuel in the reactor is replaced for each cycle. Therefore nuclear fuel generates energy in the reactor for approximately three or four cycles. As a result of this prolonged residence time of fuel in the reactor and the twenty-month lead time on fuel purchases, the optimal decision as to the fraction of the fuel in the core, f_i, to be replaced and the reload fuel enrichment, ε_i, is a function of the energy that the reactor is to produce over the following four to six years. In order to optimize the i^{th} reload batch fraction, f_i, and enrichment, ε_i, the energy that the reactor is to produce over subsequent cycles must be known. This energy is a function of the energy demanded of the entire utility system and of the other plants in the system. Due to interdependence of all the decisions over the entire planning horizon a simulation of the utility system's operation over this period must be performed in order to optimize the fueling decisions. This utility simulation and optimization is discussed further in Section 1.3.

In addition to affecting the economics of nuclear energy production, the nuclear fuel decisions also affect the power density and burnup variation throughout the nuclear fuel in the core. Power density is a function of position in the core and is affected by the distributions of uranium and plutonium fuel, fission product buildup and control poisons. The power peaking factor in the reactor is the ratio of the maximum power density at any point in the reactor to the average reactor core power density. If the power peaking factor is too large for a particular fuel loading strategy, fuel rod burnout (14) can occur resulting in the rupture of fuel rods and the release of radioactive fission products to the coolant. This situation is avoided by placing a maximum limit on the power peaking factor for each reactor. The in-core simulator used for this study, the CORE code (see Section 1.4), calculates this power peaking factor which is one of the physical constraints on the nuclear refueling optimization (see Section 1.5).

Burnup is a local measure of the total energy produced by nuclear fuel given in units of MWD/tonne of fuel. Like power density it also is a function of position in the reactor and therefore local burnup peaking does occur. Excessive fuel burnup is not permitted in order to avoid fuel rod failure caused by excessive neutron damage, gaseous fission product pressure, or fuel swelling. The maximum burnup permitted is another physical constraint on the nuclear refueling optimization considered in this study.

1.3 The Nuclear Power Management Multi-Year Model

The nature of nuclear energy production results in the coupling over the five- to ten-year mid-range horizon of the decisions on energy production and scheduling of fuel purchasing, plant maintenance and nuclear refueling. Consequently a simulation of these decisions for the utility system is required if optimal decisions are to be found. The Nuclear Power Management Multi-Year MOdel, Figure 1.1, is under development at M.I.T. (12) to perform this utility simulation and optimization. The development of a refueling and maintenance model, block A in Fig. 1.1, is being carried out by Systems Control, Inc. (28) and Commonwealth Edison Company (8). These refueling and maintenance models develop feasible schedules of all required nuclear refuelings and all required maintenance periods for all nuclear, fossil, hydro, etc., plants on the utility system. For each refueling and maintenance schedule generated by this model, an optimum fueling pattern is developed by the remainder of the Nuclear Power Management Model which also then indicates the lowest cost schedule. The fewer the number of refueling and maintenance schedules which must be evaluated, the lower will be the computing costs incurred by the entire multi-year model. The maintenance and refueling model should, therefore, perform an initial economic filtering process which would select only the more economically preferable schedules and pass only these to the system integration model, see Rees (28).

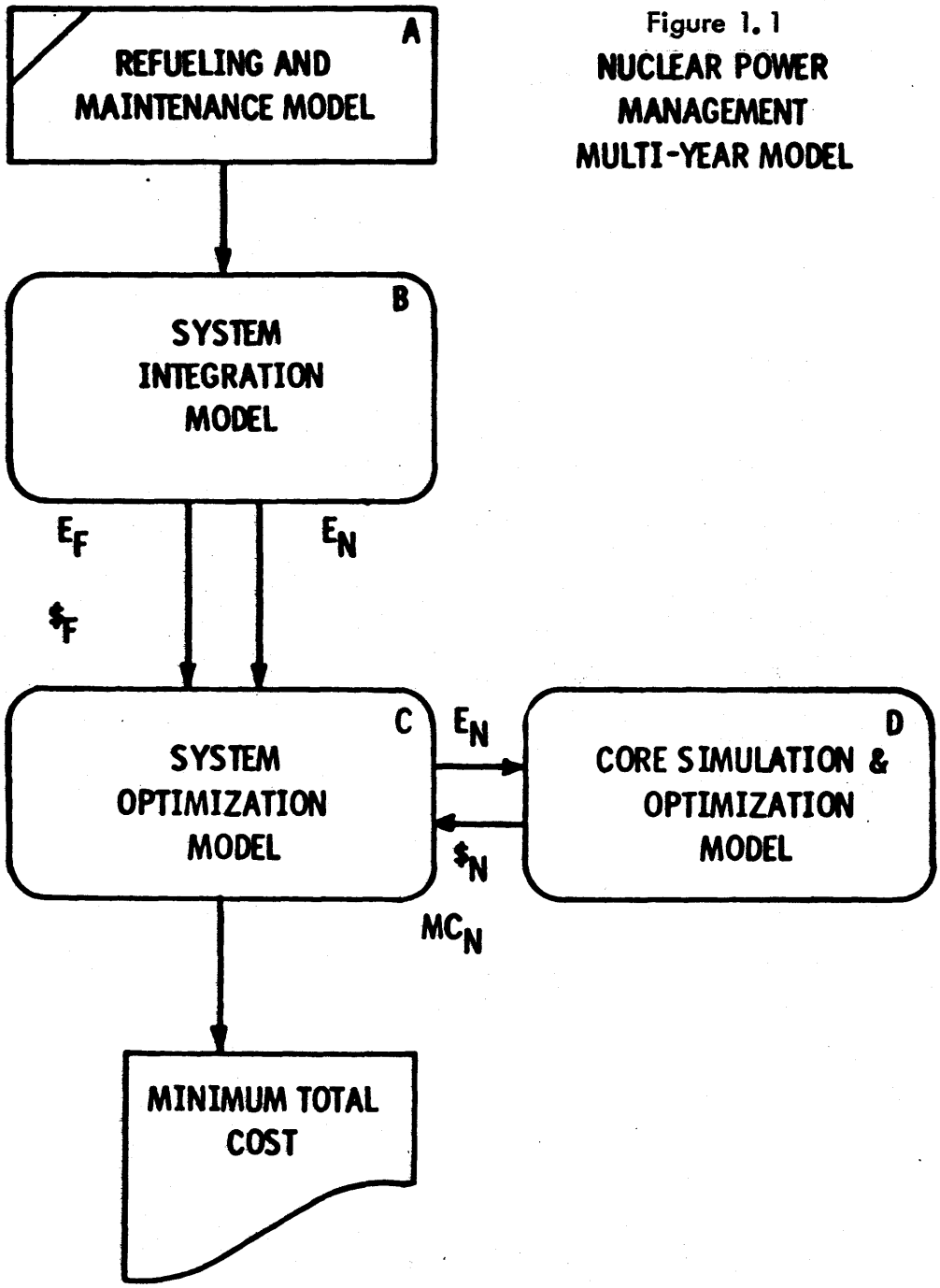

Figure 1.1
NUCLEAR POWER MANAGEMENT MULTI-YEAR MODEL

The system integration model (11) block B in Fig. 1.1 uses probabilstic simulation in determining the amount of energy to be produced during all periods of time within the planning period by each of the plants. The loading order, i.e., the sequence in which each of the plants is to start producing electricity for the system, is input for this integration model. This model generates the energy to be produced by each of the fossil plants, E_F, the total cost of producing this energy, $\$_F$, and the total nuclear energy referred to as nuclear potential to be produced by all of the nuclear plants, E_N, for each period.

The system optimization model (11), block C in Fig. 1.1, takes the total nuclear potential required in each period and uses a network algorithm to allocate that potential among all the nuclear plants available during the period. A nuclear reactor cycle is defined as the operation of a nuclear plant from the beginning of power generation after one refueling to the same point following the next refueling. Practically, a reactor cycle can vary in duration from about six to twenty-four months. In this study the reactor cycle energy, $E_{r,i}$, for reactor r in cycle i, is the sum of the period energies calculated by the System Optimization model for each reactor. The duration of each cycle for each reactor, $T_{r,i}$, is specified by the refueling and maintenance model. The goal of the core simulator and optimization model, block D in Fig. 1.1, is to minimize the cost of producing

$E_{r,i}$ during the cycle times $T_{r,i}$ by selecting a refueling pattern for each reactor. The refueling pattern in this context refers to the series of reload batch fractions $f_{r,i}$, and enrichments, $\varepsilon_{r,i}$, chosen for each reactor for all cycles in the planning horizon.

The core simulation and optimization model returns to the system optimization model the cost, $\$_N$, of producing the energy it requested and the marginal cost, MC_N, of changing any one of the energies, $E_{r,i}$. Based upon these marginal costs a new calculation of energies, $E_{r,i}$'s, is performed by the system optimization model; and the in-core simulation and optimization model is again called to optimize this new set of energies. Convergence is achieved when the new $E_{r,i}$'s are the same as the old or when the total expenditures on nuclear fuel, $\$_N$, remain unchanged. The minimum total system cost, the cost of all fossil fuel plus all the nuclear fuel, $\$_F + \$_N$, is then calculated.

The goal of the work reported herein is to design a core simulation and optimization model, to test it on a realistic basis so as to determine the feasibility, structure and sensitivity of the model and to determine the magnitude of the economic gains to be made by this optimization and how these can be achieved.

1.4 The Nuclear In-Core Simulation and Optimization Model

In-core simulation and optimization models (19, 34) presently known to be under development elsewhere utilize

simulators which are based entirely on correlations developed from precalculated results (19) or on the assumption of constant power shape throughout each cycle (34). The objective of this work was to develop an in-core simulator that performs a more realistic nuclear fuel depletion calculation which would include provisions for calculating the magnitude of power peaking and local burnup for use in establishing the feasibility of the refueling patterns being considered. The secondary objective of this work was to develop ranges of feasibility and economic attractiveness for the optimized variables so that researchers working on alternate simulation and optimization models have some aid in the directioning of their efforts.

The in-core simulation required to achieve these objectives is performed by the computer codes CELL and CORE (21 and Appendix A). Figure 1.2, The Nuclear In-Core Simulation and Optimization Model, illustrates the role this in-core simulator, CORE, performs in the refuel decision optimization procedure. CORE simulates all fuel management decisions made in each cycle. The CORE code performs a two-dimensional, (R-Z), modified two energy group fuel depletion calculation for water moderated and cooled reactors. For all refuelings the fresh fuel is inserted in the outer annulus of the reactor core and all the previously irradiated fuel remaining in the reactor is scattered in inner portions of the core. The CORE code has been programmed so that any amount of fresh

Figure 1.2

THE NUCLEAR IN-CORE SIMULATION AND OPTIMIZATION MODEL

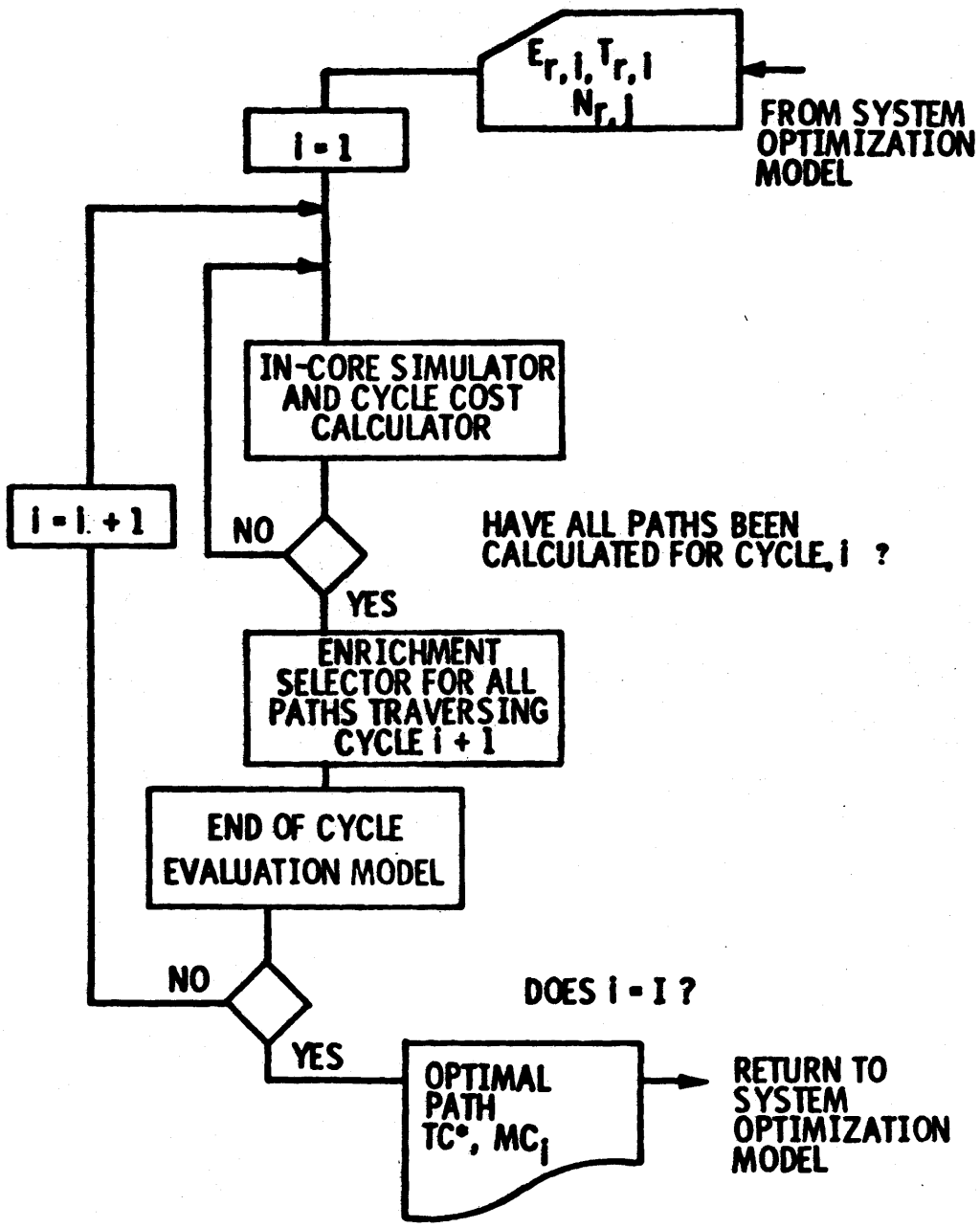

fuel can be loaded into the reactor at the beginning of each cycle. This fresh fuel can be of any enrichment. The identity of each batch of fuel is maintained throughout its lifetime in the reactor. When necessary, batches can be split so that portions of them can be unloaded. The unloading of fuel within a batch at the end of each cycle is done on the basis of most burned fuel being unloaded first. The CORE code also calculates the power peaking in the reactor and indicates when a specified maximum power peaking limit has been violated. Accuracy checks of the CORE code were made (21) using Westinghouse calculations for the San Onofre-1 reactor as a basis. All of the parameters of interest - cycle burnup, end of life nuclide masses and batch-by-batch fractional energy release - calculated by CELL-CORE agreed to within 97.5%, with the exception of the energy released in the outer zone which varied in error by 6%.

The cycle cost calculator, Fig. 1.2, is an optional subroutine of the CORE code called CYCOST. CYCOST calculates the discounted revenue requirement for producing E_i in cycle i which is the sum of the costs incurred by each batch of fuel in the reactor during cycle i, or:

$$C_i = \sum_{k=1}^{NOZONE} \frac{1}{1-\tau} \{Z(k,t_1) - PVEOC \cdot Z(k,t_2) - \tau[Z(k,t_1) - Z(k,t_2)] \cdot PVE\} \quad (1.2)$$

where k is the batch notation,

$Z(k,t)$ is the value of the fuel in batch k at time t

t_1 is the beginning of the cycle,

t_2 is the end of the cycle

PVEOC and PVE are present value factors which discount values (PVEOC) from the end of the cycle and (PVE) from the time when revenues are received to the beginning of the cycle.

The value of nuclear fuel at any time, $Z(k,t)$, is taken as the value of the uranium and plutonium isotopes in the fuel plus the depreciated fabrication and appreciated reprocessing service charges for the fuel. The fixed fab - rication costs for each batch are depreciated linearly and fixed reprocessing costs are appreciated linearly with batch energy production. This requires that at any time the energy produced to date and the total energy that the batch will eventually produce are both known. To a first approximation the total energy produced by a batch is a function of the initial enrichment of that batch. For the Zion type PWR, which was the example reactor used for this study (see Appendix D), the expected average energy production, B_k, regardless of the reload batch fraction could be approximated by:

$$B_k = -2919.25 + 10789.3 \cdot \varepsilon_k \qquad (1.3)$$

where B_k is the average discharge burnup in MWD/T, and

ε_k is the initial U-235 enrichment of batch k in w/o.

1.5 Dynamic Optimization of Nuclear Refueling Decisions

The nuclear in-core optimization problem with respect to each reactor can be succinctly stated as the problem of minimizing the discounted total revenue requirement, $\overline{TC}$, of producing the required energy, E_i, over the planning horizon.

$$\text{Min } \overline{TC} = \text{Min} \sum_{i=1}^{I} C[x(i), \varepsilon_i, f_i, i] \qquad (1.4)$$

where C is the discounted cycle revenue requirement, Equation (1.2),

x(i) is the state of the reactor at the beginning of the i^{th} cycle,

ε_i, f_i are the decision variables, reload enrichment and batch fraction, respectively, and

I is the total number of cycles in the planning horizon.

In Equation (1.4), C is also a function of the various unit costs of nuclear fuel, e.g., cost of fuel rod fabrication. Any changes in these unit costs over the planning horizon must be considered in the calculation of the objective function, but since they will not affect the optimization procedure they have not been included explicitly in Equation (1.4).

This objective function, $\overline{TC}$, must be satisfied within the constraints that the required cycle energies, E_i, are all met and the power peaking and burnup limitations are not violated.

Since for a given reactor state, x(i), the selection of a reload batch fraction uniquely determines the required enrichment to produce E_i, the decision variable reduces to only f_i for each cycle i.

The calculation of $\overline{TC}$ for all feasible batch fractions that satisfy the constraints, an exhaustive search, is possible but highly impractical. The objection of the dynamic programming approach is to recognize that there will eventually only be one optimal path of reload batch fractions from cycle to cycle and therefore to reduce the computing burden by only evaluating a few of the remaining least expensive alternatives at each decision point. The End-of-Cycle Evaluation Model, see Fig. 1.2, performs this screening process. The selection process is based on the costs already incurred for each path up to cycle i, $\sum_{j=1}^{i} \hat{C}_j$, the projected costs of meeting the required energy, E_{i+1}, and the value of the core at the end of cycle i for each path. The projected costs are estimates, see Section 4.3.3, of the cost of producing E_{i+1} by all feasible combinations of enrichment and batch fraction. These estimates are based upon correlation fits to data previously collected on the reactor being optimized. The value of the core at the end of the i^{th} cycle is taken as the book value of the nuclear fuel in the reactor, the discounted value of uranium and plutonium isotopes and the discounted depreciated fabrication and appreciated reprocessing service charges.

The End-of-Cycle Evaluator selects the n-best paths for traversing the (i + 1) cycle. A complete depletion and costing of these n paths is then performed by the In-Core Simulator and Cycle Cost Calculator (see Fig. 1.2). The enrichment selector which chooses the reload enrichment required to produce the desired energy also performs a check to see if the maximum burnup limit is likely to be violated by this batch of fuel. This check is accomplished using Equation (1.3) and comparing the estimated value of B with the maximum allowable average discharge burnup.

This dynamic programming approach, D.P., was chosen for the nuclear fuel optimization model to be used in the overall Nuclear Power Management Model (see Section 2.2) for the following reasons:

1. The D.P. approach requires little computation time itself. It is limited by computer storage space only if a very large number of paths must be contained in the n-best set for each cycle. As is shown in Section 1.8 the results of sample optimizations indicate that an n-best set of five yields acceptable results. A 5-best set does not present computer storage problems for computers with storage capacities greater than 250 K bytes.
2. The majority of the computation time used by this algorithm is devoted to performing the

in-core simulation of the nuclear fuel decisions. However, a 5-best set of paths does permit the use of accurate multi-dimensional in-core simulations. This approach to optimizing nuclear fuel loading decisions allows for a higher degree of accuracy in the in-core simulation than has been provided previously. Therefore, a better understanding of the behavior of the optimization decision variables can be observed and used in future improved optimization models.

3. The coupling effects between decisions in different cycles can be minimized in the D.P. approach by correctly evaluating the fuel in the reactor at the end of each cycle.

4. The D.P. approach can be significantly improved with additional experience. The selection procedure used to find the n-best optimal paths for each cycle can be improved as experience with the model leads to the deduction of new selection guidelines. For example, early in this study the observation was made that reload enrichment very closely correlated with average discharge burnup. Quantifying this correlation, Equation (1.3), and including it

in the end-of-cycle evaluation permits the elimination of paths that, although economically optimal, would violate the average discharge burnup constraint many cycles later. Similar guidelines for improving future D.P. optimizations of nuclear refuel decisions are presented in Section 1.9.

1.6 Correlations to Previously Accumulated Data

There are two portions of the Nuclear In-Core Simulation and Optimization Model, Fig. 1.2, which require the correlation of previously accumulated information on the reactor being modeled. The first is the Enrichment Selector and the second is the End-of-Cycle Evaluation Model. The enrichment selector chooses the enrichment, ε_i, required to produce the energy, E_i, demanded from the reactor for any reload batch fraction, f_i, for any given reactor state, $\mathbf{x}(i)$. Least squares polynomial fits can be derived relating all of these variables for the reactor being modeled. In the case of the Zion reactor, the example reactor used in this study, the state of the reactor could be defined adequately by two parameters, the average fissile enrichment, εII, and the average burnup, BII, of the (1 - f) fraction of the reactor core remaining from the previous cycle.

If a reactor is refueled with a batch fraction f, all of the fuel remaining in the reactor from the previous cycle,

(1 - f) of the total fuel present, is located in the inner cylindrical region. Placement of fresh fuel is simulated in the outermost annular region of the core by the CORE code's fuel management procedure, out-in scatter refueling. The state of the fuel in the inner region is defined by εII and BII. εII, the average fissile enrichment of the fuel in the (1 - f) region of the core, is defined as

$$\varepsilon II \equiv \frac{M(U\text{-}235) + M(Pu\text{-}239) + M(Pu\text{-}241)}{\text{Total Uranium and Plutonium Mass}} \qquad (1.5)$$

where M(X) is the mass of isotope X.

Both εII and BII, the average burnup of the (1 - f) region, are related to the physics of the reactor operation as it affects energy production. εII is a measure of the potential number of energy-producing nuclear fissions that could take place in the (1 - f) region of the core. BII, on the other hand, is a measure of the buildup of neutron-absorbing fission products in this region of the core. Using these two parameters the enrichment required to produce cycle energy E_1 for any f is predicted by the enrichment selector in Figure 1.2 to within an accuracy of 99.3% for the Zion-I reactor.

The End-of-Cycle Evaluator requires estimates of the cost of producing energy during the next cycle. Data can be accumulated relating this cycle cost to the state of the reactor and the decision variables over a wide range in these parameters for the reactor being modeled. A least

squares polynomial is then fit to these data for use by the end of cycle evaluator. For the example Zion-I reactor, the cycle cost was divided into two portions and correlations were developed for each. The first was a correlation with the costs associated with the burnup of uranium and plutonium during energy production. The second was a correlation with the fixed service charges for the nuclear fuel, the fabrication, reprocessing and conversion of the fuel. The accuracy* of the burnup cost predictions in comparison with the CORE-CYCOST calculated costs is greater than 99%. For the fixed service charges the accuracy of the predictions based on these correlations was greater than 95%. The accuracy of the fixed costs is low because of the difficulty in adequately accounting for the distribution of energy production among the several batches of fuel in the inner region of the reactor core using only the average parameters, ε_{II} and B_{II}. This accuracy, however, is high enough to permit these estimated costs to be used by the End-of-Cycle Evaluation Model in comparing feasible paths.

1.7 The Sample Optimization Problem

In order to demonstrate the effectiveness of this in-core simulation and optimization procedure a number of

---

* For all of this discussion the accuracy, A, is defined by

$$A \equiv \frac{\text{Predicted Value}}{\text{Calculated Value}}$$

sample optimizations of the Zion-I reactor were performed starting with a set of cycle energies, E_i, and cycle durations, T_i, for the Zion-I reactor over five cycles. The problem was to minimize the total cost of producing these energies in the Zion reactor. Fig. 1.3, The Sample Optimization Problem, describes the refueling energy production schedule to be optimized. The refueling schedule given is one which meets the following constraints:

1. No refuelings occur during the summer, June, July and August, or the winter, December and January, to avoid assumed system load peaks.
2. The refueling down time is 0.125 years/cycle.
3. The capacity factors during reactor operation are equal to or less than 0.95.

Furthermore, in order to best observe the ability of the model to handle large variations in cycle energies, variations in E_i of 36.6% occur between cycles 1 and 2 and of 28.6% between cycles 2 and 3.

In order to account for differences in the value of the fuel in the reactor for the n-best paths at the end of the planning horizon, an "end-effect" calculation must be performed. If the energy demands on the reactor for subsequent cycles were known, this end-effect calculation would consist of extending the optimization for two or three more cycles. However, the future energy demands on the reactor are

Figure 1.3

THE SAMPLE OPTIMIZATION PROBLEM

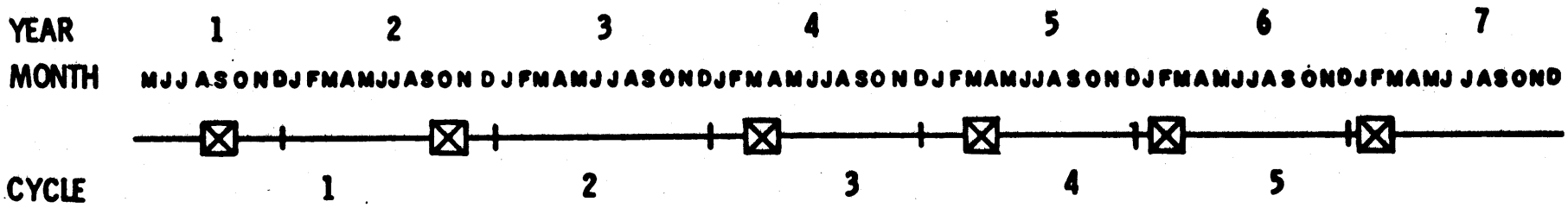

CYCLE i	CYCLE ENERGIES (GWD/CYCLE)	CAPACITY FACTOR	T_i (MONTHS)	REFUELING PERIODS YEAR	DURATION
1	324.4	0.95	11.2	2	SEPT 15 TO NOV 2
2	411.7	0.85	16.0	4	MARCH 2 TO APRIL 16
3	301.0	0.90	11.0	5	MARCH 16 TO MAY 1
4	260.8	0.95	9.0	6	FEB 1, TO MARCH 16
5	279.1	0.90	10.2	7	JAN 22 TO MARCH 7

presumed not to be known past the planning horizon. Consequently some assumption must be made regarding future operation so that the end of the planning horizon value of the fuel can be determined. For all of the optimizations performed for this study the end-effect calculation returned the reactor to the operating condition prevailing prior to the start of the planning period. Calculations of the sample problem were made for two different cases of initial operating conditions.

Constraints on fuel burnup and power peaking were imposed on the optimization for this sample problem. An average discharge burnup of the fuel of 50,000 MWD/T was selected for this problem. The power peaking in the reactor, however, poses the greatest limitation on reactor core operations and nuclear fuel management. Methods (13) for minimizing the power peaking while taking advantage of flexible fuel loading schedules are being developed. For the sample problem a limiting nuclear hot channel factor of 3.3 was used for the Zion-I reactor in Case II. The values of both these engineering constraints are higher than currently in use in the nuclear industry. The higher-than-normal values were used in this case to insure that the economic optimization capabilities of the model were tested as well as the capability to eliminate infeasible refueling strategies.

The decision variable that will be optimized is the selection of a reload batch fraction, f_i, for each cycle i.

For this sample case, the optimization model was allowed to select from four discrete values of batch fraction.

The values of batch fraction were:

Path Designation		Batch Fraction*
A	=	$0.37\dot{3}$
B	=	$0.33\dot{3}$
C	=	$0.29\dot{3}$
D	=	$0.25\dot{3}$

A path is defined as the specification of a unique combination of the decision variables, batch fraction, that have supplied the required energy and brought the reactor to its present state. For example, if a path through three cycles was refueled with batch fractions of 0.33 in cycle 1, 0.25 in cycle 2, and 0.37 in cycle 3, the designation for the path would be P(B-D-A).

1.8 Results of the Sample Optimization Problems

1.8.1 Case I

For Case I the initial and final conditions of the reactor were 3-zone refueling with a cycle energy production of 306.8 GWD. Since all of the optimization calculations for Case I were performed prior to the inclusion of the automatic check for power peaking constraint violations, only the average discharge burnup constraint was considered in Case I. Under these conditions the optimal refueling policy found to satisfy the cycle energies for the sample problem, given in Figure 1.3, is presented in Table 1.1. The

*In the remainder of this test only two digits shall be used for all batch fractions but they will always refer to the batch fractions as listed here.

Table 1.1. Optimal Nuclear Refueling Policy - Case I
Initial and Final Condition: Three Zone
Equilibrium Cycle, 3.2 w/o Fuel Loading
(305.9 GWD/cycle)
Path (C-A-D-D-C)

Cycle i	E_i GWD	f_i	ε_i (w/o)	MC_i (mills/kwhr)	C_i (10^6\$)	$\sum_{j=1}^{i} C_j$ (10^6\$)
1	326.3	0.29	4.2148	1.1706	12.420355	12.420355
2	407.7	0.37	3.3687	1.3095	14.446574	26.866928
3	299.2	0.25	4.3932	1.4388	9.472094	36.339008
4	267.5	0.25	2.8467	1.2077	7.428905	43.767904
5	285.8	0.29	3.2650	1.3061	7.537723	51.305616

E_i = Cycle energy production

f_i = Reload batch fraction for the cycle

ε_i = Reload enrichment

MC_i = Marginal cost of varying E_i

C_i = Discounted cycle cost

$\sum_{j=1}^{i} C_i$ = Total discounted cost of the optimal policy through cycle i

$\overline{TC}^*$ = 51.305616×10^6 \$

total revenue requirement for this policy, $\overline{TC}^*$, is $\$51.305616 \times 10^6$.

The optimal policy tends to meet the energy demanded of the reactor by reducing the batch fraction from the equilibrium initial condition of f = 0.33 except in the second cycle. In the second cycle the largest reload batch fraction of 0.37 was used to produce the largest cycle energy, 406.3 GWD.

In order to illustrate the competition among various feasible paths, Fig. 1.4 depicts the difference in total revenue requirements, $\overline{TC}_i - \overline{TC}^*_1$, for a few of the paths which were eliminated by the dynamic programming optimization procedure. $\overline{TC}_i$ is defined by the following equation:

$$\overline{TC}_i \equiv \sum_{j=1}^{i} C_j \qquad (1.6)$$

Some paths, e.g., P(B-B), P(B-A), quickly diverge from the optimal and are never really in the competition. Those in the competition are usually within a few hundred thousand dollars of each other. Examples of paths which were terminated due to a violation of the discharge burnup constraint were P(D-A-C) at 50,346 MWD/T, P(D-A-B) at 50,976 MWD/T, and P(D-D-D) at 58,261 MWD/T. X's in Fig. 1.4 denote paths eliminated by the burnup constraint and O's signify paths eliminated on economic grounds.

Figure 1.4

THE DEVIATION OF SUB-OPTIMAL PATHS FROM THE OPTIMAL POLICY - CASE I

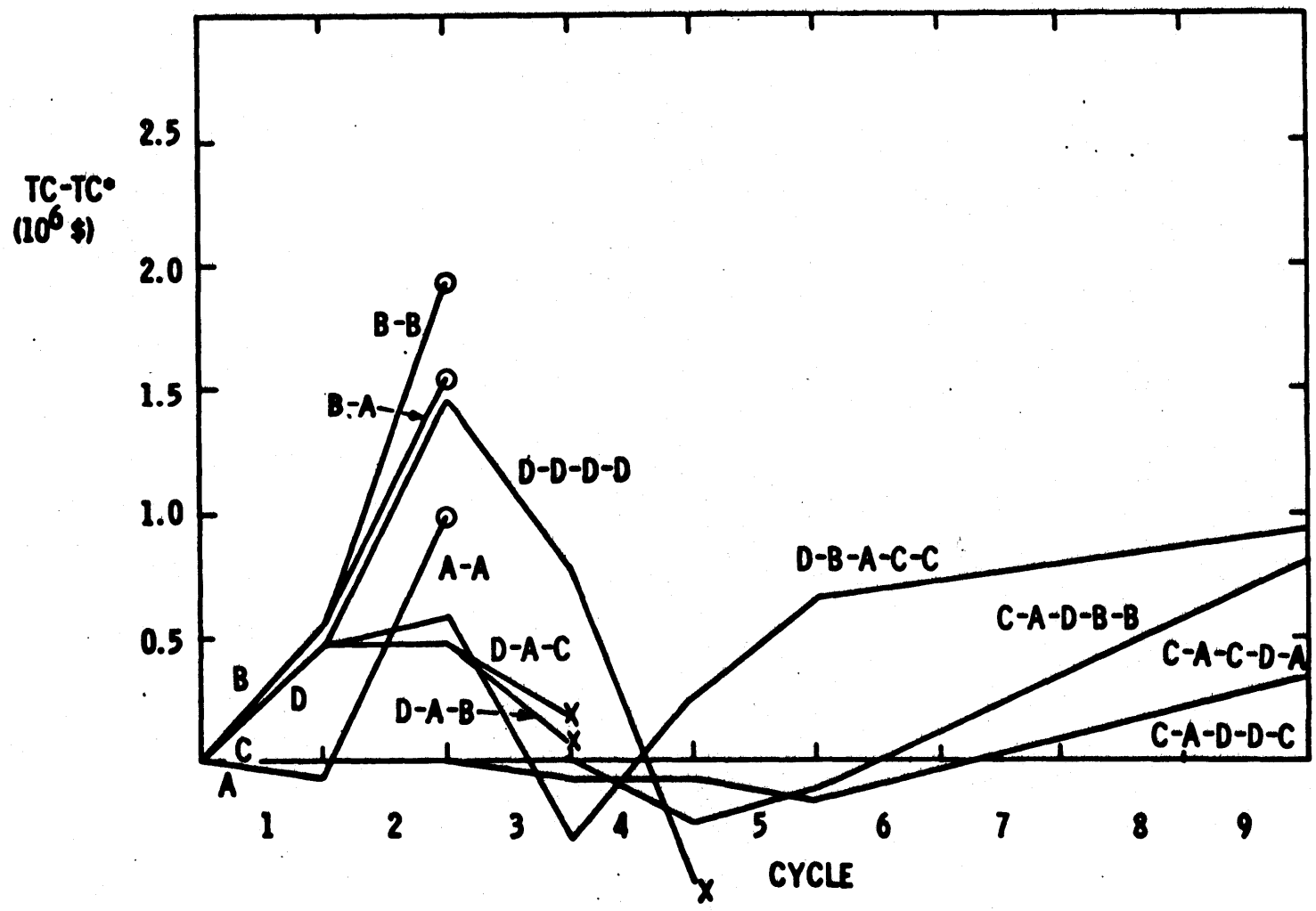

Although paths of constant f, e.g., P(A-A-A-A), were eliminated by the optimization procedure by the end of the first or second cycles (with the exception of f = 0.25) a separate calculation of these paths were performed by CORE-CYCOST. Table 1.2 shows the results of this calculation.

Comparison of Table 1.2 with Table 1.1 indicates that continually reloading the reactor with the smallest batch fraction available, f = 0.25, is not optimal. Likewise comparison of these results point out the savings, $\$1.981 \times 10^6$, to be gained in allowing the batch fraction to vary from the three zones, f = 0.33, refueling pattern.

Another interesting characteristic (see Table 1.6) of the optimal path is that the difference, $\Delta\varepsilon$, between the reload enrichment, ε_1, and the enrichment of the fuel in the remainder of the reactor, $\varepsilon(1 - f)$, is smaller than with other paths. Table 1.3 shows the difference in these enrichments for the optimal path, $\Delta\varepsilon^*$, and for one of its competitors P(D-D-D-D-D), $\Delta\varepsilon^D$. In general small $\Delta\varepsilon$'s result in lower core power and burnup peaking factors, and as Table 1.6 indicates low $\Delta\varepsilon$'s also tend to result in economical optimal paths. This fact can be used to aid future optimizations (see Section 1.9).

1.8.2 Sensitivity Evaluation of the D.P. Optimization

The essential part of the dynamic programming approach to the nuclear refueling optimization problem is the selection

Table 1.2. The Revenue Requirements, $\overline{TC}$, of Constant Batch Fraction Paths in Satisfying the Energy Requirements of the Sample Problems

Path	Batch Fraction	$\overline{TC}$ (10^6\$)	$\overline{TC} - \overline{TC}^*$ (10^6\$)
A-A-A-A-A	0.37	52.9789	1.6733
B-B-B-B-B	0.33	53.2863	1.9807
C-C-C-C-C	0.29	51.9377	0.6321
D-D-D-D-D	0.25	51.4576	0.1520

Table 1.3. The Difference $\Delta\varepsilon$ Between Reload Enrichment and the Enrichment of the Remainder of the Core for the Optimal Path, $\Delta\varepsilon^*$, and a Rival Path, P(D-D-D-D-D), $\Delta\varepsilon^D$.

Cycle	E_i GWD/Cycle	$\Delta\varepsilon^*$	$\Delta\varepsilon^D$
1	324.4	1.8649	3.1203
2	411.7	0.6194	2.2263
3	301.0	1.8711	-0.7907
4	260.8	0.1508	0.3542
5	279.1	0.7666	1.8096

of the n-best optimal paths at the end of each cycle. Two tests were performed to evaluate the sensitivity of the optimal solution to the use of a 5-best set. In the first test the n-best set was expanded to six at each cycle. Tracing this sixth path included in the n-best set revealed that none of its progeny ever reappeared in the subsequent cycle's 6-best set. From this fact it can be concluded that, with high probability, paths eliminated in one cycle by use of the 5-best set of paths do not reappear in the sub-optimal set of five paths for the next cycle.

However, a path which is not in the 5-best set in one cycle may return to the competition after two or three more cycles to become the optimal path. This would imply that the 5-best set found only a local optimal solution. In order to evaluate the possibility that paths eliminated early in the optimization could result in the optimal path the second sensitivity test was performed. This test consisted of performing another optimization commencing after the second cycle of the sample problem with the sixth through tenth best paths. Starting with this sub-optimal set the same optimization procedure with an n-best set of five paths was carried out for the third cycle through to the end of the planning horizon. The end effect calculation for this optimization was identical to that used in the previous optimization. Table 1.4 shows the results of this optimization for the sub-optimal path P(A-B-D-C-B) which was the lowest cost path

Table 1.4. Sub-Optimal Policy Resulting from the Sixth Through Tenth Best Paths in Cycle 2 Path (A-B-D-C-B)

Cycle i	E_i GWD	f_i	ε_i (w/o)	MC_i (mills/kwhr)	C_i (10^6\$)	$\sum_{j=1}^{i} C_j$ (10^6\$)	$\left(\sum_{j=1}^{i} C_j - \sum_{j=1}^{i} C_j^*\right)$ (\$)
1	326.5	.37	3.0940	1.2044	12.41032	12.41032	-100,350.
2	406.7	.33	4.8832	0.9757	15.35029	27.76061	893,683.
3	301.0	.25	3.3119	1.3002	9.253950	37.01456	675,553.
4	257.8	.29	2.5186	1.4250	7.04045	44.05801	285,971.
5	277.5	.33	3.0540	1.2139	7.812404	51.86742	561,799.

that resulted from the sixth through tenth best paths at the end of the second cycle. Path P(A-B-D-C-B) is $561,799 more expensive than the optimal policy. Furthermore, all of this difference originated in the first two cycles when path P(A-B) was eliminated from the first optimization where it was the sixth best path.

From these two sensitivity studies an n-best set of five paths was concluded to be sufficient to find an optimal policy and that with high probability this optimal policy is not a local optimum. Furthermore, since the optimal policy was the fifth best policy entering cycle 2 the use of a 5-best set was necessary, i.e., the use of n-best sets of 1 through 4 would not have found the optimal policy in the sample problem.

1.8.3 Case II

In the Case II optimization the initial and final conditions of the Zion-I reactor were altered from those used for Case I. The assumption was made for Case II that the reactor had been operating on an equilibrium 4 zone, 3.5449 w/o, equilibrium reloading pattern prior to the first cycle of the planning horizon. The cycle energy for this equilibrium operation is 286.3 GWD/cycle. To achieve the end effect correlation the reactor is returned to this operating condition after the fifth cycle of the planning period, namely, producing 286.3 GWD/cycle energy with a reload batch fraction

of 0.25 for each cycle. The same sample problem, Fig. 1.3, used in Case I is optimized in Case II. The physical constraints on the optimization are the limit on power peaking of 3.3 and the limit on average discharge burnup of 50,000 MWD/T.

The optimal refueling policy under these conditions was found to be path P(C-B-D-D-D), see Table 1.5. This path is a slightly different policy from the optimal path for Case I, P(C-A-D-D-C), shown in Table 1.1, which reflects the differences in the initial and final conditions between the two cases. The differences in the revenue requirements for both optimal policies is presented in Table 1.6.

The primary difference in the revenue requirements between both paths occurs in Cycle 2. The reason for this very expensive Cycle 2 in Case II was the elimination of paths due to the violation of physical constraints. Eleven of sixteen feasible paths were eliminated in Cycle 2 due to power peaking (four paths) and burnup (seven paths) constraint violations. This large number of constraint violations limited the choice of paths for an economically optimal policy through Cycle 2 and resulted in the high cost of that cycle in the optimal policy. The optimization did not have enough leverage to pre-plan for the large energy required during Cycle 2 since all of the paths leaving Cycle 1 were in approximately the same state and that state, unlike the

Table 1.5. Optimal Nuclear Refueling Policy - Case II
Initial and Final Condition: Four Zone Equilibrium Cycle
3.5449 w/o Fuel Loading
(285.4 GWD/cycle)
Path (C-B-D-D-D)

Cycle i	E_i GWD/cycle	f_i	ε_i (w/o)	MC_i (mills/kwhr)	C_i (10^6\$)	$\sum_{j=1}^{i} C_j$ (10^6\$)
1	326.1	0.29	3.5257	1.2676	12.032710	12.032710
2	413.7	0.33	4.3405	1.1009	15.098749	27.131509
3	298.6	0.25	3.5449	1.3484	9.253234	36.384743
4	263.4	0.25	3.1847	1.2612	7.301789	43.686532
5	282.5	0.25	3.8133	1.3570	7.655820	51.342352

Table 1.6. The Differences in Total Revenue Requirements Between the Case II Optimal Policy and the Case I Optimal Policy

Cycle i	$\left[\sum_{j=1}^{i} C^*j(II) - \sum_{j=1}^{i} C_j(I)\right]$ ($)
1	-388,350.
2	264,581.
3	45,735.
4	-82,508
5	36,736.

situation in Case I, was not prepared to meet a large energy requirement. Had there been a variety of paths with differing states traversing Cycle 1 the large number of constraint violations would not have occurred. This leads to the conclusion that in order to assure flexibility in meeting large variances in energy demand these large variances should not be among the first few cycles in the planning horizon.

The total computation time required for each optimization on an IBM-370M165 is 3.75 minutes.

1.9 Conclusions and Recommendations

Conclusions drawn from the development of this in-core simulation and optimization model are:

1. The Nuclear In-Core Simulation and Optimization Model outlined in Section 1.4 is effective in finding reactor refueling schedules which achieve significant savings by taking advantage of flexibility in reload batch fractions and enrichments.
2. This optimization model can be used to optimize energy schedules that have large variances in required energies from cycle to cycle within the physical constraints on maximum power peaking and burnup.
3. Significant savings can be realized by optimizing both reload enrichment and batch fraction

as compared to optimizing only reload enrichment with constant batch fraction.

4. In the dynamic programming procedure an n-best set of 5 paths is necessary and sufficient to contain the optimal policy through each cycle.
5. Large variances in cycle energy demands in the first two cycles of a planning period result in the violation of the physical constraints by a large number of paths. This results in the reduction of the number of feasible paths through these cycles and consequently limits the choice of an economic optimal path through the first two cycles.

Experience with the optimizations performed in this thesis leads to the suggestion of the following guidelines for future optimizations of nuclear refueling decisions.

1. The use of large reload enrichments leads to high batch discharge burnup. Experience has shown that a relationship similar to Equation (1.3) can be readily derived for a reactor which will indicate the maximum enrichment that the optimization procedure should consider.
2. Large differences, $\Delta\varepsilon$, between the reload enrichment, ε_1, and the average fissile enrichment of the remaining fuel in the reactor

result in violation of power peaking constraints. For the Zion-I reactor this Δ_ϵ should be less than 2.2 w/o to avoid power peak to average ratios greater than 3.3. A similar guideline for other reactors and for other constraint limits can be derived prior to optimizing the refueling decisions for that reactor which will enhance the efficiency of the dynamic programming optimization.

3. Large variances in cycle energy demands in the first two cycles of the planning horizon should be avoided by utility system optimization models.

4. The system optimization model should specify the set of requirements for energy, $E_{r,i}$, and time, $T_{r,i}$, for three or four refueling cycles out beyond the planning horizon on the basis of over-all utility system considerations. This would obviate the need for the in-core optimization to make and effect assumptions based on individual reactor considerations, see Section 1.7.

5. Since optimal policies select large reload batch fractions for cycles with large energy requirements the batch fractions available to the optimization should be a function of

the energy demanded in each cycle. For example, if the cycle energy demanded of the Zion reactor is greater than 400 GWD the available batch fractions should be in the range between 0.3 and 0.4. If the cycle energy demand is less than 300 GWD the range of batch fractions surveyed by the optimization program should be between 0.2 and 0.3. For energy requirements between 300 GWD and 400 GWD the range of f's should be between 0.2 and 0.35.

2. INTRODUCTION

2.1 The Need for Nuclear Utility System Planning

Although electricity was first produced from nuclear fission in the 1950's, only recently has nuclear power amounted to more than a small fraction of the total electric generating capacity of any utility system. As a result, existing nuclear power stations have usually been operated in a base-loaded (i.e. full power) fashion due to the fact that their incremental costs are lower than those of the conventional, fossil, plants. However, now with the nuclear capacity of certain utilities approaching, or exceeding, the minimum system demand for power* this base loading of nuclear plants is no longer feasible. As a consequence of such system considerations, nuclear plants can no longer all be operated at their design power level at all times, so that the total energy produced by individual nuclear plants between refuelings will be determined by system demand rather than by plant capacity and availability. The amount of energy each nuclear plant is to generate between refuelings determines the fuel loading that must be

---

* Commonwealth Edison Company of Chicago will have approximately 45% of its total electrical capacity supplied by nuclear plants by 1974. The TVA system will be comprised of 48% nuclear capacity by 1978 when TVA's installed nuclear capacity will total 10,600 MWe (26).

purchased for each plant. Since each batch of nuclear fuel produces energy in the reactor for periods of about three to five years (see Section 2.2.2) the system planner must know the energy demanded from each reactor over such time periods if the nuclear fuel loading is to be correct. Thus the production of energy must be simulated for the entire utility system, i.e. all the nuclear, fossil, etc., electricity generating plants on the system over a planning horizon of about five years.

This utility system simulation and optimization must indicate the optimal maintenance schedule for all equipment, the optimal refueling schedules for each nuclear plant and the optimal plant energy production schedule. In this context, optimal refers to that providing minimal total system cost.

Probabilistic simulation methods have been developed (1, 29) that are capable of finding these optimal schedules for utility systems that do not have significant amounts of nuclear capacity. It has been the objective of the Utility System Planning Project at M.I.T. to develop a calculational model for utility simulation and optimization that considers the utility's fossil and nuclear electricity generating capacity over a planning horizon of five to ten years, referred to here as "mid-range planning".

Section 2.4 of this report discusses Utility System Mid-Range Planning in more detail. Likewise see Deaton's "A System Integration and Optimization Model for Nuclear Power Management" (11).

The goal of this thesis has been to develop nuclear fuel simulation and optimization techniques for use in the overall utility simulation and optimization model.

2.2 Operating Characteristics of Nuclear Reactor and Nuclear Fuel

Before discussing the nuclear fuel optimization portion of the utility system planning project at M.I.T., a brief outline of nuclear reactor operation shall be presented. The objectives of this outline of nuclear reactor and nuclear fuel operation are to review the basic concepts of nuclear energy production and to highlight the nuclear operating parameters that can be optimized. This section is further intended to describe the limiting constraints on these parameters within which the optimization must be performed.

2.2.1 Nuclear Energy Production

Energy is produced in the form of heat by the fissioning of uranium and plutonium fuel in a reactor vessel; see Figure 2.1 for a sketch of a modern large pressurized water reactor vessel. This heat is transferred to the water coolant, in this type of reactor, under pressure. The

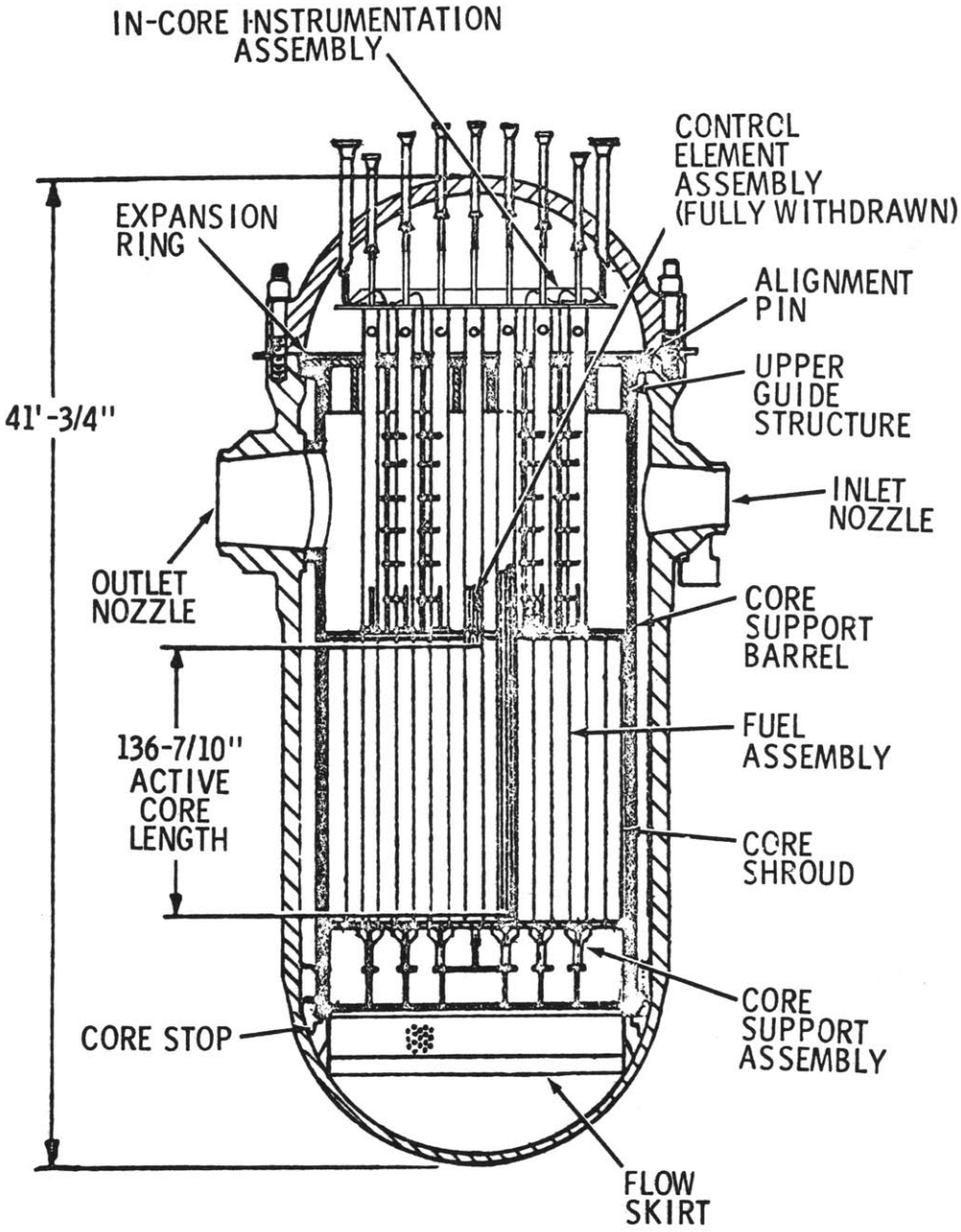

BALTIMORE GAS & ELECTRIC CO. Calvert Cliffs Nuclear Power Plant	REACTOR VESSEL ARRANGEMENT* * Extracted from Calvert Cliffs Nuclear Power Plant Final Safety Analysis Report (2)	Figure 2.1

coolant is continuously pumped from the reactor to a heat exchanger where steam is produced. Finally this steam is passed through a conventional turbine generator which produces electricity.

Fission is caused by the collision of neutrons, which diffuse throughout the reactor, with fissile (uranium and plutonium) atoms. Each fission reaction produces energy, converts the fissile atom involved into fission products (atoms with about one-half the atomic mass of uranium and plutonium atoms), and releases several neutrons. These neutrons diffuse away: (1) some cause more fissions by reaction with remaining fissile atoms in the nuclear fuel, (2) some are absorbed in fuel, fission products, coolant or structural and control materials without causing fission, and (3) the remainder leak out of the reactor. The process of neutrons causing fission, which produce neutrons, which cause more fission is called a neutron "chain" reaction. A stable self-sustaining chain reaction (one that proceeds at a steady rate and thus operates at steady power) is one in which the three general processes described above are in balance so that for each neutron causing fission in one interval of time, one other (no more nor less) neutron causes fission in the next interval of time. When the reactor is in this state it is said to have an effective multiplication factor, k_{eff}, of unity.

The fissioning of uranium and plutonium fuel occurs in fuel rods which are approximately one-half inch in diameter, twelve feet in height, and are arranged in groups of rods bound together into one fuel assembly. See Figure 2.2 which pictures two fuel assemblies each containing 217 fuel rods, for a pressurized water reactor of the 1000 MWe capacity class. One hundred and ninety three fuel assemblies make up a reactor core. The number of assemblies varies widely with the type of reactor and with the power capacity of the reactor.

The objective of nuclear fuel design is to assure that all of the heat generated in these rods is transferred to the coolant while at the same time containing the radioactive fission products (produced when a uranium or plutonium atom fissions). The transfer of heat from the fuel rods to the coolant is limited by the heat flux from the rods. If the heat flux is raised beyond the "critical heat flux" point, the temperature difference between coolant and clad rises abruptly, resulting in clad temperatures beyond safe limits. This is referred to as fuel element burnout and may result in fuel element rupture and release of fission products to the coolant (20). The critical heat flux for fuel rods with the same dimensions can be directly related to the power density, kw/l, of the fuel at any point in the

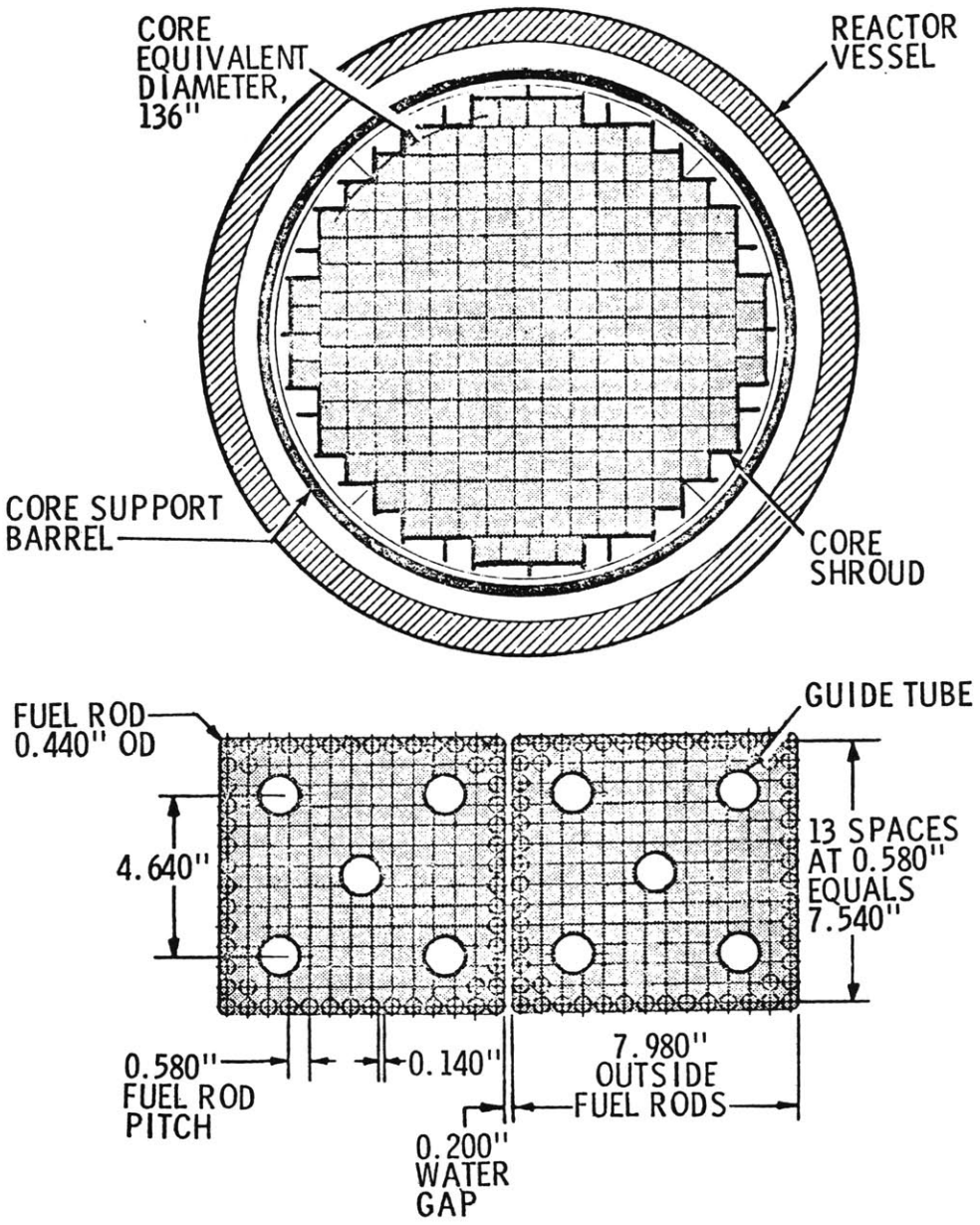

BALTIMORE GAS & ELECTRIC CO. Calvert Cliffs Nuclear Power Plant	FUEL ASSEMBLY AND REACTOR CROSS SECTIONS* * Extracted from Calvert Cliffs Nuclear Power Plant, Final Safety Analysis Report (2)	Figure 2.2

reactor core. One of the objectives of light water reactor fuel design is to prevent fuel element burnout, which implies keeping the power density below a specified level throughout the core.

In most instances the local power density is expressed in terms of the ratio of the peak power density at a point to the average core power density, which is referred to as the peak to average power density ratio or the power peaking factor. The power density, $q'''(r)$, at any point r in the reactor in kw/liter, is a function of the number of fissions occurring at that point,

$$q'''(r) = K \cdot \Sigma_f(r) \cdot \phi(r) \qquad (2.1)$$

where:

$\Sigma_f(r)$ is the microscopic fission cross section at r

$\phi(r)$ is the neutron flux at r

$\Sigma_f(r) \cdot \phi(r)$ is the number of fissions/sec occurring at r and k is a composite conversion factor needed to yield power density in kw/l.

Accurate predictions of power peaking factors obviously require detailed knowledge of the spatial distribution of Σ_f and ϕ. The nuclear fuel simulator used in this work

calculates both of these to assure that the power peaking maximum limit for a reactor is never violated (see Chapter 3). Furthermore, the economic optimization of the nuclear fuel described in Chapter 4 eliminates from further consideration any decisions which have resulted in power peaking factors above a previously defined safe level, referred to as the Power Peaking Constraint.

Besides the fuel rod temperature there are two other operating parameters which can have deleterious effects on the integrity of fuel elements. These are thermal cycling and maximum fuel burnup of the assemblies. Extensive thermal cycling due to raising and lowering the power and therefore the temperature of fuel elements can result in the rupture of fuel elements. Due to the complexity of the problem it is not considered explicitly in the nuclear fuel optimization being presented in this report.

Fuel burnup is a measure of the energy produced by the nuclear fuel and is usually expressed in units of thermal megawatt-days per metric tonne of fuel (MWD/T). As was the case with power density the fuel burnup, B(r), varies with fuel position, r, in the reactor. The higher the energy production at one point in the reactor core, the higher will be the associated number of fissions at that point and consequently the greater will be the radiation effects

at that point. In addition to radiation damage to cladding, high burnups result in fuel swelling, leading to fuel clad interactions, and in large fission product gas pressure buildup in the fuel rods. All three of these consequences of high burnup neutron damage to clad, fuel-clad interactions, and fission product gas pressure buildup--can cause fuel clad rupture. As a result there is a limit to the amount of burnup allowed for nuclear fuel. This limit referred to as the Maximum Burnup Constraint is the second physical constraint which is considered by the optimization procedure (see Section 3.2.2.2.2, Refueling Procedures in CORE). No fueling decisions which result in the violation of this constraint are treated by the economic optimization.

Returning to the energy produced by a reactor, the total thermal power, $P_{th}(t)$ in kw, for a reactor can be calculated by integrating Eq. (2.1) over the entire volume of the reactor core

$$P_{th}(t) = \int_{vol} q'''(r)dV = \int_{vol} K \cdot \Sigma_f(r) \cdot \phi(r)dV \qquad (2.2)$$

The energy produced by the reactor over any time period T is calculated by integrating Eq. (2.2) over that time period

$$E = \int_0^T P_{th}(t)dt = \int_0^T \int_{vol} K \cdot \Sigma_f(r,t) \cdot \phi(r,t)dVdt \qquad (2.3)$$

From Eqs. (2.2) and (2.3) a number of observations can be made:

1. The total amount of energy available from one reactor is an integrated function of the amount of fissionable material $\Sigma_f(r,t)$ and the flux $\phi(r,t)$ throughout the reactor. As energy is produced, Σ_f decreases and the concentration of neutron absorbing fission products increases. As more and more fissions occurs, without the addition of fissile species or the removal of fission products, a point is reached where the absorption of neutrons in fission products has increased to the point where less than one neutron per fission is left to cause fission in the next time interval. Then, as was previously described, the chain reaction is no longer self-sustaining. The reactor is then refueled by removing that part of the fuel in the core that has the highest burnup and replacing it with fresh fuel.
2. The power produced by the reactor at any time can be adjusted by changing the flux, $\phi(r,t)$.
3. When the period of time T in Eq. (2.3) is the time from reactor startup after a refueling to the time when the reactor must shutdown for the next refueling, the energy produced is referred

to as the cycle energy. This energy can be varied by adjusting the fissionable material $\Sigma_f(r,o)$ that is put into the reactor at the beginning of the cycle. $\Sigma_f(r,o)$ is affected by the enrichment ε, of the fresh fuel and by the reload batch fraction f, which is the amount of fuel that is discharged and replaced with fresh fuel. The primary subject of this thesis is the economic optimization of the f and ε variables to achieve a specified cycle energy E.

4. The energy that is produced over short periods of time, less than T, can be altered by changing the flux $\phi(r,t)$ over that period of time.
5. Eq. (2.3) can be simplified by defining the capacity factor L for a reactor. L is the ratio of the energy produced during any time period to the energy that would have been produced had the reactor operated at full power during that period. Using L Eq. (2.3) can be expressed as:

$$E = P_{th} \cdot L \cdot T \qquad (2.4)$$

P_{th} is the total thermal capacity of the reactor in kw. Eq. (2.4) indicates that if different amounts of energy are required from the reactor both L and T can be manipulated to accomplish this. As will be discussed in Section 2.4.1, the problem that this thesis deals with is the design of f and ϵ for a given reactor for a series of cycles in which both E and T can vary from cycle to cycle. In this study since E and T are specified for each cycle, the capacity factor L is fixed for each cycle so that Eq. (2.4) is satisfied. However, E, T and L all are allowed to vary from cycle to cycle for the cases studied.

The total cycle energy produced is a function of the fuel, coolant, and poison material in the reactor during that cycle. For the situation that this thesis considers, the type of coolant, the total number of assemblies in the reactor, the density of the fuel and the control poison strategy are all fixed. The variables for this study are f, ε and cycle energy E. Furthermore, for the optimization procedure as discussed in Chapter 4 the energy to be produced in each cycle is given. In this constrained situation if the reactor is to produce cycle energy E_i in

cycle i and f is fixed, ϵ is uniquely determined. This unique coupling between batch fraction, f, and reload enrichment, ϵ, simplifies the optimization of nuclear reload decisions.

2.2.2 Nuclear Fuel Management

The energy produced by a reactor core, $q'''(r)$, the power peaking factors in the core and the spatial distribution of burnup, $B(r)$, are all affected by the decisions of the nuclear fuel manager. The decisions that a fuel manager can make vis à vis nuclear fuel are

1. The amount of fissionable uranium and plutonium and the density of the fuel, UO_2 and PuO_2, in each assembly.
2. The location of each assembly inside the reactor core.
3. The amount and the positioning of control poisons throughout the core.

The decision as to what fuel density is to be used is not considered in this study since the fuel density used in one reactor is not altered very frequently. The decision as to the amount of fissionable uranium and plutonium in the form of UO_2 and PuO_2 in a core are made during refuelings at the beginning of each cycle. Practically speaking, cycle lengths can vary from about 6 months to 12 months.

At the beginning of each cycle some of the fuel assemblies are removed from the reactor, those remaining are shuffled around to minimize power peaking during the next cycle and fresh assemblies are loaded into the reactor.

The number of assemblies to be removed and the uranium -235 enrichment of the fresh replacements for these assemblies are the decision variables of primary interest in this report. The fraction of the core that is replaced by fresh fuel at a refueling is referred to as the reload batch fraction f, and the enrichment of this reload batch is referred to as ε. In practice f can vary from about 0.2 to 0.4. Another refueling decision is the amount of recycled plutonium that is to be inserted in the reload batch replacing some of the U-235. The simulation and optimization models described in Chapters 3 and 4 do not consider recycled plutonium. Consequently, the decision variables for the optimization are the reload batch fraction, f, and reload enrichment ε.

The decisions on the optimal locations of the fuel assemblies in the reactor at the beginning of each cycle have been extensively studied (35, 15). As a result this study does not consider optimizing the positioning of fuel assemblies.

Control poisons, high neutron absorbing materials, are used in the reactor to control the neutron flux. The purpose of their use is to maintain the core at just the critical level, i.e. $k_{eff} = 1.0$. PWR's normally employ soluble neutron poisons - usua-ly boron dissolved at a uniform (but time-dependent) concentration, see McLoed (25). Soluable boron control is the poison method used in this study. Additionally, control poisons in the form of full and part length rods are used to control the spatial distribution of power production and, therefore, can be used to minimize power peaking in the core. However, these control rod maneuverings are used only to compensate for short lived power peaks associated with changes in reactor power levels. Therefore, they are not taken into consideration in this study.

Assuming a mid-range planning horizon five to ten years, the decisions which are optimized in this study are the reload batch fraction, f, and reload enrichment, ε, for each reactor cycle within that horizon. Since only a fraction between 0.2 and 0.4, of the nuclear fuel is replaced at the beginning of each cycle, fuel is in the reactor for periods of up to four or five years. Furthermore, the lead time on making refueling decisions for a cycle is between one and two years prior to the beginning of that cycle*.

---

* The choice of reload batch fraction must be made about 20 months (22) prior to insertion into the reactor if the uranium is purchased in the form of UF_6. If nuclear fuel is purchased as U_3O_8 the batch fraction decision must be made 22 months (22) in advance of its use. The decision as to the enrichment of the reload fuel must be made about 15 months prior to fuel loading.

Consequently decisions are made today which will affect nuclear fuel in the reactor and thus energy produced by the reactor for upwards of five to seven years hence. An optimal decision on f and ϵ therefore, requires knowing the energy demanded of the reactor in question to a high degree of accuracy for five to seven years into the future. Simulating the operation of the entire utility system over this period is one way of finding that energy. Section 2.3 outlines the Utility System simulation used in this study and Chapter 3 describes the nuclear simulation performed over the same five year period.

As was mentioned the location of fuel assemblies in the reactor is changed at each cycle as some fuel is removed and fresh replacement fuel added. The fuel management scheme used to locate all of the fuel in the reactor at the beginning of each cycle for this study was the **modified scatter refueling** method. For this method the reactor is divided into two regions, an outer annular ring where fresh fuel assemblies are always placed and an inner "scatter" region for the remainder of the fuel which is homogeneously distributed within the region regardless of when it was loaded into the reactor. This is not to imply that the identity of fuel within each batch is lost in this scatter region but that each batch of fuel is distributed in the same manner through-

out the entire region. At each refueling a fraction, f, of the fuel in the entire reactor is removed from the scatter region. The fuel removed is the fuel that has been in the reactor the longest, see Appendix A. The fuel that was in the outer annulus is scattered homogeneously in the inner region and fresh fuel, amounting to the fraction f of the reactor's fuel, is loaded in the outer region. This procedure is performed automatically by the in-core simulator, Chapter 3, at the end of each reactor cycle that is simulated during the optimization procedure.

2.2.3 Nuclear Fuel Cycle Costs

No review of nuclear fuel management would be complete without a summary of the costs associated with nuclear fuel. The costs of each batch of fuel can be divided into those incurred prior to insertion into the reactor and those incurred upon discharge from the reactor.

Those costs incurred prior to insertion in the reactor are

1. Purchase of U_3O_8,
2. Refining and conversion to UF_6,
3. Enrichment of the uranium in U-235, and
4. Conversion to UO_2 and fabrication into fuel rods and fuel assemblies.

Those costs incurred and credits received after discharge from the reactor are

1. Shipping of spent fuel,
2. Reprocessing of spent fuel and disposal of waste products,
3. Conversion of the reprocessing product UNH to UF_6, and
4. Credits for uranium and plutonium.

The discounted value of revenue required to meet all these nuclear fuel costs is the quantity which is minimized in all of the simulation and optimization procedures described in this report. A more detailed discussion of nuclear fuel cycle costs is presented in Section 3.2.3.

2.3 Utility System Planning and Nuclear In-Core Simulation

The objective of any utility system optimization procedure considering the mid range horizon, five to ten years, is to indicate to utility planners maintenance and refueling schedules and an electricity production schedule for each plant that minimizes system costs over the planning horizon. The amount of energy that must be produced and the time sequence for that production by each of the nuclear plants on the system that minimizes total system costs is known. The nuclear fuel simulation and optimization model selects the schedule of reload batch fractions, f_i, and

enrichment, ε_i, that minimizes the nuclear fuel costs of meeting the nuclear energy requirements as specified by the utility system optimization.

2.4 Nuclear Power Management Multi-Year Model

A model is under development in the Department of Nuclear Engineering at M.I.T. which performs the utility system planning analysis for the mid range which was mentioned in the previous section. The overall power management model was divided into two portions. One is the integration of existing nuclear plants into the probabilistic simulation of the operation of the entire utility system; the development of this portion of the model was carried out by P.F. Deaton (11). The second portion, which is the basis for this report, is the nuclear fuel simulation and optimization of individual nuclear electricity generating plants on the system.

Figure 2.3, is a schematic drawing of the interaction of the different parts of the model which performs the simulation and optimization of utility system operation. The development of a refueling and maintenance model, block A in Figure 2.3, is being carried out by Systems Control Inc. (28) and Commonwealth Edison Company (8). These refueling and maintenance models develop feasible schedules of all required nuclear refueling and all required mainten-

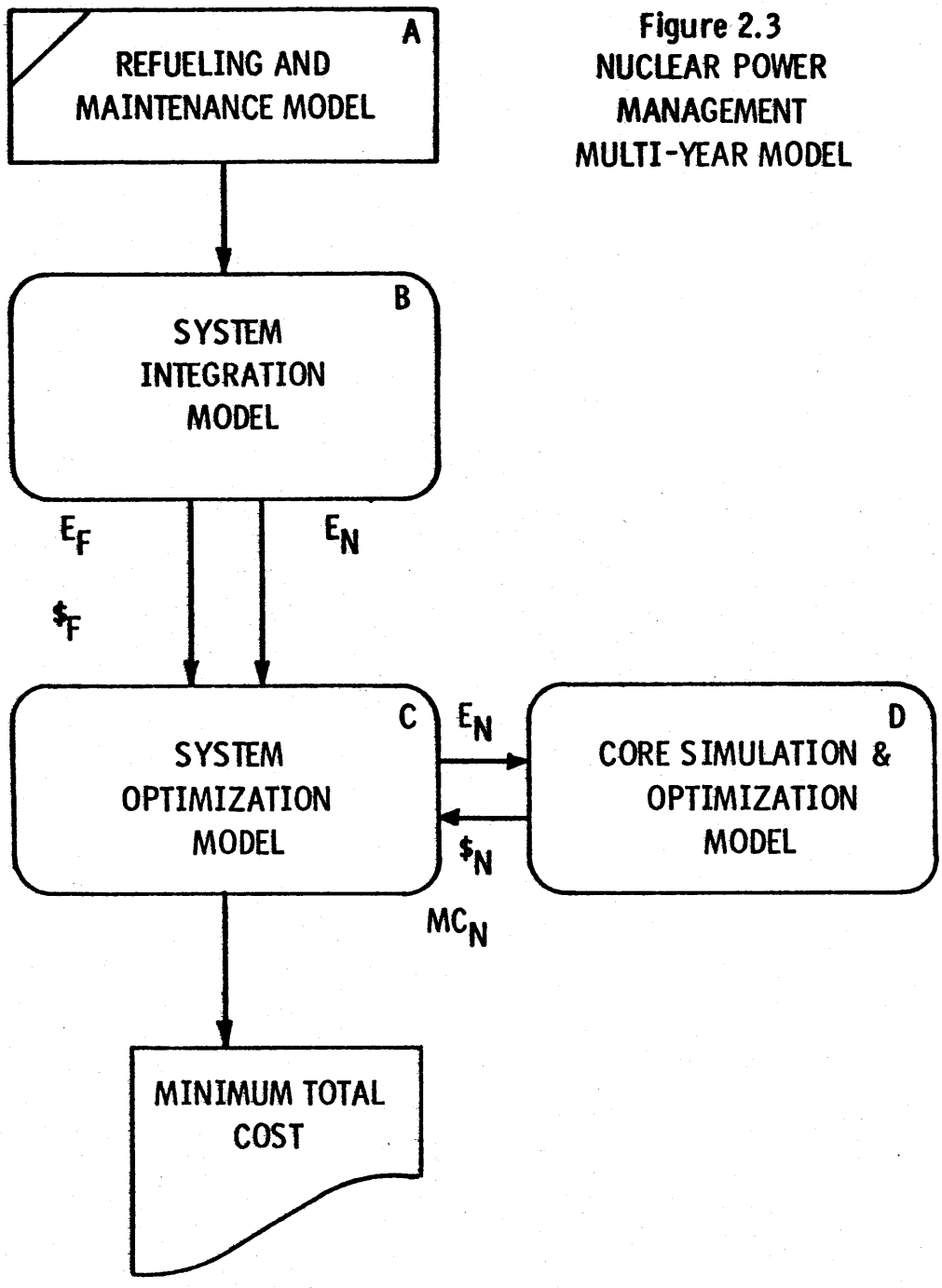

Figure 2.3
NUCLEAR POWER MANAGEMENT MULTI-YEAR MODEL

ance periods for all nuclear, fossil, hydro, etc., plants on the utility system. For each refueling and maintenance schedule generated by this model, an optimal fueling pattern is developed by the remainder of the Nuclear Power Management Multi-Year Model, which also then indicates the lowest cost schedule.

The System Integration Model (11) block B in Figure 2.3 divides the mid-range planning horizon into periods usually one or two months in duration. This system integration model uses a probabilistic* simulation model to determine the energy production of each plant during each of these periods. The following information is required by the system integration model:

1. The electric capacity of each plant on the system.
2. The number of valve points and the power level and heat rate in BTU/kwhr at each valve point for all plants.
3. The cost of fuel consumption for each plant at each valve point.
4. The system loading order, i.e., the sequence in which each of the plants starts producing electricity for the system.

---

* For a simplified explanation of probabilistic simulation with examples, see R.R. Booth's "The A-B-C- of Probabilistic Simulation" (5).

The system integration model calculates the energy to be produced by each of the fossil plants, E_F, the total cost of producing this energy, $\$_F$, and the total nuclear energy, E_N, to be produced by all of the nuclear plants for each one month period.

The System Optimization Model, block C in Figure 2.3, allocates the required nuclear energy production, E_N, among all of the nuclear plants available to the system during a period. Considering one reactor, r, the amount of energy, $E_{r,i}$, that it must produce during one cycle, i, is the sum of the energies allocated to reactor r for the periods that are included in cycle i. The duration of each cycle for each reactor, $T_{r,i}$, was specified by the refueling and maintenance model. $E_{r,i}$ and $T_{r,i}$ are commonly referred to as the energy and time vectors which must be satisfied by each reactor r. Given the energy and time vectors for each reactor, the In-Core Simulator and Optimizer, block D in Figure 2.3, must satisfy these at minimum fuel cost. As was previously mentioned in Section 2.2.2, the decision variables in this optimization of nuclear fuel are the reload batch fraction, f_i, and enrichment, ε_i, for each cycle i, in the planning horizon. The task of the In-Core Simulator and Optimizer is to select the optimal, i.e. minimum nuclear fuel cost, schedule of f_i's and ε_i's

for each reactor. One of the objectives of this thesis is to describe the design and development of an in-core simulation and optimization model to be used by a nuclear power management system.

Returning to the Nuclear Power Management model in Figure 2.3, it can be seen that the in-core simulation and optimization model must calculate the total nuclear fuel cost, $\$_N$, and the nuclear marginal cost, MC_N, which are to be used by the system optimization model. $\$_N$ is the total system revenue requirements for nuclear fuel planning horizon. MC_N refers to the marginal cost, $MC_{r,i}$, incurred by changing any one of the reactor cycle energies, $E_{r,i}$. Based upon these marginal costs, $MC_{r,i}$, the system optimization model calculates a new set of nuclear energies, $E'_{r,i}$. The in-core simulation and optimization model is then called again to optimize this new set of energies, $E'_{r,i}$. When

$$E'_{r,i} = E_{r,i}$$

or

$$\$_N' = \$_N \tag{2.2}$$

convergence is achieved.

At this juncture the optimization is concluded and the total system cost, $\$_F + \$_N$, the sum of the fossil and nuclear fuel costs during the planning horizon, is calculated. Recall that this optimization procedure was for one refueling and maintenance schedule. This same procedure is repeated for each refueling and maintenance schedule produced by the refueling and maintenance model. When all of these schedules have been optimized the schedule that incurred the minimal total system cost is the optimal schedule. This optimal schedule defines the minimal cost scheme for operating the entire utility system over the planning horizon.

2.5 Nuclear Fuel Optimization Problem

As was pointed out in Section 2.2, the nuclear in-core simulator calculates the neutron flux, power density, and energy production for each reactor after the refueling decisions for that reactor are made. The refueling decisions which are to be simulated are determined by the optimization algorithm, which is discussed at length in Chapter 4.

Figure 2.4 outlines the procedure used to optimize the nuclear fuel decisions. A dynamic programming algorithm was chosen to perform the nuclear fuel optimization. This procedure divides the planning horizon into stages, each

Figure 2.4
THE NUCLEAR IN-CORE SIMULATION AND OPTIMIZATION MODEL

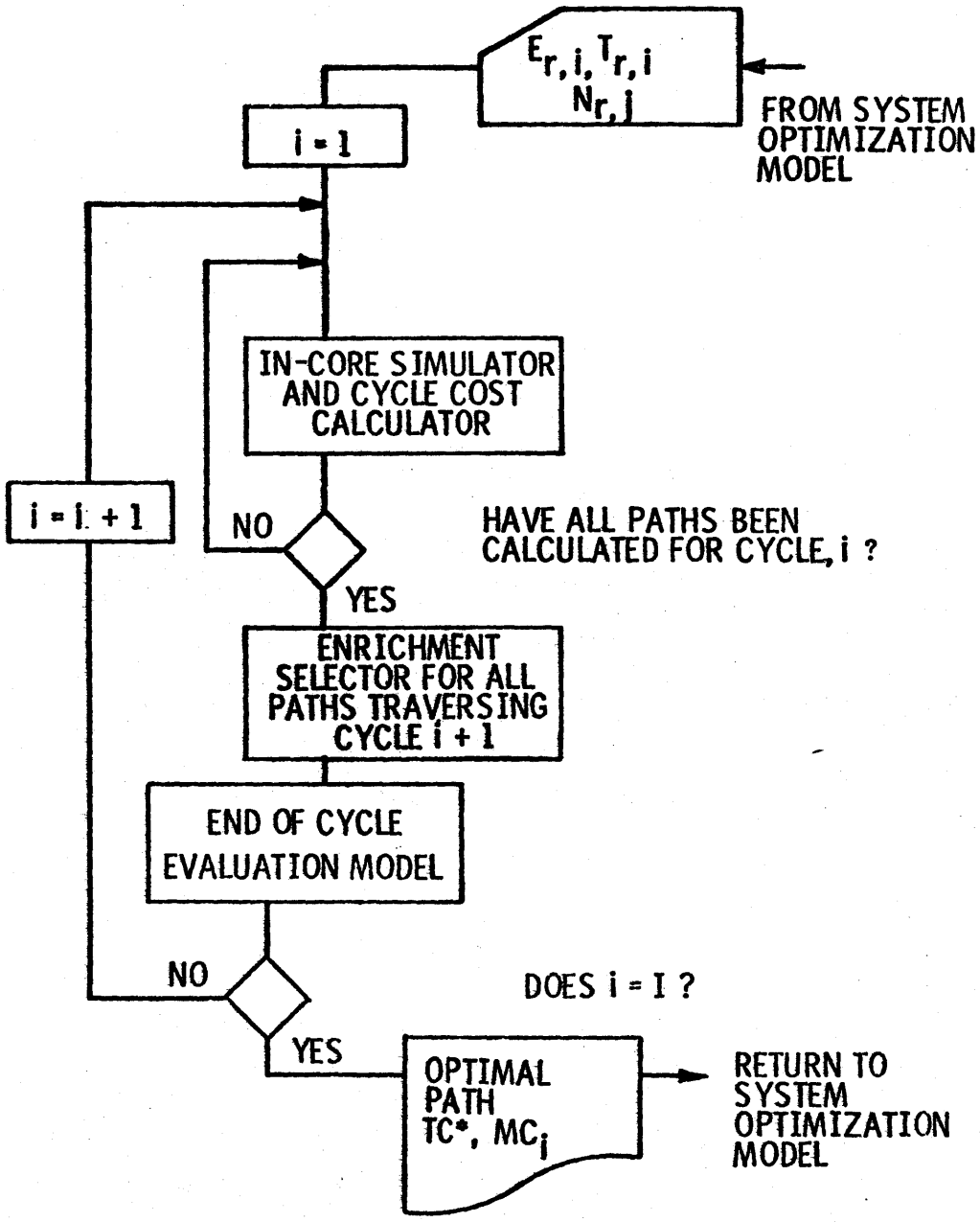

stage corresponding with a reactor cycle. At each stage a sub-optimization is performed which indicates the best set of refueling decisions from all feasible refueling decisions. It is the End-of-Cycle Evaluation Model, see Section 4.3.3, that performs this sub-optimization at the end of each cycle to find the best set of refueling decisions. Likewise, in Figure 2.4 the In-Core Simulator and Cycle Cost Calculator simulates only the best set of decisions as directed by the End-of-Cycle Evaluation Model. At the end of the optimization the algorithm finds the optimal refueling policy for the reactor from this best set.

The nuclear refueling optimization problem solved by this dynamic programming algorithm can be succinctly stated as the problem of minimizing the total revenue required from reactor r, $\overline{TC}_r$, of producing the required energy, $E_{r,i}$, over a planning horizon in I cycles. Since this optimization is performed in an identical fashion for each reactor on the system, the reactor subscript r shall be dropped in all future notation with the understanding that the procedures and equations described apply to each reactor on the system. Reiterating, the nuclear refueling optimization problem is to

$$\text{Min. } \overline{TC} = \text{Min. } \sum_{i=1}^{I} C[x(i), \epsilon_i, f_i, i] \qquad (2.3)$$

where $C[x(i), \varepsilon_i, f_i, i]$ is the revenue required to produce energy in the i^{th} stage or cycle and where x(i) is the state of the reactor at the beginning of the i^{th} cycle. x(i) is a function of the spatial distribution, r, of nuclide concentrations,

$$x(i) = x(N(r,i)) \tag{2.4}$$

ε_i, f_i are the decision variables of reload enrichment and batch fraction respectively, i is the stage designation, namely each cycle. In Equation (2.3) C is also a function of the various unit costs of nuclear fuel, e.g. cost of fuel rod fabrication. Any changes in these unit costs over the planning horizon must be considered in the calculation of the objective function. However, since these costs are not a function of the refueling strategy for which an optimum is sought they have not been included explicitly in Equation (2.3). This total cost function, $\overline{TC}$, is subject to the constraints that

1. E_i is given for all i and is a constant for each i, and,
2. The state vector x(i) shall not violate certain specified limits on power peaking and burnup.

In this formulation of the problem the state transformation function G which describes the effects of the decision variables on the state variable from one stage, i, to the next, i + 1,

$$x\ (i + 1) = G[x\ (i),\ \epsilon_i,\ f_i] \qquad (2.5)$$

is calculated by the in-core simulator.

The remainder of this report describes the solution of the nuclear fuel optimization problem as outlined in the above equations by the in-core simulation and optimization model.

2.6 Objectives of This Thesis

This thesis describes the computer tools developed to simulate both the reactor physics and the economic aspects of nuclear fuel utilization which perform the in-core simulation and optimizations within the nuclear power management model. The development of certain correlation fits to previously accumulated data on a specific reactor, a Zion-I type reactor*, which significantly improve and speed up the optimization procedure for that reactor are also described. Finally this thesis discusses

---

* The Zion-I reactor is a 1060 MWe Westinghouse pressurized water reactor scheduled for operation by the Commonwealth Edison Company in 1973. See Appendix D for a detailed description of the design of this reactor.

the application of these simulation and optimization procedures in designing refuel loadings for the Zion reactor to meet a specified energy-time vector, $E_{r,i}$, $T_{r,i}$, over a six year planning horizon.

The development of this thesis proceeded along four distinct lines:

1. In Core Reactor Physics Simulating

   The development of calculation techniques to perform nuclide transformations as functions of space and time. These transformations are performed by the CORE computer code which is discussed in Chapter 3.

2. Nuclear Fuel Costing

   The calculation of the costs of these nuclide transformations which is necessary to find the most economic method of producing the energy demanded by the system. CYCOST, a subroutine of CORE, which is described in Section 3.4, calculates these costs.

3. Feasible Path Surveying

   The development of rapid means of evaluating the feasible combinations of enrichment and batch size that will supply the required energy at each loading. These evaluative procedures are discussed in Sections 4.3.2 and 4.3.3.

4. Nuclear Fuel Optimization

   The optimization procedure that finds the minimum cost refueling method of producing the required nuclear energy. The procedure used is a dynamic programming algorithm, see Section 4.3.1.

This report

1. Discusses these four portions of the nuclear simulation and optimization problem in great detail.
2. Describes the use of the simulation and optimization techniques developed in optimizing an example case for a Zion Reactor.
3. Analyzes the results of this example and,
4. Directs attention to where future work in this area can be most productive.

3. THE IN-CORE SIMULATOR AND COST CALCULATOR

3.1 Objectives of In-Core Simulation

The function of the In-Core Simulator and Cycle Cost Calculator shown in Figure 2.4 is to simulate all the nuclear fuel management decisions and calculate the costs associated with each of those decisions. The simulation of the fuel management decisions requires a capacity to perform nuclear fuel depletion calculations for a broad set of enrichment and batch fraction decisions. In terms of the dynamic optimization notation, Section 2.5, see Eq. (2.6), the in-core simulator must perform the state transformation

$$x(i + 1) = G[x(i), \varepsilon_i, f_i] \qquad (3.1)$$

Given the state of a reactor at the beginning of the i^{th} cycle, $x(i)$, it must simulate reloading that reactor with enrichment ε_i and batch fraction f_i and then calculate the state of the reactor $x(i + 1)$ at the beginning of the $(i + 1)^{st}$ cycle. As was previously noted, the state of the reactor is defined as the spatial distribution of all the uranium and plutonium isotopes and fission products.

The two other functions that the in-core simulator must perform are the checks to assure that neither the power peaking or maximum burnup constraints on the fuel have been violated.

Since the optimization scheme (see Chapter 4) requires a large number of these state transformation calculations, the in-core simulator must calculate this transformation very rapidly. The remainder of this Chapter discusses the computer codes developed to perform the in-core simulation and cycle cost calculation.

3.2 The Components of the In-Core Simulator and Cost Calculator

Three computer codes CELL, CORE and CYCOST make up the in-core simulator and cost calculator shown in Figure 3.1. Figure 3.1 indicates how these three codes interact to accomplish the state transformation, $x(i) \rightarrow x(i+1)$, and the costing of that transformation. The CELL code (17) is a point depletion code which generates time dependent cross section, $\Sigma(\theta,k)$, and nuclide density, $N(\theta,k)$ data for fuel of any initial enrichment. CORE, see Appendix A, is a modified two group, two dimensional code that calculates the reactivity and spatial flux and power density changes during each cycle. CYCOST (see Appendix B) uses the average nuclide mass information, $\bar{N}(\theta,k)$, for each batch k to calculate the discounted cost, C_i, of producing E_i, during cycle i.

3.2.1 The CELL Code

The role of the CELL code is to generate information needed by CORE for nuclear fuel of any initial enrichment.

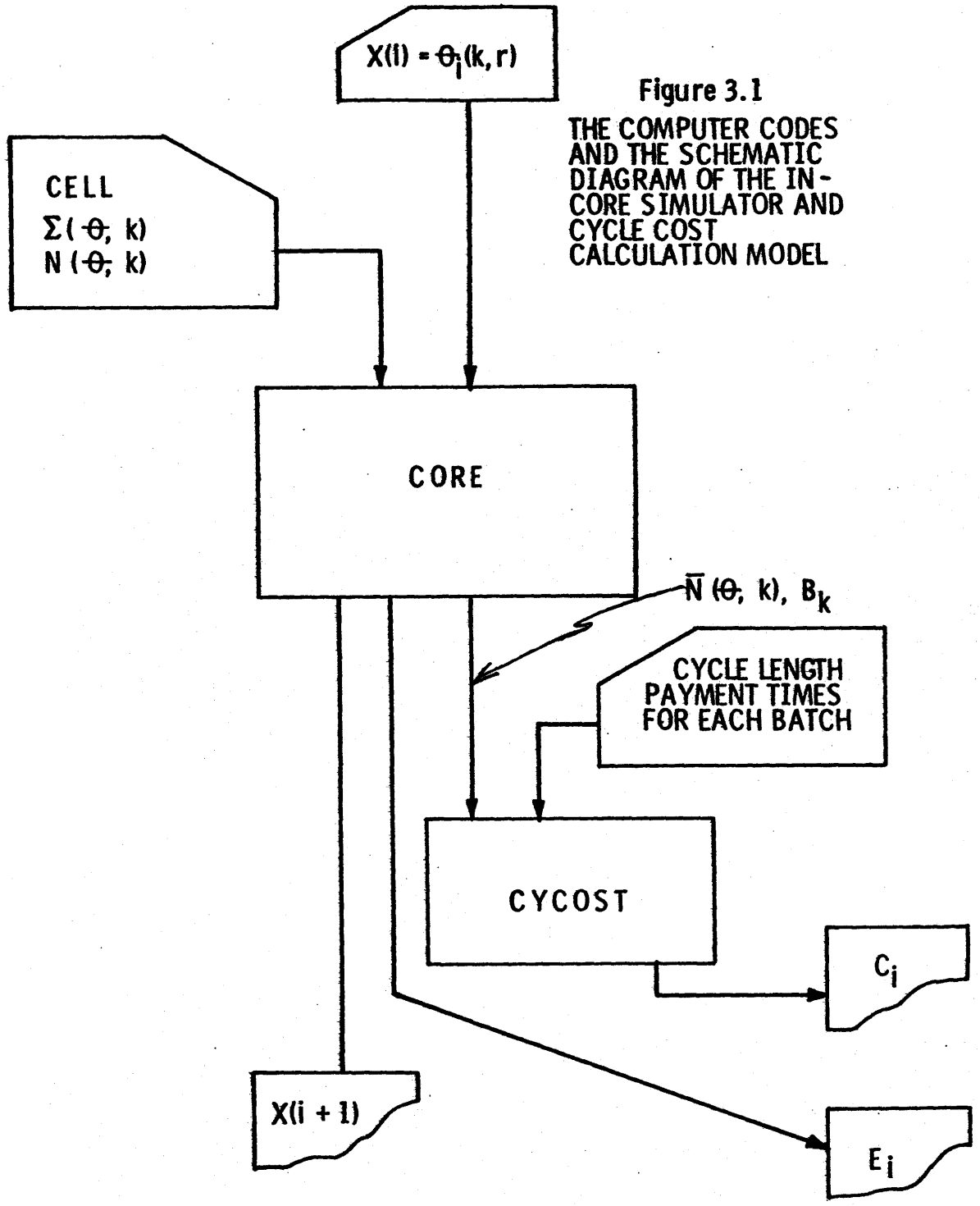

Figure 3.1

THE COMPUTER CODES AND THE SCHEMATIC DIAGRAM OF THE IN-CORE SIMULATOR AND CYCLE COST CALCULATION MODEL

CELL performs a point depletion calculation to determine the time dependent nuclear characteristics of a unit reactor cell. These nuclear characteristics which include uranium and plutonium nuclide concentrations and macroscopic nuclear cross section information (see Appendix B) are stored on tape or on cards for future use by CORE. Each CELL calculation requires 4.3 sec of computation time on an IBM-370 M165 computer. The CELL code need only be run once for each fuel enrichment of interest.

CELL calculates all burnup dependent parameters as functions of one variable, the flux-time, θ assuming that these parameters are independent of flux magnitude and flux history. As a result the state of a reactor at the beginning of the i^{th} cycle can now be defined in terms of θ, the flux-time.

$$x(i) = \theta_i\ (k,r) \tag{3.2}$$

where $\theta_i(k,r)$ is the flux-time for fuel batch k at position r at the beginning of the i^{th} cycle. Knowing $\theta_i(k,r)$ (see Figure 3.1) for a given reactor, the CORE program refers to the batch k CELL information to get all of the nuclear parameters $\Sigma(\theta,k)$, required for the depletion calculation and all the nuclide concentrations, $\bar{N}(\theta,k)$ necessary for the cost calculation. The nuclear parameters required for the modified two energy group calculation performed by CORE are:

$\nu\Sigma_f$: the number of neutrons released by thermal fissions per unit of thermal flux, cm^{-1}.

Σ_f : the homogenized macroscopic thermal fission cross-sections, cm^{-1}.

$\frac{1 - P}{1 + \alpha}$: the number of resonance fissions per unit of slowing down density entering the resonance region.

$\eta(1-P)$: the number of neutrons released by resonance fissions.

P : the overall resonance escape probability.

Σ_x : the maximum Xe-135 macroscopic absorption cross-section, cm^{-1}.

Σ_a : the cell macroscopic absorption cross-section excluding Xe-135, cm^{-1}.

3.2.2 The CORE Code

Using the CELL calculated properties, $\Sigma(\theta,k)$ and $N(\theta,k)$ the CORE code calculates the spatial flux and power distributions, the changes of these distributions with time and the energy generated during each cycle. CORE considers two spatial dimensions (R-Z) and solves the modified two energy group, five point difference equation for the flux at each depletion step (see McLeod (25)).

3.2.2.1 The CORE Depletion Calculation

The CORE code in its present state represents the pressurized water reactor being studied by as many mesh points as the operator desires. However, in the case where

very rapid simulation of reactor performance is a requirement, the number of mesh points can be reduced to as low as 75 without affecting the accuracy of the code. For a description of a mesh point sensitivity study done for this code see Appendix G. For the Zion reactor used in the Sample Optimization problem, Chapter 5, fifteen radial and five axial mesh points were employed.

At the beginning of a cycle the necessary nuclear parameters are calculated at each mesh point from the CELL data. From this information CORE solves the five point difference form of the diffusion equation for the flux and iterates until the soluble boron concentration needed to bring the effective core multiplication factor, k_{eff}, to unity is found. This calculation also produces the beginning of life power distribution at which point the power peaking constraint can be checked for the first time. The spatial distribution of the flux-time is now incremented on the basis of the assumption that the spatial distribution of the flux remains constant during that time increment. The time steps taken by CORE can be adjusted by changing the input to the code. For this study the time steps were approximately 40 to 45 days and vary inversely with the maximum flux in the reactor at the time of the step. At the end of each time step new spatial properties are calculated and another flux and boron con-

centration search is performed. At the end of a cycle when k_{eff} equals unity with no soluble boron present CORE calculates for that cycle the energy produced by each batch, B_k, the uranium and plutonium nuclide masses in each batch, N(k), and the average reactor energy production, E_1. The power density peak to average ratio is checked at every time step to assure that it is below the allowable limit. The computation time, on an IBM 370-M165, required to perform this one cycle calculation is 4.1 seconds.

3.2.2.2 Nuclear Fuel Representation in CORE

Major changes were made to the CORE code, formerly called MOVE (21), in order to use it as the reactor in-core simulator in the nuclear fuel optimization model. These changes were mainly involved in altering the fuel handling procedures so that CORE has the flexibility to consider reload batches of different enrichments and different sizes. Each batch k was assigned an integer, IPROP(k), that specifies the block of CELL information in which the CORE code will find the correct nuclear parameters for that batch. The remainder of this section describes the method by which CORE treats batches of different sizes.

3.2.2.2.1 The Mesh Point Property Calculation

The reactor core is spatially represented by a matrix of discrete mesh points (see Figure 3.2). The outer rings

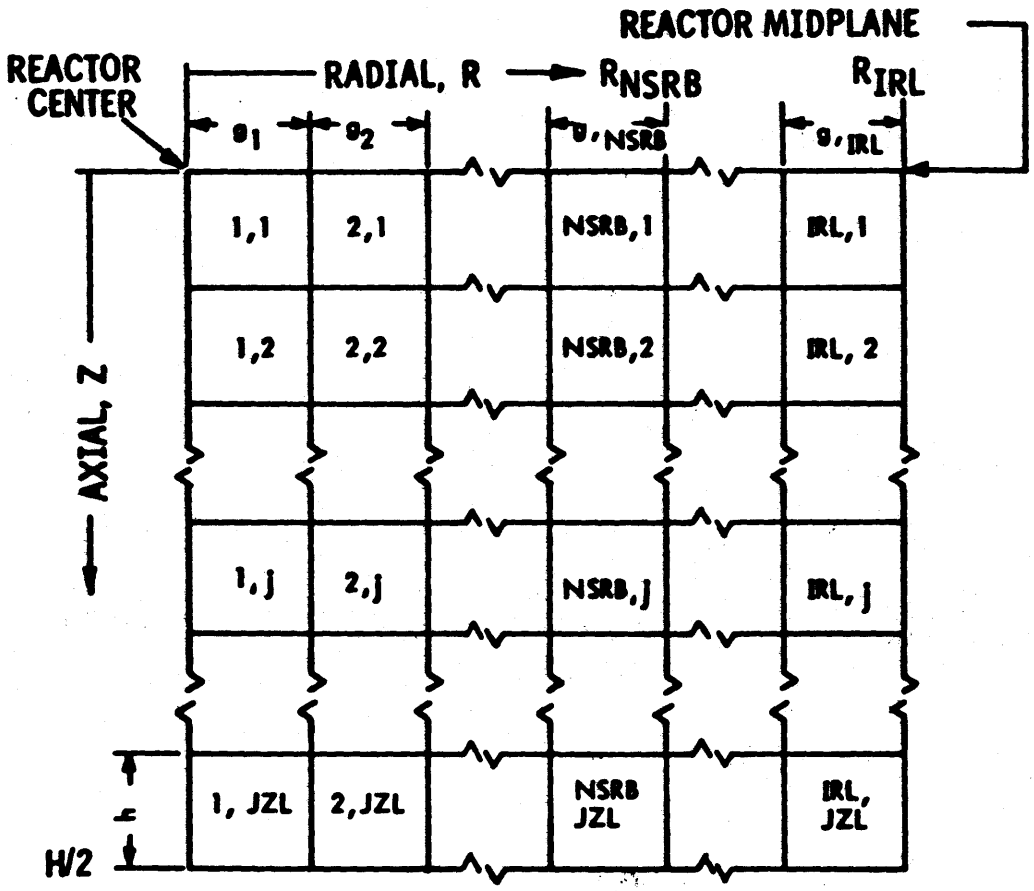

Figure 3.2
MESH REPRESENTATION OF A REACTOR QUADRANT IN-CORE
EXCERPTED FROM McLEOD (24)

from radial mesh point NSRB to IRL in Figure 3.2 contain only fresh fuel. This outer region, R_{NSRB} to R_{IRL}, therefore specifies the reload batch fraction, f_i, for each cycle $_i$. NSRB can be changed at the beginning of each cycle, and in this fashion batch fractions of different sizes can be loaded into the reactor core. Using this method only discrete values of f_i are permitted. However, since the position of all radial mesh points is an input parameter, the level of discreteness in f can be decreased by the addition of more radial mesh points in the proper locations in the core. Recall (see Section 2.2.2) that the fuel in this outer region is of only one type and therefore, the calculation of the spatial nuclear parameters required to solve the diffusion equation simply reduces to looking for them in the appropriate CELL data set designated by IPPROP. This is not the case in the inner, (1-f), region.

In the inner region of the reactor core from radial mesh point R_1 to R_{NSRB} in Figure 3.2 there are several different size batches of fuel as a result of the reactor having been reloaded with differing f's in previous cycles. The fuel mass in each batch in the inner region is divided equally among all of the mesh points in this region, therefore, the name "scatter region." As a result the volume ratios of the batches at each mesh point in the 1-f region are the same as the batch volume ratios for the entire region. The

batch volume fraction, VOLFRC(k), specifies the ratio of the k^{th} batch volume to the volume of the entire inner region. That is:

$$VOLFRC(k) = \frac{Vol(k)}{\sum_{k=1}^{NZ} Vol(k)} \tag{3.3}$$

where Vol(k) is the volume of the k^{th} batch and NZ is the total number of batches in the inner region.

$\theta(k,r)$ is the flux-time value for batch k at position r. In order to calculate the value of any property, VU(r), at any position r the CORE code averages that property from each batch at r in the following manner:

$$VU(r) = \sum_{k=1}^{NZ} VU[\theta(k,r)] \cdot VOLFRC(k) \tag{3.4}$$

where $VU[\theta(k,r)]$ is the value of the property VU at flux-time $\theta(k,r)$ which is found in the CELL information for batch k.

3.2.2.2.2 The Refueling Procedure in CORE

Refueling is automatically performed at the beginning of every cycle calculation on the basis of an out-in scatter refueling scheme. In this scheme the most burned fuel, amounting to the fraction f of the fuel in the reactor, is removed from the inner scatter zone, an equal mass of fresh fuel is placed in the outer region, and the fuel not dis-

charged after the previous cycle including the fuel which had been irradiated in the outer region is scattered uniformly within an inner region. Permitting variable size batches to be loaded as fresh fuel complicates the automatic fuel-shuffling done in CORE for it requires the nonintegral unloading of batches. For example, if the most burned batch in the core is 1/3 of the core volume and the reload batch fraction is 1/4, then some fuel from this most burned batch must remain in the reactor for another cycle.

Assuming that the reactor is to be loaded with a batch fraction f_i for the i^{th} cycle CORE performs the refueling according to the following fuel discharge order until the reload fraction, f, of the reactor has been discharged

1. The chronologically oldest batches of fuel in the reactor.
2. When required batches are divided and the most burned elements within a batch are discharged first. All sub-divisions of a batch become new batches, some of which remain in the reactor and some are discharged.

After the fuel has been unloaded it is necessary to change the dimensions of the scatter region in the reactor if the reload batch fraction f_i is different from the previous

cycle's batch fraction f_{i-1}. This necessitates a recalculation of the volume fractions of all batches still remaining in the scatter region and also the averaging of the flux-time, θ, values within each batch. As was mentioned in the previous section, the mass of each batch in the inner region is divided equally among all of the mesh points in the inner region. Consequently, when the number of mesh points in the inner region is changed the mass of each batch at each mesh point must be changed in order to maintain conservation of mass within each batch and this equal, i.e. homogeneous, distribution of fuel.

CORE adjusts the fuel material in each batch in the following manner:

1. The code averages the flux-time exposure of all the fuel in one batch for all radial mesh points at the same axial mesh point.
2. CORE then assigns this average flux-time value, θ_k, to that fuel batch k for those radial mesh points for that one axial mesh point.
3. The mass in this fuel batch is then redistributed among all the radial mesh points in the newly defined scatter region. Each mesh point is given an equal mass of batch k.

These three steps are then repeated for each axial mesh point, in the reactor.

This procedure closely simulates the standard fuel shuffling scheme of moving highly burned fuel into close proximity to much less burned fuel in an attempt to minimize the power peaking in a local region. The only parameter that is significantly affected by this batch homogenization procedure is the maximum burnup for a fuel batch. Since the values of θ_k for all radial mesh points are averaged for each axial plane and then this average θ_k value is used for all radial mesh points occupied by batch k in the next cycle the maximum value of θ_k is lost. Consequently the maximum point burnup for batch k calculated at the end of the next cycle is low by ten to fifteen percent. For this reason the elimination of feasible paths in the optimization program is done on the basis of the average batch discharge burnup and not the maximum discharge burnup.

3.2.2.3 Power Peaking Constraint Calculation

The power density peak to average ratio calculated by the CORE code is based on the maximum mesh point power density. Due to the coarse mesh spacing (only 75 mesh points describe half of the reactor core) used in this simulation this ratio is much lower than is expected in actual reactor operation. As a result the elimination of certain paths upon the basis of this power peaking factor would be unrealistic.

A comparison was performed between the CORE code and a much more detailed code, CITATION (16). The comparison was made for similar calculations with both codes for the beginning of life, no Xenon and Samarium fission product buildup, for the Zion-I reactor's first core. An R-Z CITATION calculation with 37 axial and 44 radial mesh points calculated a point peak to average power density ratio of 2.811. This calculation was performed with no soluble boron in the core. Two more CITATION calculations in X-Y geometry were used to calculate the effect of soluble boron on this power peaking factor. It was found that soluble boron reduced the power peak by 8.7%. Adjusting the R-Z power density factor by this 8.7% yields the power peak to average ratio of 2.567 for the Zion-I reactor, first cycle, beginning of life, with soluble boron and no Xe, and Sm fission products. A CORE run for precisely the same conditions calculated the power peaking factor to be 2.080. The normalization factor, NF, required to adjust the CORE calculation to the CITATION calculation is

$$NF = \frac{2.567}{2.080} = 1.23 \qquad (3.5)$$

In practice this normalization factor should be calculated on the basis of many comparisons between the CORE code and a more detailed code, among which a diversity of re-

fueling conditions are represented. However, only one CITATION run for the Zion-I reactor was made in this model development study.

A more realistic power peaking factor to eliminate paths in the optimization procedure would be normalized power peaking factors and not the CORE calculated factors. For the sample problem described in Chapter 5 the maximum power peak to average ratio allowed was 3.3. Elimination of paths occurred when

$$PDMXTA \cdot NF > 3.3 \qquad (3.6)$$

where PDMXTA was the peak to average power density ratio as calculated by CORE.

3.2.2 The Cycle Cost Calculation

3.2.3.1 The Necessity for Cycle Costing

Nuclear fuel costing is traditionally done on the basis of calculating all of the costs incurred by one batch of fuel and all the energy that that batch produces during its residence of many cycles in the reactor. This requires that all of the information pertaining to all of the reactor cycles during which this batch of fuel was in the reactor be calculated before this batch cost can be calculated. If this batch costing is to be used in the optimization of the decisions as to the reload enrichment and reload batch fraction for any cycle it would be necessary to calculate the cost of

many subsequent cycles in order to observe all the effects of each decision. In reality this implies making decisions for all of the cycles in the planning horizon and then calculating the cost of that entire set of decisions with existing nuclear fyel cycle costing codes such as REFCO (31) or MITCOST (10). This procedure is being used in nuclear fueling optimization procedures under development (19). Using this approach of calculating costs for the entire planning horizon requires linearization approximations (37) or an exhaustive search of all feasible alternatives (19) in order to perform the optimization.

Since the decisions to be optimized, the reload enrichment and batch fraction, must be made at the beginning of each cycle another approach to the optimization problem is to divide the planning horizon into stages, each stage being equivalent to each cycle, and to calculate the revenue requirements incurred in traversing each stage. This is a dynamic programming approach to the optimization to nuclear fuel decision making. Chapter 4 describes this approach and alternate optimization techniques in detail. The dynamic programming approach eliminates the necessity to make linearization assumptions about nuclear fuel costing and the necessity to do an exhaustive search of all feasible alternatives. However, the dynamic programming approach does require the development of a nuclear fuel costing

procedure that can calculate the cost of each cycle in a planning horizon and not each batch of fuel loaded into the reactor during this horizon. The CYCOST routine was written to perform this cycle by cycle nuclear fuel costing. It also was written to link directly to CORE so that the cycle cost is calculated automatically with every cycle depletion calculation done by CORE.

3.2.3.2 The CYCOST Routine

The CYCOST subroutine, see Figure 3.1, of the nuclear in-core simulation and optimization package receives from CORE the energy, B_k, produced by each batch k of fuel and the nuclide masses, $\bar{N}_k$, in each batch. Along with this information from CORE, the CYCOST code needs the time schedule of all payments made for each batch and the beginning and end of cycle times in order to calculate the cycle by cycle nuclear fuel revenue requirements, C_i. The equation that CYCOST solves is:

$$C_i = \sum_{k=1}^{NOZONE} \frac{1}{1-\tau} \{ Z(k,t_1) - PVEOC \cdot Z(k,t_2) - \tau(Z(k,t_1) - Z(k,t_2)) \cdot PVE \} \qquad (3.7)$$

where:

k is the batch notation,

NOZONE is the total number of batches and sub-batches in the reactor during cycle i,

τ is the income tax rate,

$Z(k,t_1)$ is the "value" of the fuel in batch, k, at the beginning of the cycle, defined by Eq. (3.8),

$Z(k,t_2)$ is the "value" of the fuel in batch, k, at the end of the cycle, also defined by Eq. (3.8),

t_1 and t_2 are the time at the beginning and the end of each cycle respectively,

PVEOC is the end of cycle present value factor which discounts the value of each batch of fuel to the beginning of the cycle, and

PVE is the present value factor which discounts the revenues received for energy produced in cycle i to the beginning of the cycle.

The value of any lot of fuel, k, at time t, is:

$$Z(k,t) = U(t)\cdot c_U(t)\cdot PVAUP + [(1/F'-1)c_U(t_o) + c'](1 - \frac{\int_{t_o}^{t} dE_k}{\int_{t_o}^{t_f} dE_k})\cdot PVFAB$$

continued

$$- U(t_f)[F''c''' + (1-F''F''')\cdot c_U + c'']\cdot \frac{\int_{t_o}^{t} dE_k}{\int_{t_o}^{t_f} dE_k} \cdot PVREP$$

$$+ F''P(t)\cdot c_p \cdot PVAUP \qquad (3.8)$$

where:

$U(t)$ is the mass of uranium in batch k at time t,

$P(t)$ is the mass of plutonium at time t,

PVAUP is the present value factor which discounts the purchase or sale of uranium and plutonium to the beginning or end of the cycle depending upon whether t equals t_1 or t_2 respectively,

PVFAB is the present value factor which discounts payments for fabrication to the beginning or end of the cycle,

PVREP is the present value factor for reprocessing and conversion payments,

F', F'', F''' are the fractional yields of uranium and plutonium in the fuel fabrication, reprocessing and conversion processes respectively,

c_p is the unit salvage value of plutonium,

c', c'', c''' are the unit costs for fabrication, reprocessing and conversion respectively,

$\int_{t_o}^{t} dE_k$ is the amount of energy produced by batch k from time t_o to t, and,

$c_U(t)$ is the unit cost, \$/kg, of uranium for the batch at time t.

As the fuel is irradiated its enrichment decreases. Therefore, c_U is a function of enrichment which is a function of time. t_o refers to the beginning of the first irradiation of this fuel batch. t_f refers to the end of the last irradiation of this batch.

The factor $1 - \frac{\int_{t_o}^{t} dE_k}{\int_{t_o}^{t_f} dE_k}$ calculates the cost of fabrication which has not yet been depreciated by time t, the time at which the value of the fuel batch k is being calculated. Similarly the factor

$$\frac{\int_{t_o}^{t} dE_k}{\int_{t_o}^{t_f} dE_k}$$

applied to the reprocessing and conversion costs calculates the amount of those costs which are incurred by batch k up to time t. In order to calculate both of these factors $\int_{t_o}^{t_f} dE_k$, the total amount of energy produced by batch k must be known. Since this total batch energy production

is not known until the batch is finally discharged from the reactor, it must be estimated. It has been found through the experience gained by many CORE cycle calculations for the Zion-I reactor (the reactor used in the sample problem Chapter 5) that to a first approximation this total batch energy in MWD/T is a function of the initial enrichment of the batch regardless of batch size over the range of $0.25 < f < 0.37$. This relationship of initial enrichment was calculated by correlating existing results for the Zion-I reactor that CORE had previously developed with a least square polynomial fit. This function was found to be

$$E_k = -2919.25 + 10789.3\ \varepsilon_k \qquad (3.9)$$

where E_k is the total energy produced by batch k in MWD/T if its initial enrichment was ε_k in w/o. This estimation is performed automatically by CYCOST, see Appendix C. This assumption used in the depreciation of fabrication, reprocessing and conversion revenue requirements only affects the present value of these costs and not the total amount of revenue required for each. As a result the error introduced into Eq. (3.9) which is about 10% in E_k has only a second order effect on the cycle revenue requirements as calculated by CYCOST.

All discounting is done on a continuous basis. That is, the present value factors, PV, are calculated as follows (31):

$$PV = e^{-[\ln (1 + x) \cdot t]} \tag{3.10}$$

where x is the discount factor and t is the time over which the discounting is being done.

In their present forms Eq. (3.7) and (3.8) calculate the revenue required to produce energy during that cycle discounted to the beginning of the i^{th} cycle. C_i is further discounted by the factor $PVTOT_i$ to the beginning of the planning horizon and it is this discounted revenue requirement which is added to the cycle costs for all other cycles,

$$\overline{TC} = \sum_{i=1}^{I} C_i \cdot PVTOT_i \tag{3.11}$$

This total revenue requirement, $\overline{TC}$, is the objective function that is minimized by the optimization procedure described in Chapter 4.

Figure 3.3, which shows the time sequence of payments used in costing energy produced in Cycle i, presents the time parameters required to calculate the present worth factors in Equations (3.7) and (3.8). Part A of Figure 3.3 depicts the times at which payments were made for the fabrication, reprocessing and conversion services for all

A. PURCHASE OF FABRICATION, REPROCESSING AND CONVERSION SERVICES

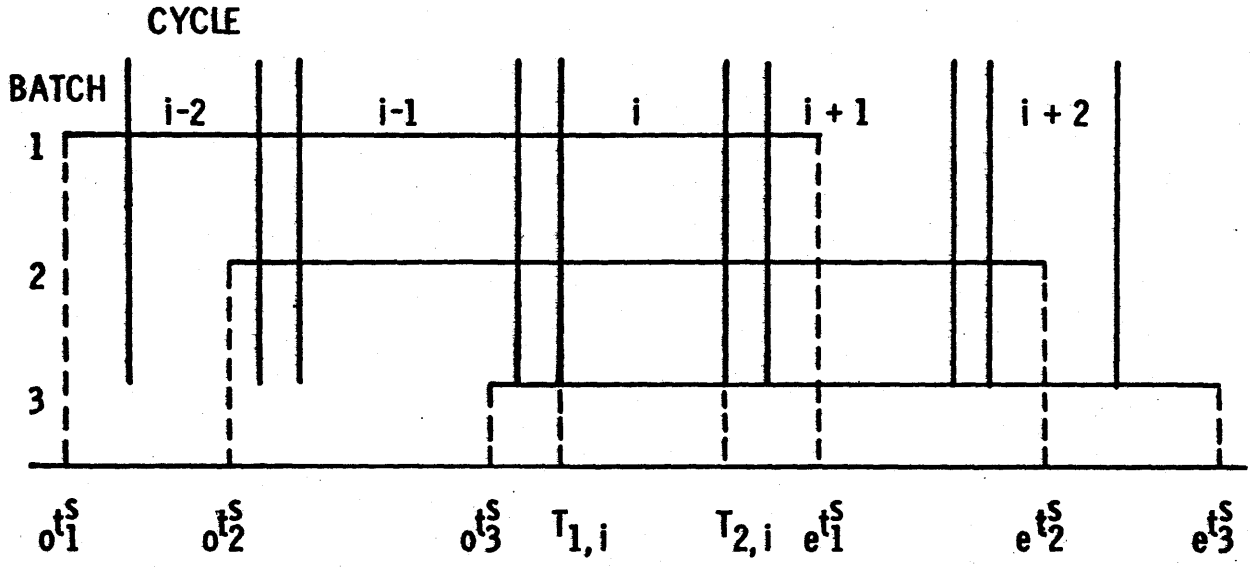

$$T_{1,i} - o t_3^S = \text{TAPRE}$$

$$e t_1^S - T_{2,i} = \text{T POST}$$

B. URANIUM AND PLUTONIUM PURCHASES AND CREDIT RECEPTIONS

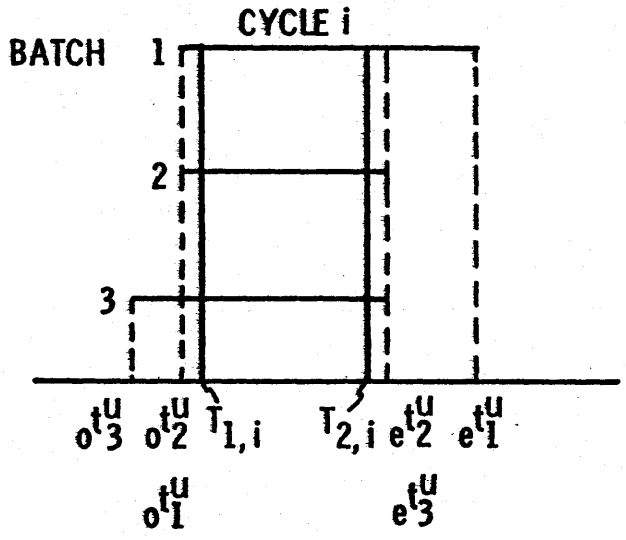

Figure 3.3
THE TIME SEQUENCE OF PAYMENTS USED IN
COSTING ENERGY PRODUCED IN CYCLE i

batches of fuel in the reactor during cycle i. The time sequence for these payments are handled in the same manner as they are in most nuclear fuel cycle cost codes (31, 10). The notation used in Figure 3.3 and in the following discussion is based on the use of ${}_{y}t_{k}^{x}$ where:

- x is either s or u and refers to the time that a service payment is made, s, or a purchase or sale of uranium or plutonium is transacted, u.
- y is either o or f for a payment or credit occurring prior to irradiation or subsequent to irradiation, respectively.
- k is an integer and is the batch notation

$T_{1,i}$ and $T_{2,i}$ are the times at the beginning and at the end of cycle i.

For the case shown in Figure 3.3 there are three batches of fuel in the reactor during cycle i. ${}_{o}t_{1}^{s}$, ${}_{o}t_{2}^{s}$, and ${}_{o}t_{3}^{s}$ are the times at which fabrication services were paid for each batch. This fabrication payment time, ${}_{o}t_{k}^{s}$, for any batch k is calculated as

$$ {}_{o}t_{k}^{s} = T_{1j} - \text{TAPRE} \qquad (3.12) $$

Cycle j as used here is the reactor cycle into which batch k is first loaded. TAPRE is the time before insertion of fuel when payment is made for the uranium in the batch,

for the fabrication and for the enrichment of the uranium. TAPRE is an input parameter to CYCOST, see Appendix C.

The time for reprocessing, conversion, and shipping payments is given by ${}_{e}t_1^s$, ${}_{e}t_2^s$ and ${}_{e}t_3^s$ for the three batches shown in Figure 3.3. The ${}_{e}t_k^s$ times are calculated in a similar fashion to the ${}_{o}t_k^s$ times. That is

$$ {}_{e}t_k^s = T_{2,j} + \text{TPOST} \tag{3.13} $$

where $T_{2,j}$ is the time at the end of the last cycle, cycle j, during which batch k is in the reactor and TPOST is the time period after discharge when reprocessing, conversion and shipping charges are paid. TPOST is also an input parameter to CYCOST.

The end of cycle times, $T_{2,j}$, are all known over a particular planning period for the optimization problem under consideration, see Section 2.4. However the number of cycles during which a batch of fuel will be in the reactor is not known when that batch is first inserted. Consequently, an estimate must be made of the number of cycles during which each batch will reside in the reactor in order to calculate ${}_{e}t_k^s$. This estimate is made on the basis of the batch fraction f_k for each batch, k. Namely, the number of cycles during which batch k is in the reactor is given as the nearest integer to $1.0/f_k$.

Part B of Figure 3.3 depicts the times used in the calculation of uranium and plutonium burnup charges to cycle i. For the batch inserted into the reactor at the beginning of cycle i, batch 3, the uranium purchase payments and enrichment service payments are made at ${}_{o}t_{3}^{u}$ which is TAPRE years prior to the beginning of cycle i. It is assumed that the uranium and plutonium in batches 1 and 2 are purchased at the midpoint of the refueling down period.

$$ {}_{o}t_{1}^{u} = {}_{o}t_{2}^{u} = \frac{T_{1,i} - T_{2,i-1}}{2} \tag{3.14} $$

where:

$T_{1,i}$ is the time for the beginning of cycle i, and

$T_{2,i-1}$ is the time at the end of the (i-1)st cycle.

Likewise all fuel not discharged, batches 2 and 3, from the reactor at the end of cycle i, $T_{2,i}$ are sold at ${}_{e}t_{2}^{u}$ and ${}_{e}t_{3}^{u}$, where:

$$ {}_{e}t_{2}^{u} = {}_{e}t_{3}^{u} = [T_{2,i} + T_{1,i+1}]/2 \tag{3.16} $$

For the batches being discharged the uranium and plutonium credit is received at ${}_{e}t_{1}^{u}$ where

$$et_1^u = T_{2,i} + TPOST \qquad (3.17)$$

This cycle costing routine is used as the objective function which is optimized by the nuclear optimization model described in Chapter 4.

4. DYNAMIC PROGRAMMING APPROACH TO NUCLEAR REFUELING OPTIMIZATION

In Section 2.5 the nuclear refueling optimization problem was described. The purpose of any optimization procedure is to minimize or maximize an objective function. Equation (2.3) repeated here for convenience, is the objective function of the nuclear refueling optimization problem.

$$O.F. = \text{Min } \overline{TC} = \text{Min} \sum_{i=1}^{I} C[x(i), \epsilon_i, f_i, i] \qquad (4.1)$$

where

$\overline{TC}$ is the total discounted revenue required to produce energy from one reactor over I cycles,

$C[x(i),\epsilon_i,f_i,i]$ is the discounted revenue required to produce energy in the i^{th} cycle,

$x(i)$ is the state of the reactor at the beginning of the i^{th} cycle,

ϵ_i, f_i are the decision variables of reload enrichment and batch fraction and

i designates each cycle in the planning horizon.

$x(i)$ is a function of the spatial distribution, r, of the nuclide concentrations in the reactor, $N(r,i)$. This objective function can be calculated by any nuclear fuel depletion computer code in tandem with a nuclear fuel cycle cost code. Chapter 3 described the use of the codes CORE and CYCOST in

calculating this objective function. Chapter 4 will concentrate on the optimization procedures developed to minimize the nuclear refueling objective function, Equation (4.1).

4.1 The General Characteristics of the Nuclear Refueling Optimization Problem

One of the major difficulties in optimizing the objective function in Equation (4.1) is that the function is by no means a simple analytic function. There is a superfluity of optimization techniques available to handle well behaved functions (36). However, the nuclear refueling objective function has only slight resemblances to the functions which have general optimization solutions. As a result optimization techniques for minimizing the costs of a stream of nuclear refueling decisions must be developed. There are two general approaches to developing this optimization procedure. The first is to simplify, e.g. linearize, the objective function so that it is well behaved and established optimization procedures can be utilized. The second is to reduce the complexity of the objective function by simulating the interactions of the variables in Equation (4.1) as the optimization is performed. This simulation can be extremely coarse or performed in great detail (34).

Simplifying the objective function or simulating it in a very coarse fashion may reduce the accuracy of any

optimization technique. On the other hand, however, performing the objective function calculation in great detail requires inordinate amounts of computer time. Simulating energy production from one reactor cycle by the CITATION (34) code requires five minutes of CPU time on the IBM 370, M-165. If only fifty cycle calculations are required for each reactor optimization this results in over four hours of computer time. This four hour calculation must be repeated for each reactor in the system. Both of these approaches to calculating and optimizing the objective function are outlined in Section 4.2 of this Chapter.

Another thorny aspect to nuclear refueling optimization is the interconnectedness of the decision variables f_i and ε_i from cycle to cycle. Fuel loaded into the reactor at the beginning of cycle i may remain in the reactor for several cycles. Consequently, refueling decisions made in cycle i affect the energy produced through approximately cycle i + 4 and hence the cost of nuclear fuel through cycle i + 4. This implies that the refueling decisions made in cycle i should consider future reloadings and future energy production. Again there are two approaches to resolving this dilemma. The first is to evaluate the objective function in such a fashion that the effects between cycles are eliminated, i.e. decouple the decisions. The second approach is to optimize all of the decisions over the entire planning horizon simul-

taneously. The decoupling approach is discussed in detail in Sections 4.3 and the simultaneous optimization approach is outlined in Section 4.2.1.

Besides reviewing various optimization techniques and their applicability to the nuclear refueling optimization problem, the remainder of this chapter discusses the general characteristics of the dynamic programming algorithm (Section 4.3) chosen to perform this optimization in the Nuclear Power Management Model presented in this report. In order to demonstrate the effectiveness of this algorithm and its method of application, a typical pressurized water reactor of the Zion-I type was modeled (Section 4.3.2) and sample optimization problems were solved (Chapter 5).

4.2 Optimization Techniques for Nuclear Refueling Decisions

There are a variety of optimization techniques which are applicable to the nuclear refueling optimization problem. This section presents a cursory review of those optimization approaches of major interest, some of which are being developed for the nuclear refueling problem and others which are not. Much of the art of optimizing is not in finding an optimization technique but in formulating the problem being considered such that the concepts of a particular technique can be readily applied. With this in mind it is not the intention of this review to describe in detail the application of each technique to the nuclear

refueling problem but rather to describe how this problem must be formulated to take advantage of each technique.

The two basic criteria which should be used in evaluating the use of any optimization procedure are:

1) Is the calculation of the objective function accurate enough to assure the reliability of the optimal solution and
2) Is the total computation time required by the nuclear fuel optimization procedure small enough so that this procedure can be used in an overall utility system optimization model?

All of the techniques described in this section can be characterized by how they calculate the objective function, O.F. In general two methods are used.

1) The O.F. is reduced to simplified analytic functions by the use of correlations to previously accumulated data. The accuracy of this approach is a function of the accuracy of the fit to the data base and of interpolation and extrapolation errors between the cases being optimized and the data base but the speed of optimizations based on this reduction justifies continued and more intensified work on them.

2) An on-line simulation of refueling decisions is performed simultaneously with the optimization. These simulations can be as accurate as desired by using reactor core models of one two or even three dimensions. However, the computation time required for the simulation of each decision is prohibitive in many instances, e.g. the three dimensional simulation is always too time consuming irrespective of the optimization procedure utilized.

4.2.1 Linear and Non-Linear Optimization Procedures

Recall that the optimization problem that must be solved is that of minimizing the total discounted revenue required to produce a specified amount of energy, E_i, for each reactor cycle i over a planning horizon of I cycles, see Eq. (4.1). The decision variables are the nuclear refuel enrichment ε_i and batch fraction f_i for each cycle and the constraints are maximum limits on the power peaking factor and on the average discharge burnup, see Section 2.2.1. The objective function in Eq. (4.1) can be linearized to become

$$\text{O.F.} \quad \text{Min } \overline{TC} = \text{Min } \sum_{i=1}^{I} c_{f,i} f_i + \sum_{i=1}^{I} c_{\varepsilon,i} \cdot \varepsilon_i \qquad (4.2)$$

In this format the simplex method of linear programming is readily applicable. One approach used in solving this linear optimization problem is as follows:

1) Select a basic feasible solution, a combination of ϵ_i and f_i for all i that produces the required energies, E_i, and violates none of the constraints.
2) Calculate the total revenue requirements, $\overline{TC}$, of this basic solution by simulating these decisions in off-line nuclear fuel depletion and fuel cycle cost codes.
3) Calculate the coefficients $c_{f,i}$ and $c_{\epsilon,i}$ in Eq. (4.2) using the fact that

$$c_{f,i} = \frac{\partial \overline{TC}}{\partial f_i} \qquad \text{and}$$

$$c_{\epsilon,i} = \frac{\partial \overline{TC}}{\partial \epsilon_i} \qquad (4.3)$$

These partial derivatives can be calculated by a perturbation analysis on the basic solution cost function.

4) Solve Eq. (4.2) for the optimal solution via the simplex method (18).

5) Perform steps 2, 3 and 4 for this optimal solution until the $c_{f,i}$ and $c_{\varepsilon,i}$ from one iteration to the next remain unchanged.

The utilization of this approach to nuclear refueling optimization required by the utility system planning model will be judged on the basis of the number of iteration requires many nuclear fuel depletion and fuel cycle cost simulations over the entire planning horizon, convergence of the method must occur within a very few iterations, less than ten if a two dimensional nuclear simulation is being used. A variation of this approach is being developed at MIT by Watt (37). This procedure is referred to as the successive linear approximation approach.

In most cases the utilization of non-linear programming approaches to the nuclear refueling optimization problem requires the calculation of so many nuclear fuel cycle depletions that they preclude the use of anything more than a zero dimensional simulation. In its basic form the non-linear programming problem can be viewed as

$$\text{Min } \overline{TC} = \text{Min } \overline{TC}[\varepsilon_1,\varepsilon_2,\varepsilon_3....\varepsilon_I,f_1,f_2,f_3,....f_I] \qquad (4.4)$$

An extensive set of correlations, previously calculated, would have to be used to generate this cost function. This function would be required to calculate the total cost of nuclear fuel for all the feasible sets of decisions, ε_i and f_i, that satisfy the cycle energy, E_i, demands over the entire planning horizon. Using the relationships from this correlation the steepest ascent with Optimal Step Size non-linear programming algorithm can be used very effectively (see Wagner (36) Chapter 14). A version of this approach is being investigated by Watt (37).

There are however, potential uses for non-linear programming in solving the nuclear refueling optimization problem if the non-linear objective function can be slightly altered. The alteration required is the writing of the revenue requirements, C_i, as being only a function of the decisions made in cycle i such that the objective function becomes

$$\text{Min } \overline{TC} = \text{Min} \sum_{i=1}^{I} C_i(\varepsilon_i, f_i) \tag{4.5}$$

The single stage optimization of the previous objective function Eq. (4.4), has been divided into a multi-stage optimization, Eq. (4.5). The general procedure for solving this equation is to calculate the non-linear cost function $C(\varepsilon_i, f_i)$ at the beginning of each stage. Since the com-

plexity of this function is greatly reduced from the function in Eq. (4.4) enough combinations of ε_i and f_i could be simulated at the beginning of cycle i to generate $C(\varepsilon_i, f_i)$. This simulation could be performed by a zero dimensional calculation. Using the same non-linear programming algorithm as before, the steepest ascent with optimal step size $C(\varepsilon_i, f_i)$ can be readily optimized. From the description of this method so far it is obvious how the energy produced in each cycle is optimized but this does not guarantee an optimal strategy for the entire path. If ε_i^*, f_i^* are the optimal enrichments and batch fractions for cycle i the cost

$$\overline{TC} = \sum_{i=1}^{I} C(\varepsilon_i^*, f_i^*) \qquad (4.6)$$

is not guaranteed to be the optimal total cost nor is the strategy of ε_i^*, f_i^*'s an optimal policy because of the coupling effects between cycles.

In order to use this multi-stage non-linear approach to the nuclear refueling optimization problem it is necessary to couple the stage wise optimization together so as to account for this coupling between the stages. This can be accomplished by using the following example procedure.

1) Assume the optimization is at the beginning of stage i. On the basis of the state of the reactor entering the stage, perform the zero dimensional simulations to generate the function $C(\varepsilon_i, f_i)$. Optimize the variables ε_i and f_i.

2) Using the simulations from previous cycles calculate

$$\left.\begin{array}{l} \dfrac{\partial C_i}{\partial f_j} \\ \text{and} \\ \dfrac{\partial C_i}{\partial \varepsilon_j} \end{array}\right\} \text{for } j = 1,\ i-1 \qquad (4.7)$$

3) If $\sum_{j=1}^{1} C(\varepsilon_j, f_j)$ can be improved, which the partials in Step 2 will indicate, change any or all ε_j and f_j in order to improve the overall solution.

4) It is now necessary to retrace the optimization for all the cycles that precede cycle i. That is, if the ε_j, f_j were changed in any cycle j all cycles after cycle j would now have new initial conditions. This would require the generation

of new cost functions for all cycles after cycle j, and the re-optimization of each cycle with the non-linear programming algorithm.

5) Repeat steps 1, 2, 3 and 4 until no further changes in ε_j and f_j, for j=1, i-1, will improve the sum of the costs for cycles one through i.

6) Procede to cycle i + 1 and repeat steps 1 through 5. When the last cycle I is reached terminate the procedure.

There are two severe limitations to this optimization procedure. First is the use of a zero dimensional calculation to generate $C(\varepsilon_i, f_i)$. The ability of such a model to generate valid cost information is in doubt. Furthermore, its capacity to calculate power peaking factors as a function of fuel loading is nil. As a result the power peaking constraint may not be tested until after the entire optimization is concluded, which can present grave difficulties. The second limitation is the number of times steps 1, 2, 3 and 4 of the procedure must be repeated before they converge on a set of ε_j, f_j for cycles one through j. If convergence is slow even using a zero dimensional model to generate the non-linear cost functions for each cycle would be too time consuming. If the work presently

being carried out by Rothrock (30) on a variation of this approach can eliminate these liminations, this method could prove very valuable as a nuclear refueling optimization model.

The steepest ascent algorithm itself is very fast and the numerical characteristics of the method have been well studied both of which enhance this algorithm's value in the nuclear refueling model.

4.2.2 Dynamic Programming Optimization Procedure

The linear and non-linear algorithms described in the previous section have a great deal in common with each other in the manner in which they move toward optimal solutions. The dynamic programming procedure described in this section is very different from both of these although some similarities to the multi-stage non-linear optimization do exist. The objective function solved by the dynamic programming approach is identical to Eq. (4.1), repeated here for convenience.

$$\text{Min } \overline{TC} = \text{Min } \sum_{i=1}^{I} C[x(i), \epsilon_i, f_i] \qquad (4.8)$$

The dynamic programming approach divides the planning horizon into stages, in this case the selection of each cycle as a stage is quite appropriate since the decisions to be optimized must be made at the beginning of each cycle.

At each stage the algorithm surveys all alternative decisions that can be made before proceding to the next stage. When it performs this survey, to be described in detail in Section 4.3.3, it searches out those decisions which tend to minimize the costs incurred up to the stage in question and those decisions which will minimize future costs. In this manner the dynamic programming approach can handle the coupling of decisions between the cycles.

If all the combinations of all the decision variables were calculated, an exhaustive search, indeed the optimal refueling strategy would be found but this strategy might have taken many hours of computer time to find. The goal of the dynamic programming approach is to recognize that only certain combinations of decision variables, referred to as paths, at each stage of the solution are optimal, and to selectively reduce the computing burden by dropping the non-optimal paths.

Only the general characteristics and operating procedures of the dynamic programming approach to the nuclear refueling optimization problem will be presented in this section for the remainder of this chapter is devoted to a detailed description of the dynamic programming approach used for this study.

At each stage the decision variables are discretized in batch fraction, f, but left continuous in enrichment, ε. For the purposes of this discussion a path is designated by a unique combination of reload batch fractions for each cycle that the path has traversed. For example, the path $\bar{P}(f_1,f_2,f_3)$ designates a nuclear fuel strategy that reloads the reactor with batch fractions f_1 in cycle 1, f_2 in cycle 2 and f_3 in cycle 3. Each path represents a feasible set of reload decision parameters. That is, each path produces the required energy during each cycle and does not violate the constraints on power peaking or average discharge burnup.

The optimization procedes as follows for each cycle i:

1) Calculate the cost of each path that was considered through the i-1 cycle.

$$\overline{TC}_p = \sum_{j=1}^{i-1} C(f_j) \quad \text{For all paths p} \tag{4.9}$$

2) Evaluate the additional costs of traversing cycle i by means of all of these paths and all of the feasible decisions in cycle i. Calculate the value of the state of the reactor for each path at the end of cycle i.

3) Based on step 2, select only a few quasi optimal paths, referred to as the n-best set.

4) Perform the state transformation calculation, see Section 2.5, Eq. (2.5).

$$x(i + 1) = G[x(i), \epsilon_i, f_i] \qquad (4.10)$$

5) Calculate the revenue requirement, C_i, for this transformation, Eq. (4.10), and add it to the total path costs TC_p which were calculated in step 1.

6) If $i + 1 \neq I$, the last cycle in the planning horizon return to step 2 and do steps 2, 3 and 4 for cycle $i + 1$.

7) From among all paths considered through the entire planning horizon, select the optimal, minimum cost path.

The state transformation equation, Eq. (4.10), can be calculated by any in-core nuclear fuel simulator from a three dimensional spatial simulator to a single correlation equation depending upon the accuracy desired. All previously accumulated insights regarding nuclear fuel economics are put to use in steps 2 and 3. These insights can be in the form of correlations to previously accumulated data or in the form of general guidelines that point toward optimal future strategies. See Section 4.3.3 for

a detailed description of some of these insights and their uses in the dynamic programming algorithm.

The dynamic programming, D.P., approach was chosen for the nuclear fuel optimization model to be used in the overall Nuclear Power Management Model, see Section 2.2, for the following reasons:

1) The D.P. approach requires little computation time itself. It is limited by computer storage space only if a very large number of paths must be contained in the n-best set, the sub-optimal set for which in-core simulations are performed at each cycle.

2) The majority of the computation time used by this algorithm is devoted to performing the simulation of the nuclear fuel decisions. However, if the number of in-core simulations required at each cycle, i.e. if the n-best set is less than 10, the D.P. algorithm can use an accurate multi-dimensional in-core simulator. For this first study of nuclear in-core simulation and optimization this accuracy was essential to drawing valid conclusions.

3) The coupling effects between decisions in different cycles can be minimized by correctly evaluating the fuel in the reactor at the end of each cycle. The D.P. algorithm is ideal for exploiting this decoupling.

4) The D.P. approach can be significantly improved with additional experience. Information regarding general trends in the optimization can be readily incorporated into the evaluation performed in steps 2 and 3 above. This flexibility in the D.P. approach can significantly improve its performance in future optimizations.

The limiting factor in the use of the dynamic programming approach will be the time consumed by the in-core simulator. If the n-best set required to obtain reasonable results is very large the amount of computer time used in simulating the refuel decisions becomes prohibitive.

4.3 The Application of Dynamic Programming to the Nuclear Refueling Optimization Problem

After the selection of the dynamic programming approach the nuclear refueling optimization problem was formulated in a more specific way than outlined in the previous section in order to take full advantage of the D.P. procedure. This problem formulation will be described in Section 4.3.1.

Besides adequately formulating the refueling problem, specific nuclear fuel depletion and nuclear fuel economic information must be developed to aid the D.P. algorithm. A typical pressurized water reactor of the Zion-I type was chosen as an example reactor and the development of this information for this reactor is described in Section 4.3.2. The use of this information by the D.P. algorithm is discussed in Section 4.3.3.

4.3.1 The Dynamic Programming Procedure

For the linear and non-linear optimization techniques described in Section 4.2 the objective functions, Eq. (4.2) and Eq. (4.4) respectively were continuous in both decision variables enrichment ε and batch fraction, f. Due to physical limitations on nuclear fuel and also to the limitations of the in-core simulator it is necessary to formulate the D.P. algorithm for the nuclear refueling optimization problem in terms of discrete values of the batch fraction f. The physical limitation alluded to is the fact that nuclear fuel is loaded and unloaded by assembly where each assembly is about 0.5% of the total fuel in the reactor. This discrete nature of loading nuclear fuel gives some justification to discretizing f in the D.P. optimization. However, the major reason for discretizing f is the fact that any in-core simulation used in conjunction with the dynamic

optimization becomes increasingly more time consuming as the number of permissible batch fractions increases. This increase is due to the fact that the coarse mesh point in-core simulations require more and more mesh points as the batches of fuel in the reactor become smaller and smaller. As the number of mesh points used to model a reactor increases so also does the computation time required for each cycle calculation. The enrichment variable, ε, however, is continuous throughout the entire optimization.

The dynamic optimization as proposed here finds the optimal reload batch fraction strategy. Since the energy to be produced in each cycle and the state of the reactor at the beginning of the planning period are given the selection of a batch fraction, f_i, for each cycle uniquely determines the enrichment, ε_i, needed to achieve E_i. As a result of this unique coupling between ε_i and f_i the optimization of one variable optimizes both of these decision variables. The nuclear refueling optimization discussed from this point on optimizes the single variable batch fraction, f_i.

Figure 4.1, The Nuclear In-Core Simulation and Optimization Model, describes the various calculation models which perform the nuclear refueling dynamic optimization. The In-Core Simulator performs the state transformation

Figure 4.1

THE NUCLEAR IN-CORE SIMULATION AND OPTIMIZATION MODEL

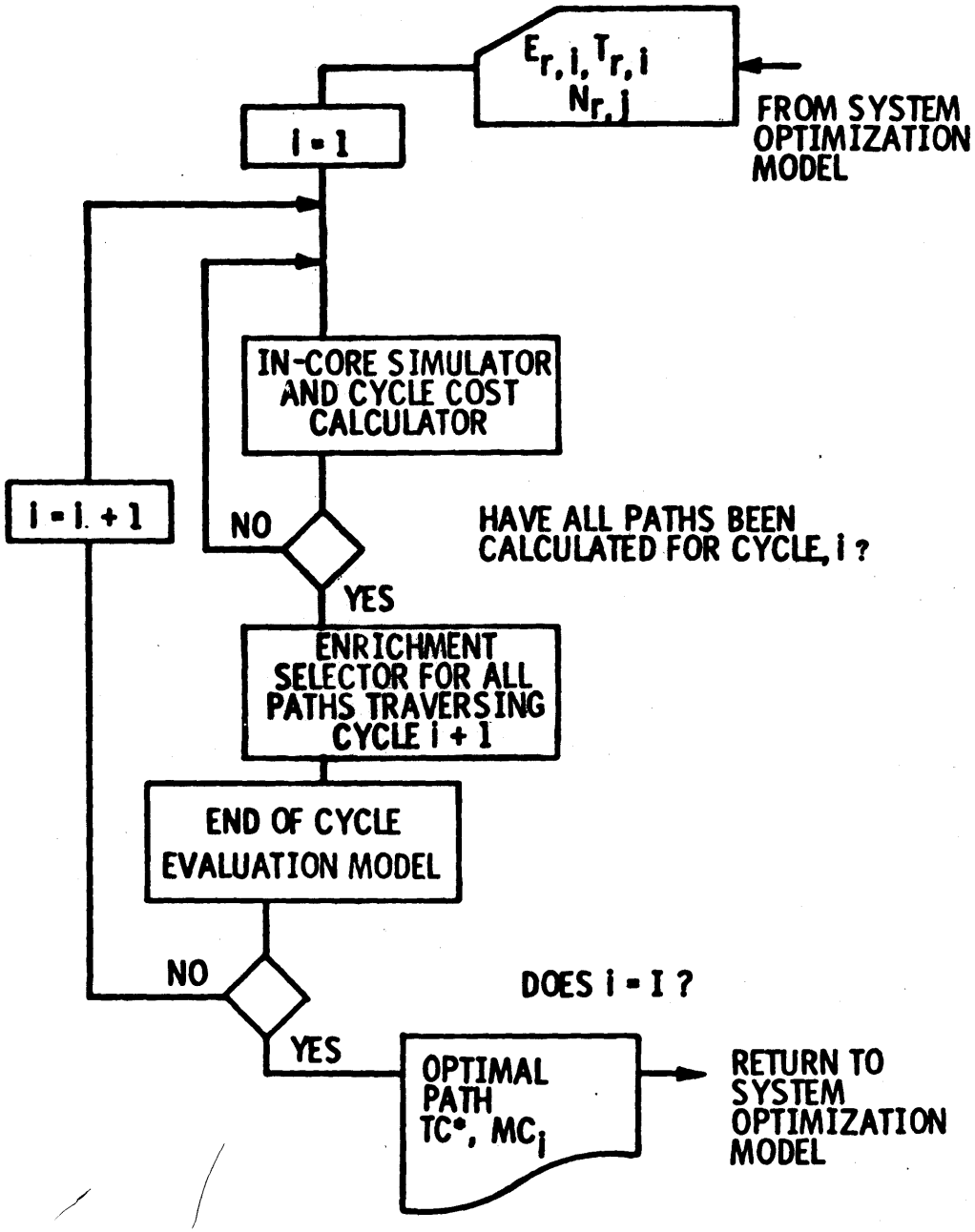

$$x(i + 1) = G[x(i), \varepsilon_i, f_i] \qquad (4.11)$$

which is step 4 in the dynamic programming dexcription outlined in Section 4.2.2. This In-Core Simulation performs the fuel depletion from the beginning of any cycle or from the middle of a cycle if the reactor refueling cycle had commenced prior to the beginning of the planning horizon. The costs incurred by each path traversing cycle i are calculated by the Cycle Cost Calculator. This calculation is step 1 of the D.P. description. The Enrichment Selector estimates the reload enrichments, ε_{i+1}, needed to achieve E_{i+1} for all feasible f_{i+1} for each path leaving cycle i.

The End-of-Cycle Evaluation Model in Figure 4.1 is the heart of the D.P. algorithm. The End-of-Cycle Evaluation model performs the evaluations required by steps 2, 3 and 6 in the D.P. description. This end of cycle evaluator decouples the decision variables in one cycle from decisions in all other cycles, which is essential to the D.P. approach to nuclear refueling optimization. This can be seen by stating Belman's Principle of Optimality which is the foundation of all dynamic programming:

> "An optimal policy has the property that whatever the initial state and initial decision are, the remaining decisions must institute an optimal policy with regard to the state resulting from the first decision" (3).

Dynamic programming uses this principle to find the optimal policy, a strategy of reload batch fractions, in the following fashion*. If the optimal path to stage i is known then the remainder of the stages can be optimized and the optimal policy found regardless of the decisions made in stages previous to i. However, if the fuel in the reactor for each path can be accurately evaluated with respect to its future economic potential in the reactor then all paths can be compared at the end of stage i-1 and the optimization can enter stage i knowing the optimal policy to that stage. If this can be done at the end of each stage a very straight forward dynamic optimization utilizing Belman's Principle produces the optimal fuel reloading policy. Since the nuclear refueling decisions at stage i effect energy production and consequently costs in future cycles these decisions unfortunately can not be fully assessed until many cycles into the future. As a result the optimal policy entering stage i is not known if cost calculations have been made only through cycle i-1. Belman's Principle of Optimality does not hold true.

An end of cycle evaluation model was developed to evaluate the future energy producing (and, therefore, economic) potential of the fuel in the reactor at the end

---

* A path is defined as the specification of a unique combination of the decision variable, batch fraction, that has supplied the required energy and brought the reactor to its present state.

of a cycle. The model is based on two evaluations.

1. The book value of the fuel in the reactor at the end of each path entering a cycle as defined by Eq. (3.8), Section 3.2.3.2.
2. The estimation of the cost of producing E_i by all feasible reload batch fractions, f_i, for all paths entering cycle i, $CE_{p,i}$, see Section 4.3.3.

These two evaluations partially decouple the effects of previous decisions on cycle i and subsequent cycles but cannot totally decouple them. Consequently more than one path is evaluated through each cycle.

The paths which are calculated through each cycle are referred to as the n-best set of paths. The number of paths n is chosen by experimentation such that the optimal policy will not be discarded by the end of cycle evaluator.

One very important aspect of the dynamic programming approach which shall now be discussed is the effect of constraints on the optimization.

As has previously been discussed, Section 2.2.1, the constraints of paramount concern in the nuclear fuel optimization problem are the power peaking in the core throughout the life of the core and the average discharge burnup of the fuel. Both of these constraints can be violated in any

cycle i as a result of decisions in previous cycles. This can be readily seen in the case of the discharge burnup constraint. Fuel that is loaded in cycle i-3 might be discharged at the end of cycle i with a burnup greater than the maximum permissible burnup. As a result of the violation of this burnup constraint in cycle i that path is eliminated from further consideration. Now, however, consider the possibility, not at all remote, that this offending path was the optimal path up to cycle i. Its elimination would result in the D.P.'s selection of the next best path with which to traverse stage i. If stage i was entered with only one path, the optimal policy through i-1 stages, then the next best path could only be a path with a different reload batch fraction in the i^{th} cycle, f_i. However, the real cause for the violation of the burnup constraint was the fuel loaded into the reactor in cycle i-3 so that it is f_{i-3} that should be altered in the optimal path and not f_i. In this manner carrying only one path from cycle to cycle prevents the correct handling of the physical constraints. Irrespective of the accuracy of the economic evaluations performed at the end of each cycle, consideration of the physical constraints which may be violated several cycles in the future, forces the optimization procedure to carry more than one or two paths in the n-best set.

4.3.2 Data Accumulation to Aid the D.P. Optimization

All of the optimization procedures mentioned in Section 4.2 require the collection and processing of operational information on the nuclear reactor being optimized. The operational information required consists primarily of data on the effects of the decision variables, ε_i and f_i or energy production and cost under as wide a range as possible of initial conditions, the state of the reactor, N(r,i). Once collected this information is used by each of the different optimization procedures to perform different functions. For example, in the non-linear single stage optimization a set of analytic functions would be derived from these data that span and tie together the entire planning horizon. In the D.P. approach the data are used in a much more limited way. The D.P. algorithm uses this operational information to relate the decision variables to energy production and cost for only one cycle at a time.

In general, this operational information is reduced to two different forms for use by the optimization routines. It is either arranged in tabular form and then referred to by the optimization routine when data are required from it or it is correlated to functional form for use in the optimization. For the dynamic programming approach described in this report correlations to precalculated opera-

tional data by least-squares polynomial fits were used at each stage to increase the efficiency of the optimization.

4.3.2.1 The Use of Precalculated Data by the Dynamicc Program

As an example of what data are required and how it is used by the dynamic program a sample reactor was modelled in a format amenable to a dynamic programming optimization. The reactor chosen was of the Zion-I type, a pressurized water reactor designed by Westinghouse and operated by the Commonwealth Edison Co. of Chicago, see Appendix E. Referring to Figure 4.1, the Nuclear In-Core Simulation and Optimization Model, the first need for pre-calculated information is for an Enrichment Selector. This Enrichment Selector must choose the enrichment, ε_i, necessary to produce the required energy E_i. The state of the reactor at the end of the previous cycle, N(r,i), is known. Recall that the dynamic program is dealing only in discrete values of batch fraction. This significantly reduces the burden on the enrichment selector for it need only predict the enrichment for the discrete values of f available to the optimization and not for a continuous spectrum of f's. This being the case, a separate predictive correlation can be found for each value of f. The problem now reduces to finding ε_i, given N(r,i), E_i and f_i, remembering that separate but similar functions will be found for each value of f being considered by the optimization.

The state of the reactor at the beginning of stage i, N(r,i), and the reload batch fraction f_i are known and the fuel are also given by the selection of a refueling and shuffling procedure (see Section 3.2.2.2 for a detailed description of the fuel handling procedures used by the in-core simulator, CORE).

Empirically, two very simple calculated parameters describing the remaining fuel in the reactor were developed to predict very effectively the required enrichments. These parameters are the average fissile enrichment, εII, and the average discharge burnup, BII, of the remaining fuel, the (1-f) fraction of the nuclear fuel in the reactor. εII, the average fissile enrichment, is defined to be:

$$\varepsilon II \equiv \frac{M(U\text{-}235)+M(Pu\text{-}239)+M(Pu\text{-}241)}{\text{Total Uranium and Plutonium Mass}} \qquad (4.12)$$

where:

M(X) is the mass of isotope X.

εII, the average fissile enrichment of the 1-f fraction of the fuel, is a measure of the potential number of energy producing fissions that could occur during the cycle. BII, the average burnup of the 1-f fraction of the fuel, is a measure of the amount of fission product poison build up in the fuel which will decrease the energy production by the reactor during the cycle.

For each f sixteen different data points relating ε_i, E_i, εII and BII were calculated for the Zion reactor, and a least squares polynomial fit procedure was used to determine the correct terms to be used and coefficients of these terms that relate these variables. The procedures used were standard data analysis procedures (4) where the validity of the correlations are measured by the correlation coefficient, the multiple linear correlation coefficient etc. See Appendix D, the Zion Reactor Data Correlations for a further discussion of this curve fitting procedure. Table 4.1 shows the equation resulting from this fitting procedure used by the enrichment selector to predict the enrichments ε_i to produce energies E_i for a batch fraction of 0.29.

The End-of-Cycle Evaluation Model shown in Fig. 4.1 and described in the next section of this report requires cost predictions at the beginning of each stage on the basis of which it selects the n-best paths for this stage. The information required is the estimated cost, $CE_{p,i}$, of producing the cycle energy, E_i, for all feasible paths p that could traverse cycle i. This information was calculated in the same manner as the data for the enrichment selector. Again, the information was calculated for each value of f independently. For example, for f = 0.25, for varying reactor states εII and BII and for various energy requirements E_i a number of CORE cycle calculations were performed and the cost of producing E_i in each case was calculated by

Table 4.1

Sample Set of Equations, for f = 0.29,
Calculated by Least Square Polynomial Fitting
for the Zion-I Reactor

$$\varepsilon_i = 3.97173 - 2.35004 \cdot \varepsilon II - 0.438245 \cdot \varepsilon II^2 + 0.506433 \times 10^{-3} \cdot E_i + 0.377401 \times 10^{-10} \cdot \varepsilon II \cdot E_i^2 + 0.148358 \times 10^{-3} \cdot BII$$

$$BU\$ = -0.555231 \times 10^7 + 0.194353 \times 10^7 \cdot \varepsilon_i - 0.595997 \times 10^5 \cdot \varepsilon_i^2 + 0.0504968 \times 10^3 \cdot E_i - 0.836234 \times 10^2 \cdot E_i \cdot \varepsilon_i + 0.236018 \times 10^{-2} \cdot \varepsilon_i \cdot E_i^2 + 0.168889 \times 10^7 \cdot \varepsilon II$$

$$FAR\$ = 0.611091 \times 10^7 + 0.279393 \times 10^8 \cdot \varepsilon II - 0.15666 \times 10^8 \cdot \varepsilon II^2 - 0.882404 \times 10^4 \cdot E_i + 0.52623 \times 10^4 \cdot E_i \cdot \varepsilon II - 0.243165 \times 10^{-1} \cdot \varepsilon II^2 \cdot E_i^2 - 0.111516 \times 10^7 \cdot E_i$$

$$\frac{\partial \varepsilon_i}{\partial E_i} = 0.506433 \times 10^{-3} + (2.0) \cdot (0.377401 \times 10^{-10}) \cdot \varepsilon II \cdot E_i$$

Table 4.1

(Continued)

$$MC_i = \frac{\partial BU\$}{\partial E_i} = 0.194353 \times 10^7 \cdot \frac{\partial \varepsilon i}{\partial E_i} - (0.595997 \times 10^5)$$

$$\cdot (2.0) \cdot \varepsilon_i \cdot \frac{\partial \varepsilon i}{\partial E_i} + 0.504668 \times 10^3 - 0.836234 \times 10^2$$

$$\cdot (\varepsilon_i + E_i \cdot \frac{\partial \varepsilon i}{\partial E_i}) + 0.236018 \times 10^{-2} \cdot (2 \cdot \varepsilon_i \cdot E_i + E_i^2 \cdot \frac{\partial \varepsilon i}{\partial E_i})$$

CYCOST, see Chapter 3. The costs were calculated for a constant cycle time T_i, equal to 1.05 yrs. This simplification reduced the number of variables required in the correlation and introduces no substantial error into the end of cycle evaluation. This is due to the fact that the end of cycle evaluation uses the estimated costs for only one cycle at a time. Since the duration T_i of each cycle is fixed for each path traversing that cycle, the evaluator is never comparing estimated costs for cycles of different durations.

The nuclear fuel cycle cost was divided into two separate portions, those costs incurred due to burnup of uranium and plutonium in the cycle and those costs associated with fabrication, reprocessing, shipping and conversion. Eq. (3.7) for the nuclear fuel cycle revenue requirements as repeated here for convenience is the same for both the burnup and fixed portions of the cost.

$$C_i = \sum_{k=1}^{NOZONE} \frac{1}{1-\tau}[Z(k,t_1) - PVEOC\cdot Z(k,t_2) - \tau(Z(k,t_1) - Z(k,t_2))\cdot PVE] \qquad (4.13)$$

However, the value of the fuel, Z(k,t), in batch k at time t is different for each portion of the cost. Namely, for the burnup portion Z(k,t) is taken to be the value of the uranium and plutonium in batch k at time t. For this

value of Z(k,t), C_i in Eq. (4.13) becomes the cycle burnup cost, referred to as BU$.

For the other costs Z(k,t) is taken to be the undepreciated portion of fabrication, reprocessing and conversion payments for batch k at time t. For this value of Z(k,t), C_i in Eq. (4.13) becomes the fixed cost component, FAR$ of the nuclear fuel costs for cycle i.

Typical equations resulting from the fitting of precalculated costs for BU$ and FAR$ are shown in Table 4.1 for f = 0.29335.

The accuracy of all three of the correlation equations for each f can be measured by the ratio of the value of the parameter calculated by the polynomial fit, V_c, to the actual value, V_a, of the data point,

$$\text{Agreement} = \left(\frac{V_c}{V_a}\right)\cdot 100 \qquad (4.14)$$

The average agreement of calculated enrichments to the actual data was 99.3%. For BU$ this agreement was 99.6% and for FAR$ the accuracy was 97.1%. The significant decrease in the accuracy of the fixed cost, FAR$, correlation is due to the failure of the average parameters εII and BII to adequately account for the distribution of energy production amongst several batches of fuel in the inner, the 1-f, region of the reactor core.

The range of enrichments used to generate the data for all of these correlation fits was from 2.25 w/o to 4.5 w/o. Reload batch fractions, f, were varied from 0.25 to 0.37 and the cycle energy produced varied from 250 GWD/cycle to 450 GWD/cycle.

There is one further parameter which the nuclear refueling optimization procedure must generate. That is the incremental cost, MC_i, of changing the energy E_i in each cycle of the optimal path. MC_i is required by the system optimization model, see Section 2.4, Figure 2.3, so that it can reallocate the nuclear potential required by the system amongst all the nuclear plants on the system. If TC* is the total cost of the optimal policy, the change in TC* due to a change in E_i can be considered in two parts ... the change in materials or burnup costs and the change in the service costs of fabrication reprocessing and conversion which are independent of each other, thus,

$$MC_i = \frac{\partial(\text{Total Burnup Costs})}{\partial E_i} + \frac{\partial(\text{Total Service Costs})}{\partial E_i} \qquad (4.15)$$

The total service costs are independent of the energy extracted during cycle i, so that the second partial derivative is equal to zero. In addition, Watt (37) has found that

most of the effect on cost due to varying cycle energy occurs in the cycle where the energy was changed so that

$$MC_i = \frac{\partial(\text{Total Burnup Costs})}{\partial E_i} \cong \frac{\partial(\text{Burnup Costs})_i}{\partial E_i} \qquad (4.16)$$

The error in MC_i as calculated by Equation (4.16) was found to be less than 6% where the fuel value is based on its uranium and plutonium content.

In practice since only a minimum of four assemblies (about 2% of the total fuel) can be removed at a time from the reactor, one from each quadrant, small changes in cycle energy demand would be met by varying the reload enrichment. Consequently, MC_i in Equation (4.16) should be calculated at constant batch fraction.

The incremental costs, MC_i^*, of the optimal path required by the system optimization model can readily be calculated at constant f using the correlation for BU$ to represent the cycle burnup costs. Differentiation of the BU$ equations for each f yields expressions for MC_i. Table 4.1 includes an example of an MC_i equation for f = 0.29.

4.3.3 The End-of-Cycle Evaluation

It is in the end-of-cycle evaluation where all insights into nuclear refueling costs must be put to use. This evaluation model in the nuclear refueling optimization

procedure chooses the best paths at the end of each cycle that shall be considered in future cycles.

This model first checks that no physical constraints have been violated by the paths that were simulated during the cycle. Figure 4.2, The End-of-Cycle Evaluation Model begins with this elimination of any of the paths, p, that were calculated through the i^{th} cycle which violated the burnup or power peaking constraints in the i^{th} cycle. Recall that the Enrichment Selector in the Nuclear In-Core Simulator and Optimization Model, Figure 4.1, has already estimated the reload enrichments ε_{i+1} needed to achieve E_{i+1} for all feasible f_{i+1} for each path leaving cycle i. This results in the expansion in the number of paths to p'.

$$p' = n \cdot m \qquad (4.17)$$

where:

n is the number of paths that were calculated through the i^{th} cycle, referred to as the n-best paths and

m is the number of f's being surveyed in the optimization.

For example in the sample problem, Chapter 5, the number of f's being surveyed by the optimization is 4 and n is 5 resulting in 20 new paths, p', being evaluated by the end-of-cycle evaluator.

Figure 4.2 The End-of-Cycle Evaluation Model

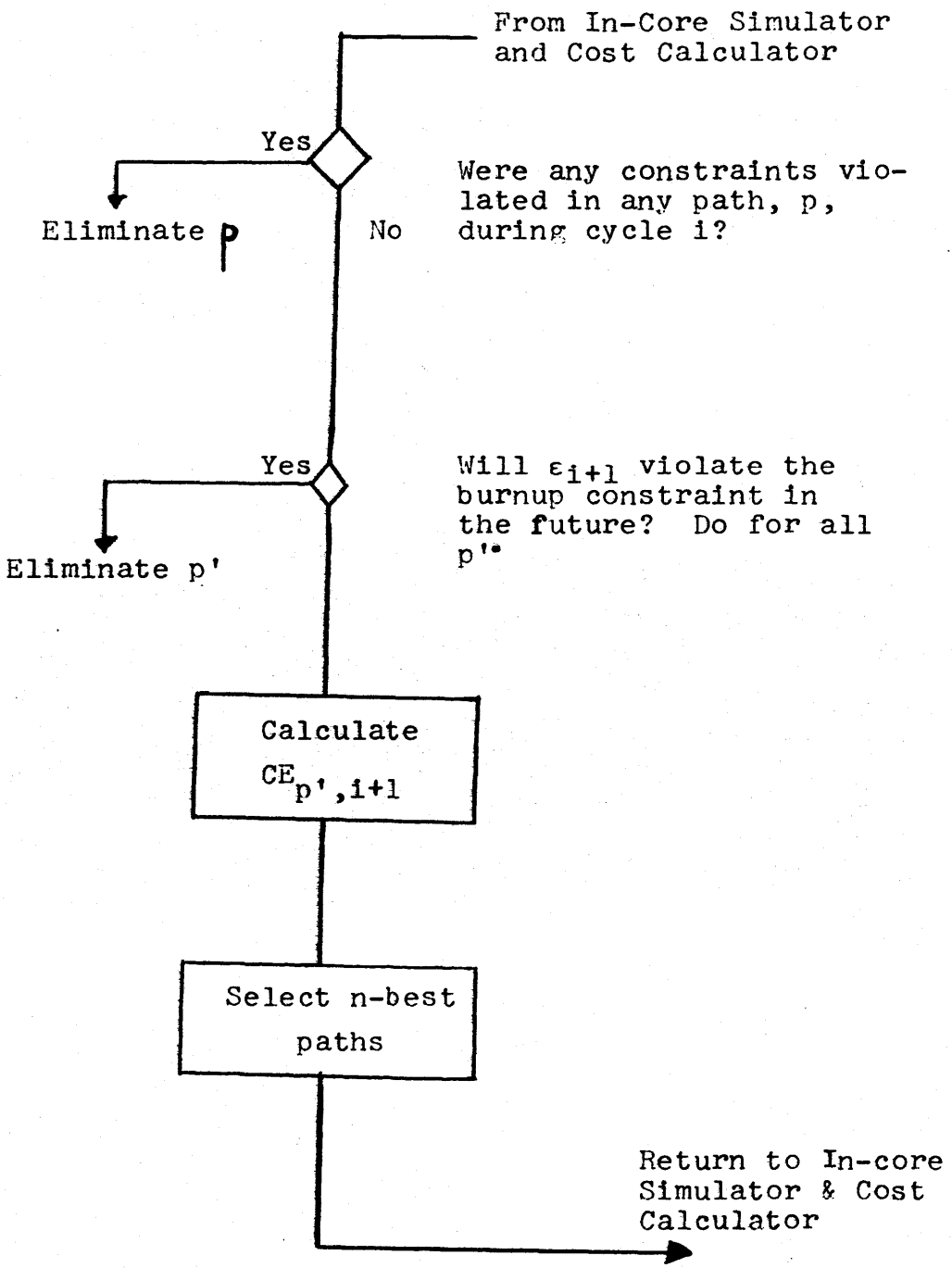

In order to minimize the possibility of carrying within the n-best set any path which will violate the maximum discharge burnup in future cycles the end of cycle evaluator estimates the average discharge burnup for the enrichments ϵ_{i+1} for all paths p'. This estimate is made using a correlation of the reload enrichment ϵ_k with the average discharge burnup B_k for many various modes of operating the Zion reactor that was derived using a least squares polynomial fit to both of these variables:

$$B_k = -2919.25 + 10789.3 \cdot \epsilon_k \qquad (4.18)$$

The effect of the reload batch fraction on this prediction of B_k is less than 5% over the range of interest in batch function, 0.25 to 0.37.

Furthermore, this equation always slightly underestimates B_k so that eliminating any ϵ_{i+1} using this equation will always be a conservative elimination. If the limit on average discharge burnup is 50,000 MWD/T the maximum allowable reload enrichment is 4.905 w/o.

At the end of cycle i the revenue requirement $\sum_{j=1}^{i} C_{j,p}$ for producing energy in cycles 1 through i have been calculated by the CYCOST code for all paths p. In order to increase the optimizations consideration of future energy production from all paths p', all the progeny of p, an

estimation is made of the revenue requirements, $CE_{p',i+1}$, for the (i+1)st cycle for all p' paths. $TCE_{p'}$, Equation (4.19), is the sum of these revenue requirements for all p' paths and is the basis for the first comparison of paths by the End-of-Cycle Evaluator.

$$TCE_{p'} = \sum_{j=1}^{i} C_{j,p} + CE_{p',i+1} \tag{4.19}$$

The second comparison of the p' paths is made on the basis of

$$TVE_{p'} = \sum_{j=1}^{i} C_{j,p} - V_{p,i} + CE_{p',i+1} \tag{4.20}$$

$$= TCE_{p'} - V_{p,i}$$

where:

$V_{p,i}$ is the book value of the reactor fuel at the end of the i^{th} cycle as defined by

$$V_{p,i} = \sum_{k=1}^{K} Z(k,t_2) \tag{4.21}$$

where:

$Z(k,t_2)$ is the value of the fuel in batch k at the end, t_2, of cycle i, see Equation (3.8), and

K is the total number of batches of fuel in the reactor during cycle i.

$V_{p,i}$ is a measure of the future (over many cycles) energy producing capabilities of the fuel in the reactor for path p' at the end of cycle i. It does consider all the uranium and plutonium in the fuel but does not reflect the negative effects of the fission product poisons in the core.

The economic significance of $TVE_{p'}$ can be seen if a more detailed consideration is made of Equation (4.20). As was mentioned $\sum_{j=1}^{i} C_{p',j}$ is the revenue required by path p' through cycle i. However, if the value $V_{p',i}$ at the end of cycle i differs from V_o, the value of the fuel in the reactor at the beginning of the planning period , an additional cost is incurred which is not reflected in the revenue requirements. Let us refer to the net costs for path p' over the period from the beginning of the horizon to cycle i as $\sum_{j=1}^{i} C_{j,p} - (V_{p,i} - V_o)$. For the purpose of comparing net costs among all p paths that originated with equal V_o's the V_o can be dropped. Adding the estimated revenue requirements, $CE_{p',i+1}$, for the next cycle to the net costs of all paths p' over i cycles yields the net costs for all paths over i+1 cycles assuming that $V_{p',i+1}$ equal $V_{p,i}$. Therefore, comparing paths on the basis of $TVE_{p'}$, Equation (4.20), is tantamount to comparing the net costs for these paths over i+1 cycles of the planning period.

Both $TCE_{p'}$ and $TVE_{p'}$ are used in the comparison of paths by the End-of-Cycle Evaluator because it is not clear how much weight to give to future, $V_{p,i}$, considerations. If $V_{p,i}$ were shown to be a complete evaluation of future energy producing potential, then only $TVE_{p'}$ would be appropriate for comparing paths. But this can not be shown nor is it at all likely that $V_{p,i}$ is that complete measure of future potential desired. This weighting is achieved by arranging all paths in order of ascending values of $TCE_{p'}$ and $TVE_{p'}$ and giving each path a ranking R in each set. The n-best paths are selected by combining the rankings of each path p' in both the $TCE_{p',i+1}$ and the $TVE_{p',i+1}$ orderings. A combined ranking R_s is found by averaging the rank, $R_{cp'}$, in the $TCE_{p',i+1}$ ordering with the rank, $R_{vp'}$, in the $TVE_{p',i+1}$ ordering in the following manner:

$$R_s = W_c \cdot R_{cp'} + W_v \cdot R_{vp'} \qquad (4.22)$$

where:

W_c and W_v are weighting functions and $W_c + W_v = 1$

Experience has shown that the TVE ordering is in fact more accurate than the TCE ordering in evaluating the future worth of a fuel so that the use of a larger value for W_v than W_c is recommended*.

---

* In the examples discussed in Chapter 5 the weighting functions used were: $W_v = 0.6$ and $W_c = 0.4$.

The n-best paths selected by the End-of-Cycle Evaluator are the n paths with the smallest R_s values.

The dynamic programming approach to the nuclear refueling optimization problem with the aid of the correlations developed in this Section for the Zion-I reactor are used to optimize a sample energy production schedule in the next chapter.

5. A SAMPLE OPTIMIZATION PROBLEM

5.1 Statement of the Sample Problem

In order to evaluate the effectiveness of the dynamic programming optimization procedure described in Chapter 4, a realistic sample problem was developed and the D.P. procedure was used to find optimal refueling policies for a single reactor under a variety of conditions. Since the role of the In-core Simulation and Optimization Model in the nuclear power management model is to minimize the cost of producing a specified amount of energy from each reactor on the system over a mid-range planning horizon, the sample problem will be to perform this minimization for one reactor for one set of energies over a planning horizon of six years. As was described in Section 2.4, the Nuclear Power Management Multi-Year Model, the nuclear in-core optimization model is given a set of cycle energies, E_i, and cycle durations, T_i, for each reactor for which an optimal refueling strategy must be found. Consequently, a realistic sample optimization problem must have a set of E_i's and T_i's that reflect the type of schedule that the system optimization model will generate. In some examples he has considered, Deaton (11) has found that the variances in E_i from cycle to cycle can be as large

as 30 percent with variations in the cycle lengths, T_i, from 9 months to as many as 16 months. Consequently the sample problem delineated in Figure 5.1 has a maximum variation in E_i of 28.6 percent, Cycle 2 to Cycle 3, a maximum cycle length exclusive of the refueling time of 16 months, T_2, and a minimum cycle length of 9 months, T_4.

Besides defining a sample problem that might cover a wide range of E_i and T_i vis à vis the overall nuclear power management model, the sample problem was also formulated so that observations could be made on the behavior of nuclear fuel under transient cycle, non-equilibrium cycle, conditions. That is, the E_i's and T_i's were chosen so that the effects of the physical constraints on power peaking and burnup could be observed on the flexibility of nuclear reactors in meeting energy requirements that vary from cycle to cycle.

The reactor selected for the sample problem was the Zion-I, 1060 MWe, PWR, described in Appendix E which was the reactor that the dynamic programming algorithm was modelled to optimize. The cycle energy requirements chosen for the sample problem are listed on Figure 5.1 and plotted on Figure 5.2 to demonstrate the variance in energy demanded of the reactor. Note that the planning horizon covers five cycles but that an end effect calculation covering four more cycles extends the total number of cycles under consideration to nine.

Figure 5.1
THE SAMPLE OPTIMIZATION PROBLEM

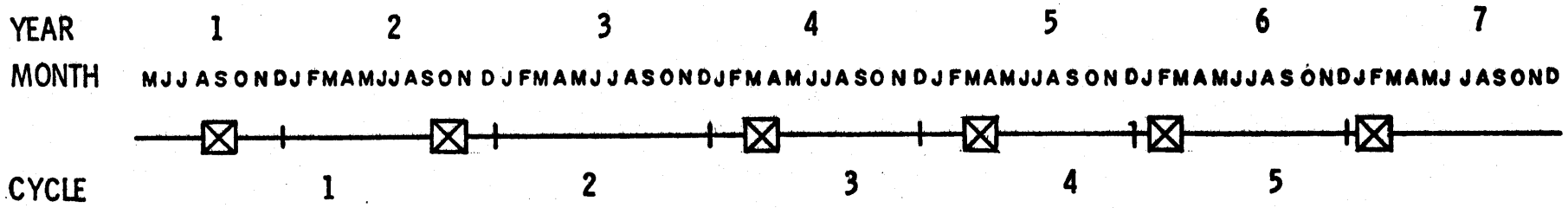

CYCLE i	CYCLE ENERGIES (GWD/CYCLE)	CAPACITY FACTOR	T_i (MONTHS)	REFUELING PERIODS YEAR	DURATION
1	324.4	0.95	11.2	2	SEPT 15 TO NOV 2
2	411.7	0.85	16.0	4	MARCH 2 TO APRIL 16
3	301.0	0.90	11.0	5	MARCH 16 TO MAY 1
4	260.8	0.95	9.0	6	FEB 1, TO MARCH 16
5	279.1	0.90	10.2	7	JAN 22 TO MARCH 7

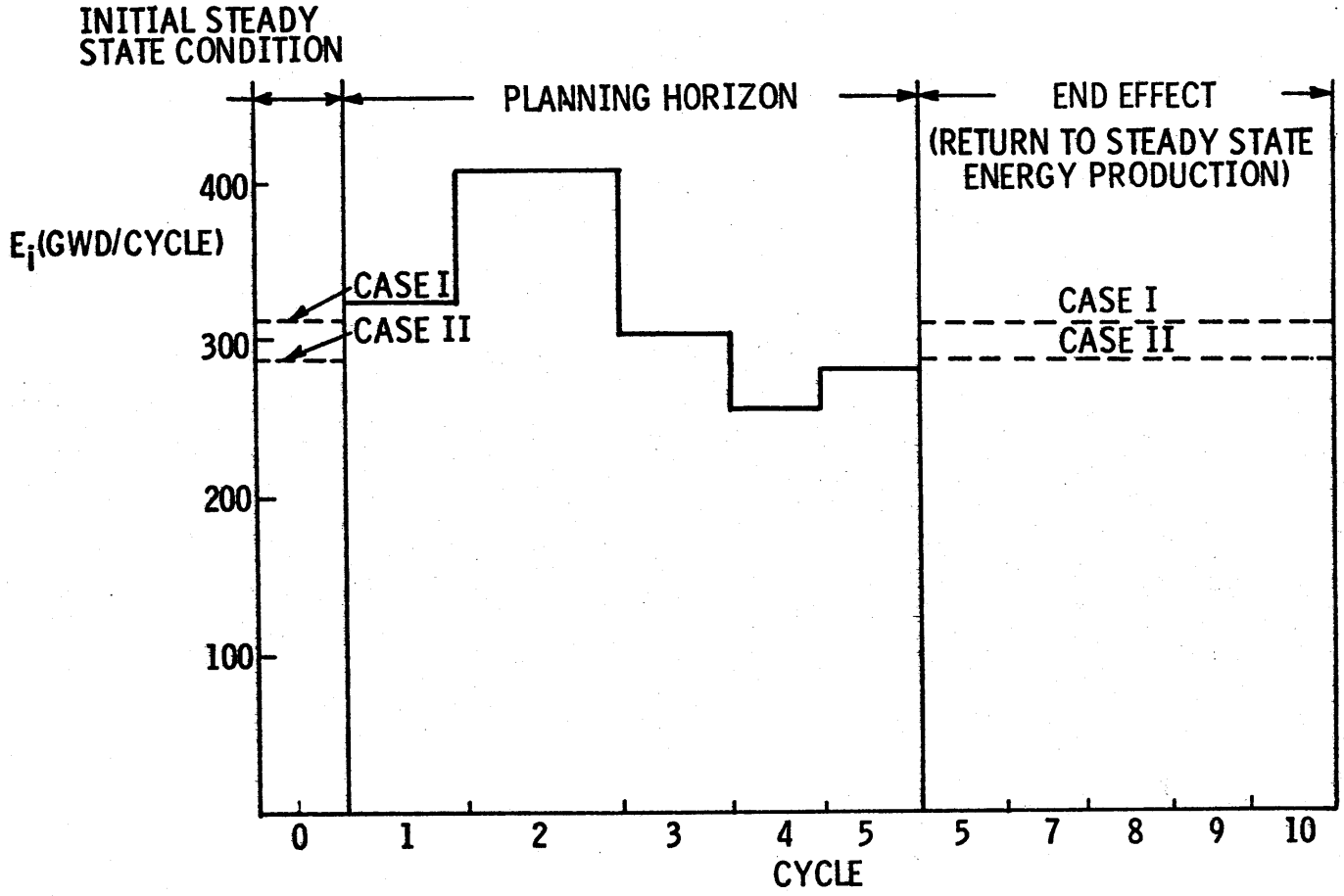

CYCLE ENERGY REQUIREMENTS IN SAMPLE PROBLEM

Figure 5.2

5.2 Planning Horizon End Effect Consideration

In order to find the optimal refueling policy for a reactor, the fuel in the reactor must be evaluated at the end of the planning horizon. Since this study is considering a six year planning horizon in the middle of the life of the reactor and not at the end of the reactor's life this plant will be producing energy in cycles beyond the five for which the mid range plan is being decided. The objective of any end effect calculation is to evaluate the future value of the nuclear fuel in the reactor at the end of the planning horizon. Knowledge of the energy demand on the reactor after the planning horizon would be a great help in this evaluation.

If this energy were known the optimization could be extended two or three more cycles (See Recommendations, Section 7.4). The optimal refueling policy over the planning horizon would then be the path of decisions that minimized costs over the planning horizon plus the additional cycles. Lacking the knowledge of future demand, a reasonable estimate must be made of this demand so that an evaluation of the future worth of nuclear fuel can be made.

For this study the assumption was made that the reactor returns to its initial operating mode at the end of the planning horizon.* If the plant was operating on a three

---

*For future work with nuclear simulation and optimization models that are operated in conjunction with the System Integration and Optimization Models this assumption is not necessary, see Section 7.4.

zone, 3.2 w/o, equilibrium cycle prior to the planning horizon it was forced to return to that operating condition after the planning horizon. This three zone (f=0.33) 3.2 w/o, equilibrium condition was the starting point for Case I, see Table 5.1. The cycle energy produced by the Zion reactor in this equilibrium condition is 306.8 GWD/cycle (10450 MWD/T) on the basis of a reactor fuel mass of 90,066 kg. Assuming annual refueling and a refueling down time of 0.125 yrs the capacity factor during operation implied by this equilibrium energy production is 0.95. This end effect energy production for cycles 5 through 9 is shown by the dotted lines on Figure 5.2.

Case II is the optimization of the same sample problem with initial and final conditions different from Case I. The initial and final conditions for Case II were a four zone (f=0.25), 3.5449 w/o equilibrium cycle, see Table 5.1.

5.3 The Constraints on Power Peaking and Burnup

Power peaking, the ratio of the power at any position in the reactor to the average core power, and the fuel discharge burnup at any point are taken as the limiting operating parameters for nuclear fuel (see Section 2.2.1). In order to operate the plant safely, upper limits are placed on these parameters, referred to as the physical constraints on the optimization. Available evidence indicates that

Table 5.1

Sample Problem Initial and Final Operating Conditions*

	f	ε (w/o)	E (GWD/cycle)	Capacity Factor	Operating Period (months)
Case I	0.33	3.2000	306.8	0.95	10.5
Case II	0.25	3.5449	285.4	0.89	10.5

* These are all equilibrium cycle conditions

behavior of UO_2 fuel remains satisfactory to a maximum exposure of 50,000 MWD/T (8, 38). Anticipating improvements in fuel design and in-core fuel operation in the future, a limit on the average discharge burnup of fuel was set at 50,000 MWD/T for this sample problem. This constraint must be met by each batch and sub-batch of fuel that is discharged from the reactor. A sub-batch is any portion of a fuel batch that is left in the reactor after any other portion of that batch has been discharged (see Section 4.2.2.2.2).

The power peaking in the reactor, however, poses the greatest limitation on reactor core operations and nuclear fuel management as attested to by this 1972 quotation.

> "It is the nature of the nuclear reactor that there is little room for further modification of the fuel management without increasing the peaking factors substantially. All reactors of current vintage are alike in this respect, and the principal factor determining the amount of flexibility available to the operator is simply whatever extra thermal margin may be present in the reactor in question, above that necessary for operation with 'optimum' peaking factors."
>
> J.R. Dietrich and J.M. West (13)
> August 1972

Current nuclear power peaking factors vary from 2.71 (9) to 2.91 (2). The power peaking maximum limit used in this study was 3.3. These higher-than-normal values for power peaking as well as discharge burnup were used in this

study to insure that the economic optimization capabilities of the model were tested as well as its capability to eliminate refueling strategies which violate engineering constraints. As pointed out by Dietrich and West, the ability to manage nuclear fuel in the presence of these constraints is essential if further economic gains from nuclear fuel are to be realized.

5.4 Nuclear Cost Data Used in the Sample Optimization Problem

The nuclear cost data used by the CYCOST routine to calculate the cost of nuclear fuel both in the optimization problem and in the previous accumulation of cost data for the end of cycle evaluation model, Section 4.3.2, are presented in Table 5.2.

The four allowable batch fractions that were selected for use in the sample problems are presented in Table 5.3.

Table 5.3

Batch Fractions Used In The Sample Problem and Their Path Designations

Path Designation	Batch Fraction* f
A	0.37$\dot{3}$
B	0.33$\dot{3}$
C	0.29$\dot{3}$
D	0.25$\dot{3}$

*In the remainder of the text only two digits shall be used for all batch fractions but they will always refer to the batch fractions as listed here.

Table 5.2

NUCLEAR COST DATA USED IN THE OPTIMIZATION PROBLEM (39)

CUF6	Cost of UF_6		23.68 $/kg [based on $8/lb U_3O_8]
CSEP	Separative Work Charges		32.00 $/kg S.W.
CFAB	Fabrication		70.00 $/kg
CRESH	Shipping and Reprocessing		34.57 $/kg
CCONV	Conversion UNH-UF_6		5.60 $/kg
CP	Pu Credit		7.50 $/kg fissile Pu
	Capital Structure	Debt	55% (@ 8%)
		Preferred Stock	10% (@ 8%)
		Equity	35% (@ 13%)
TAUT	Income Tax Rate		52.8%
XRATE	Effective Cost of Money		7.427%
XF	Uranium Feed to Enrichment Process		0.711 w/o
XW	Uranium Tails Assay		0.200 w/o
TAPRE	Time of Payments for Uranium, Enrichment and Fabrication Before Loading Fuel		0.5 years
TPOST	Time After Discharge of Fuel When Credits are Received for Spent Fuel and Reprocessing, Conversion and Shipment are Paid for		0.61 years

In the absence of information on the range of f that would be of economic interest as well as within the region of feasibility, i.e, no constraints violated, these four batch fractions were selected arbitrarily in an attempt to span both of these regions.

All costs discussed in the remainder of this chapter are discounted to the beginning of the planning period

5.5 Results of the Sample Optimization Problem

5.5.1 Case I

With Case I initial and final conditions see Table 5.1, the optimal refueling policy found by the D.P. optimization is presented in Table 5.4. Since all of the optimization calculations for Case I were performed prior to the inclusion of the automatic check for power peaking constraint violations, only the average discharge burnup constraint was considered in this case.

The total nuclear fuel revenue requirements, $\overline{TC}^*$, for the optimal policy are \$51.306 x 10^6. As Table 5.4 indicates the optimal policy tends to meet the energy demanded of the reactor by reducing the batch fraction, f, from the equilibrium initial condition of f = 0.33 with the exception of the second cycle.

In the second cycle the largest reload batch fraction of 0.37 was used in the optimal policy to produce the largest cycle energy demand of 407.7 GWD. In anticipation of the sixth cycle which has a batch fraction of 0.33

Table 5.4

Optimal Nuclear Refueling Policy - Case I

Initial and Final Condition: Three zone equilibrium cycle
3.2 w/o fuel loading: (306.9 GWD cycle)
Path: (C-A-D-D-C)

Cycle i	E_i (GWD/cycle)	Cycle Time (months)	f_i	ε_i (w/o)	MC_i (mills/kwhr)	C_i (10^6\$)	$\sum_{j=1}^{i} C$ (10^6\$)
1	326.3	12.7	0.29	4.2148	1.1706	12.420	12.420
2	407.7	17.5	0.37	3.3687	1.3095	14.447	26.867
3	299.2	12.5	0.25	4.3932	1.4388	9.472	36.339
4	267.5	10.5	0.25	2.8467	1.2077	7.429	43.768
5	285.8	11.7	0.29	3.2650	1.3061	7.538	51.306

E_i = cycle energy demanded by the system

f_i = reload batch fraction for the cycle

ε_i = reload enrichment

MC_i = marginal cost of varying E_i

C_i = discounted cycle cost

$\sum_{j=1}^{i} C_j$ = total discounted cost of the optimal policy through cycle i

Cycle Time includes the 1.5 mo. refueling down time.

and an energy of 306.9 GWD to conform to the final condition constraint, the batch fraction in cycle 5, 0.29, has increased from the 0.25 level of cycles 3 and 4.

In order to demonstrate the competition amongst various feasible paths, Figure 5.3 shows the difference in total discounted cost for various sub-optimal paths, $\overline{TC}_i$, and the optimum path $\overline{TC}_i^*$ as a function of the cycle i. A complete listing of all calculations performed for this study is given in Appendix 4. $\overline{TC}_i$ is defined as

$$\overline{TC}_i = \sum_{j=1}^{1} C_j \qquad (5.1)$$

The notation used to distinguish the paths is based upon the path designations listed in Table 5.3. For example, the path $\overline{P}$(D-A-C) denotes a path that has traversed three cycles where it was reloaded with batch fractions of 0.25 in the first cycle, 0.37 in the second cycle and 0.29 in the third cycle. Figure 5.3 shows that some paths, eg., $\overline{P}$(B-B), $\overline{P}$(B-A), quickly diverge from the optimal and are never really in the competition. Those in the competition are usually within a few hundred thousand dollars of each other. Examples of paths which were terminated due to a violation of the average discharge burnup constraint were $\overline{P}$(D-A-C) at 50,346 MWD/T, $\overline{P}$(D-A-B) at 50,976 MWD/T and $\overline{P}$(D-D-D-D) at 58,261 MWD/T. X's in Figure 5.3 denote paths eliminated by the burnup constraint and O's signify paths

---

* Indicates optimal policy.

Figure 5.3

THE DEVIATION OF SUB-OPTIMAL PATHS FROM THE OPTIMAL POLICY - CASE I

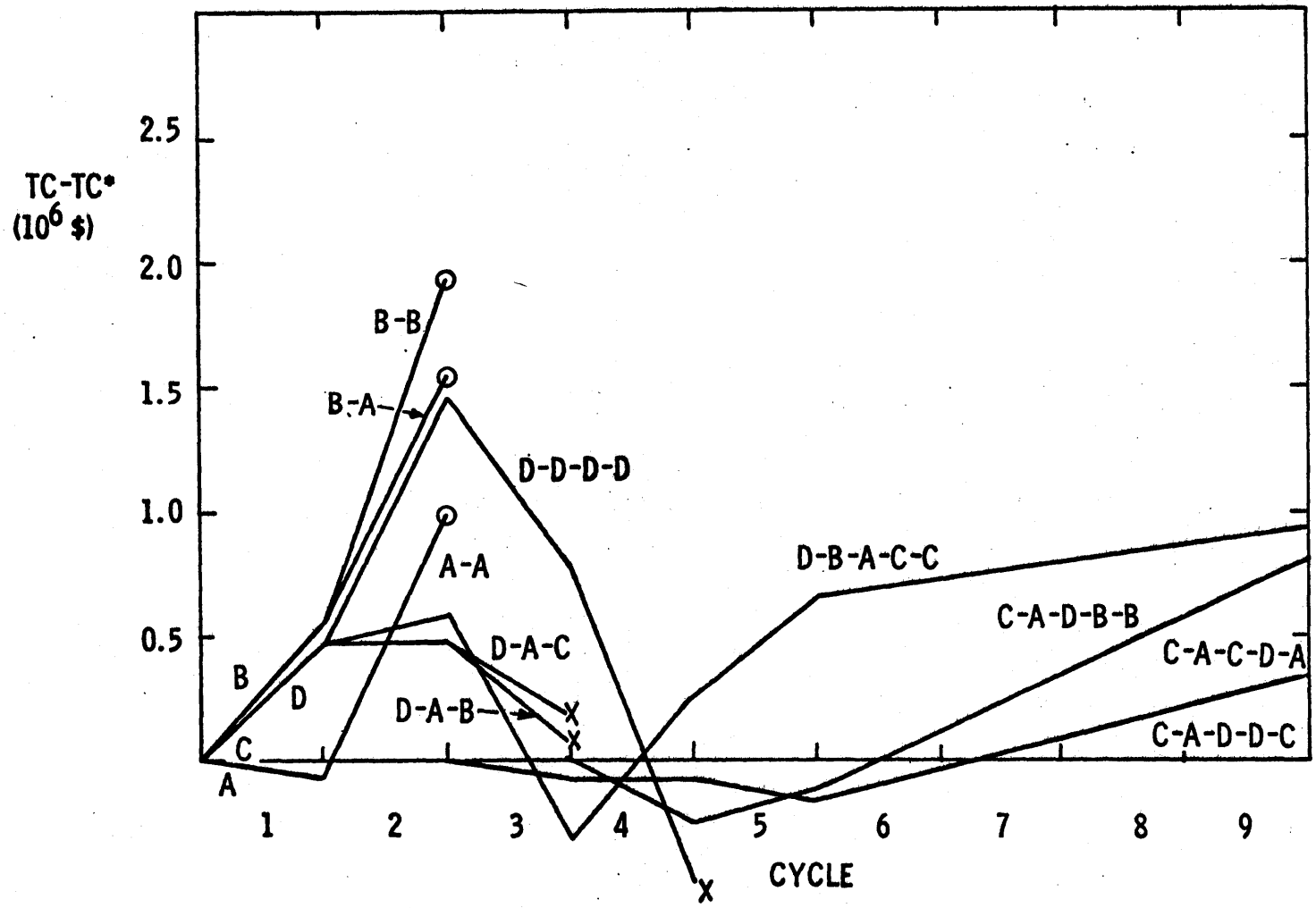

eliminated on economic grounds.+

Although paths of constant f, e.g. $\bar{P}$(A-A-A-A-A) were eliminated by the optimization procedure by the end of the first or second cycles (with the exception of f = 0.25) a separate calculation of these paths was performed by CORE-CYCOST. Table 5.5 shows the results of this calculation. This table indicates that continual reloading of the reactor with the smallest batch fraction available, f = 0.25 is not optimal. Likewise these results point out the savings to be gained in allowing the batch fraction to vary from the three zones, f = 0.33, refueling pattern. That savings is 1.98 million dollars.

Figure 5.3 also gives some insights into the effect of the End-Effect Calculation for the sixth through ninth cycles. Note that at the end of the last, fifth, cycle in the planning horizon two paths $\bar{P}$(C-A-C-D-A) and $\bar{P}$(C-A-D-B-B) are cheaper than the optimal path $\bar{P}^*$(C-A-D-D-C). However, the value, V_5, of the fuel in the reactor at the end of cycle 5 for each path is (see Section 4.3.3, Eq. (4.20)):

$$V_5\ (\bar{P}^*(\text{C-A-D-D-C})) = \$9.845 \times 10^6$$

$$V_5\ (\bar{P}(\text{C-A-C-D-A})) = \$8.638 \times 10^6$$

$$V_5\ (\bar{P}(\text{C-A-D-B-B})) = \$9.827 \times 10^6$$

+ For a full list of the calculations performed for this optimization see Appendix H.2.

Table 5.5

The Revenue Requirements of Constant Batch Fraction Paths in Satisfying the Energy Requirements of the Sample Problem

Path	Batch Fraction f	TC, Total Discounted Revenue Requirement 10^6\$	TC-TC* 10^6\$
A-A-A-A-A	0.37	52.9789	1.6733
B-B-B-B-B	0.33	53.2863	1.9807
C-C-C-C-C	0.29	51.9377	0.6321
D-D-D-D-D	0.25	51.4576	0.1520

These values for V at the end of Cycle 5 indicate that the reactor for $\overline{P}^*$(C-A-D-D-C) had a greater future energy producing potential than the other two paths. Whether this greater future potential would lower the cost of future energy for $\overline{P}^*$(C-A-D-D-C) enough to offset its higher cost than the other two paths during the planning horizon is evaluated by the End-Effect Calculation for the subsequent four cycles, i = 6 through 9. In this case the cost of future energy from path $\overline{P}^*$(C-A-D-D-C) was low enough to result in its becoming the optimal path. This can be observed by the crossing of paths $\overline{P}$(C-A-C-D-A) and $\overline{P}$(C-A-D-B-B) with $\overline{P}^*$(C-A-D-D-C) during the End-Effect Calculation, Figure 5.3.

A test of the sensitivity of the optimal path to the planning horizon length was also performed for Case I. In order to do this the planning horizon terminated after the fourth cycle of the sample problem and the End-Effect Calculation was performed for the fifth through the eighth cycles. The optimal path remained path $\overline{P}$(C-A-D-D).

Another interesting characteristic of the optimal path is the fact that the difference (see Table 5.6) between the reload enrichment $\varepsilon_i(f)$ and the enrichment of the fuel remaining in the reactor from the previous cycle $\varepsilon_i(1-f)$ was small compared with other paths. For example, Δ_ε is defined to be

Table 5.6

The Difference, Δ_ε, Between Reload Enrichment and the Remainder of the Core Enrichment for the Optimal Path and a Rival Path

Cycle	Δ_ε^*	Δ_ε^D
1	1.8649	3.1203
2	0.6194	2.2263
3	1.8711	-0.7907
4	0.1508	0.3542
5	0.7656	1.8096

$$\Delta_\varepsilon \equiv \varepsilon_i(f) - \varepsilon_i(1-f) \qquad (5.2)$$

Δ_ε for the optimal path, Δ_ε^*, and for one of its rivals, $\Delta_\varepsilon D$, path $\overline{P}$(D-D-D-D-D), are compared in Table 5.6 for each cycle. As can be seen in Table 5.6, Δ_ε is much larger on the average and in almost every cycle for the sub-optimal path $\overline{P}$(D-D-D-D-D). In general small Δ_ε's result in lower core peaking factors and from the above it can be seen that they also tend to result in economically optimal paths. To put these values of Δ_ε in perspective, the Δ_ε for 3-zone 3.2 w/o equilibrium reactor operation is 0.8147.

In all of the cycle calculations performed for the Case I optimization of the sample problem and for the additional constant batch fraction paths, 60 cycle calculations in all, the average difference between the energy produced and that desired was 0.94%. This small error validates the predictive correlations and for ε_i, the enrichment required to meet a specified cycle energy for any cycle i; refer to Table 4.1 for an example of the predictive equations and to Appendix D.2 for all equations.

5.5.2 Sensitivity Evaluation of the D.P. Optimization Procedure

Two types of sensitivity tests were performed to check the dynamic programming procedure used in the optimization of the sample problem. Recall from Chapter 4 that the

essential part of the dynamic programming approach is the selection of the n-best optimal paths at the end of each cycle. Two tests were performed to find the sensitivity of the optimal solution to the use of a 5-best set. The first test was to expand the n-best set to six at each cycle. Tracing this sixth path included in the n-best set revealed that none of its progeny ever reappeared in the subsequent cycle's 6-best set. For example, in Case I the End-of-Cycle Evaluator at the end of cycle 2 selected path $\bar{P}$(D-A-B) as the sixth best path with which to traverse cycle 3. The in-core simulation and cost calculation was then performed on all six best paths. The End-of-Cycle Evaluator working on the 24 progeny of these six paths chose the six best paths with which to traverse cycle 4. None of the progeny of path $\bar{P}$(D-A-B) were included in this six best set. This occurred for the sixth best path in every cycle. As a result it seems that the n-best set of five is sufficient to find the optimal policy. However, there was one further possibility which required looking into before this conclusion that a 5-best set is sufficient could be drawn.

The possibility does exist that one of the paths excluded at one cycle might turn out to be an optimal policy two or three cycles later. In order to ascertain whether this was a possibility another full optimization was performed. This optimization commenced at the end of

the second cycle of the Case I optimization already discussed. The sixth through the tenth best paths at the end of cycle two were optimized through to the end of the planning horizon in the same fashion as were the first through fifth best paths. These five paths were $\bar{P}$(A-B), $\bar{P}$(D-D), $\bar{P}$(A-C), $\bar{P}$(B-A), and $\bar{P}$(C-C). Table 5.7 shows the result of this optimization. The sub-optimal path $\bar{P}$(A-B-D-C-B) was the cheapest path that resulted from the sixth through tenth best paths at the end of cycle two. Path $\bar{P}$(A-B-D-C-B) is \$561,799 more expensive than the optimal policy. Furthermore, it can be seen from $(\sum_{j=1}^{i} C_j - \sum_{j=1}^{i} C_j^*)$ in Table 5.7 that all of this difference originated in the first two cycles when path $\bar{P}$(A-B) was eliminated from the first optimization when it was the sixth best path. Although the optimization of the third through the fifth cycles did prevent any further divergence of these paths from the optimal it did not find a refueling policy that was better then the optimal policy already calculated.

From this sensitivity test optimization and from the expansion of the n-best set to six as was previously described it can be concluded that an n-best set of five paths is sufficient to find an optimal policy. Furthermore, the optimal policy was the fifth best policy at the

Table 5.7

Sub Optimal Policy† Resulting from the n-best Sensitivity Test for Case I

Path (A-B-D-C-B)

Cycle i	E_i (GWD)	Cycle Time (months)	f_i	ε_i (w/o)	MC_i (Mills/Kwhr)	C_i (10^6\$)	$\sum_{j=1}^{i} C_j$ (10^6\$)	$\sum_{j=1}^{i} C_j - \sum_{j=1}^{i} C_j^*$ (\$)
1	326.7	12.7	.37	3.0940	1.2044	12.41032	12.41032	-100,350
2	408.0	17.5	.33	4.8832	0.9757	15.35029	27.76061	893,683
3	300.7	12.5	.25	3.3119	1.3002	9.253950	37.01456	675,553
4	268.6	10.5	.29	2.5186	1.4250	7.04045	44.05501	285,971
5	278.4	11.7	.33	3.0540	1.2139	7.812404	51.86742	561,799

C_j^* refers to the cost of cycle j in the optimal path for Case I

†This sub-optimal policy refers to the best fuel reload policy over the planning period if the optimization commences with the sixth through tenth best paths at the end of the second cycle of the Case I optimization.

end of cycle one and thus would have been eliminated had an n-best set of four been used. Therefore, for this sample problem the 5-best set was necessary and sufficient to find the optimal nuclear refueling policy.

5.5.3 Case II

In the Case II optimization the initial and final conditions of the Zion-I reactor were altered from those used for Case I. The assumption was made for Case II that the reactor had been operating on an equilibrium 4 zone 3.5449 w/o enrichment reloading pattern prior to the first cycle of the planning horizon. Under these steady state conditions the Zion Reactor produces 285.4 GWD/cycle, see Table 5.1.

Case II optimizes the same sample problem, Figures 5.1 and 5.2, as Case I. It optimizes within both the power peaking constraint of 3.3 and the average discharge burnup constraint of 50,000 MWD/T.

The optimal refueling policy under these conditions was found to be path $\overline{P}$*(C-B-D-D-D), see Table 5.8. This path is slightly different from the optimal path for Case I, $\overline{P}$*(C-A-D-D-C), which reflects the differences in the initial and final conditions. More important, however, than this difference in strategies is the difference in costs for the two optimal policies. Table 5.9 shows these

Table 5.8

Optimal Nuclear Refueling Policy---Case II

Initial and Final Condition: Four zone equilibrium cycle 3.5449 w/o fuel loading (285.4 GWD/cycle)

Path: (C-B-D-D-D)

Cycle i	E_i (GWD)	Cycle Time* (months)	f_i	ε_i (w/o)	MC_i (mills/kwhr)	C_i (10^6\$)	$\sum_{j=1}^{i} C_j$ (10^6\$)
1	326.1	12.7	0.29	3.5257	1.2676	12.03271	12.032710
2	415.0	17.5	0.33	4.3405	1.1009	15.098799	27.131509
3	299.5	12.5	0.25	3.5449	1.3484	9.253234	36.384743
4	264.2	10.5	0.25	3.1847	1.2612	7.301789	43.686532
5	283.4	11.7	0.25	3.8133	1.3570	7.655820	51.342352

* Cycle Time includes the 1.5 month refueling down time.

Table 5.9

The Differences in Total Revenue Requirements Between the Case II Optimal Policy and the Case I Optimal Policy

Cycle i	$\sum_{j=1}^{i} C_j^*(II) - \sum_{j=1}^{i} C_j^*(I)$
1	- 388,350
2	264,581
3	45,735
4	- 82,508
5	36,736

cost differences. From Table 5.9 it can be seen that it is primarily Cycle 2 which makes the optimal policy in Case II more expensive than the optimal policy in Case I. The principle reason for this was the elimination of paths that violated the power peaking or burnup constraints in traversing Cycle 2*. Of the sixteen feasible paths for traversing Cycle 2, eleven were eliminated for constraint violations. Those paths that violated the power peaking constraint were $\overline{P}$(A-A), $\overline{P}$(A-B), $\overline{P}$(B-A) and $\overline{P}$(B-B). Those paths that would eventually violate the burnup constraint were $\overline{P}$(A-C), $\overline{P}$(A-D), $\overline{P}$(B-C), $\overline{P}$(B-D), $\overline{P}$(C-C), $\overline{P}$(C-D) and $\overline{P}$(D-D).

From this large number of constraint violations which limited the choice of an economically optimal policy through Cycle 2, it seems that the optimization did not have enough leverage to pre-plan for this large energy demand in Cycle 2. All of the paths leaving Cycle one, $\overline{P}$(A), $\overline{P}$(B), $\overline{P}$(C), $\overline{P}$(D) were in very similar states since they had only one cycle of a different loading pattern. Had there been various paths traversing Cycle 1 the states of the paths would have been different and the large number of constraint

---

* Although the power peaking constraint was not automatically considered in the Case I optimization a separate calculation of $\overline{P}$*(C-A-D-D-C) revealed that only Cycle 1 of this path had a power peak, 3.4, larger than the 3.3 constraint used in Case II.

violations would in all likelihood not have occurred. Of course there is a limit to how large an energy increase from one cycle to the next can be met within the constraints regardless of the diversity of paths entering Cycle 2. However, the initial conditions for the Case I study did not result in reactor states entering Cycle 2 that eventually violated as many constraints as were violated in Case II. This leads to the conclusion that large changes in energy demand from one cycle to another must be anticipated in planning so that the adjustments in batch fraction and enrichment necessary to meet the increased energy demand are required over several cycles preceeding the large change in energy demand. Hence large changes in cycle energy cannot be accommodated in the first few cycles of a planning period.

In general comparing Cases I and II it can be seen that both the optimal policy and the cost of the optimal policy are dependent upon the initial conditions of the reactor at the beginning of the planning horizon. The final reactor condition (i.e. the return of the reactor to the equilibrium cycle conditions from which it began) has its predominant effect on the final cycle reloading decision but little effect on the overall policy cost. Consequently it would be advantageous to have a reasonable idea as to what the energy strategy for this reactor will be after the planning horizon so that the strategy for the final cycle might be a better preparation for the future.

5.6 The Computer Time Used by the Optimization Procedure

The total computer time, TI, used by the D.P. optimization algorithm is a function of the n-best set size. Namely,

$$TI = n.(m+4)\cdot t_c \qquad (5.3)$$

where n is the number of best paths carried through each cycle, m is the number of cycles in the planning horizon and t_c is the reactor cycle computation time.

On an IBM-370 M165 computer t_c is 0.084 min/cycle. The computation time, TI, therefore, required to optimize the refueling strategy to meet the energy demands in the sample problem was 3.75 min, where 45 CORE cycle calculations were required. For the Zion-I reactor 80 cycle calculations were performed prior to the optimization to develop the correlations required by the dynamic programming algorithm. These consumed 8.4 min. of computer time but are used for all subsequent refueling optimizations performed on the Zion-I reactor. The 3.75 min computation time and the 8.4 min pre-calculation computer time consumed by this dynamic programming model are not inordinately high considering the objectives of this study, see Section 2.6. If this model were to be used in an on-line fashion with the System Integration and Optimization Models (11) the total time consumed in on-line nuclear simulations would

be about 18.75 hrs. This assumes that 10 iterations are required with the System Optimization Model to find the optimal reactor cycle energies, that there are 6 reactors on the utility system and that there are five refueling and maintenance schedules to be optimized (3.75 x 10 x 6 x 5 = 18.75 hrs). At $300/hr computation costs this implies a $5025 computer bill for the nuclear simulation portion of the Nuclear Power Management Model. The total savings in nuclear fuel costs gained by this optimization can be as high as 10 million dollars which justifies the $5025 expense. However, other optimization methods, especially a complete correlation fit of all variables method (37), could be used that would reduce this expense a great deal. To date these analytic fit methods do not consider the power peaking constraints which do have a large impact on the optimization. Certain guidelines may be deduced, see Section 7.4, from this study which may aid these other methods in their consideration of the engineering constraints.

6. OPERATING INSTRUCTIONS FOR THE IN-CORE SIMULATION AND OPTIMIZATION MODEL

This chapter describes in detail how the in-core simulation and optimization models developed in this study are applied to any given reactor. This description of the way in which these models are used is meant for the reader who is interested in using the approach to nuclear in-core simulation and optimization presented in this report to optimize the energy production by a given reactor. Results of the application of the dynamic programming approach to sample nuclear refueling optimization problems and the general conclusions drawn from this application are to be found in Chapters 5 and 7.

The application of the in-core simulation and optimization models presented in this report involves four basic tasks. These tasks are:

1. The modelling of the reactor whose refueling schedule is to be optimized using the CELL and CORCOST codes so that depletion calculations and cost calculations can be made for all refueling decisions.
2. The collection of nuclear fuel revenue requirements and energy production data for the reactor over a wide range of refueling conditions which are to be used by the optimization model.

3. The preparation of the required polynomial correlations of these data which relate cycle reload enrichment and cycle revenue requirements to the state of the reactor and the energy to be produced during that cycle.
4. The use of the dynamic programming algorithm, (see Chapter 4) to find the optimal refueling policy.

All of these tasks are described in the following four sections.

6.1 Modelling the Reactor Using the CELL and CORCOST Codes

The first step in applying the in-core simulation and optimization model is the setting up of the CELL and CORCOST codes to perform the neutron depletion and cost calculations for the reactor under investigation. CELL and CORCOST are used both to produce operating and cost information for the reactor prior to performing any optimization and are also used as the on-line simulator in the optimization procedure. The CELL code (17) is the point depletion code which generates time dependent cross section and nuclide density data for nuclear fuel (see Appendices B, F and I). This time dependent data must be calculated for each reload enrichment, ε, that will be needed in the optimization procedure. The range of

reload enrichments to be used by the optimization routine is dependent on the individual reactor being optimized. However, before optimization experience is gained with a reactor the use of a very broad range of enrichments is recommended. Experience with the Zion-I, a 1060 MWe PWR, reactor has shown that a reasonable range of enrichments extends from 1.8 w/o to 5.0 w/o.

Since enrichment is a continuous variable in the dynamic programming, D.P. optimization (see Chapter 4), the number of enrichments within this range for which CELL data are required is very large. The number of different CELL enrichment data, N_ε, which must be available to the D.P. algorithm depends on the error between cycle energy demand and cycle energy production, ΔE, which is to be tolerated. Again this relationship of the N_ε required to the error in cycle energy is a function of the individual reactor being described. However, if the sensitivity of cycle energy production to reload enrichment, ρ_ε [w/o/MWD/t], is known N_ε can be calculated using the following relationship:

$$N_\varepsilon = \frac{(\varepsilon_{MAX} - \varepsilon_{MIN})}{2 \cdot \rho_\varepsilon \cdot \Delta E} \qquad (6.1)$$

where $\varepsilon_{MAX}-\varepsilon_{MIN}$ is the range of enrichments being used by the optimization and where the 2 reflects the fact that the mesh spacing in enrichment can be double the allowable variance in enrichment, $\rho_\varepsilon \cdot \Delta E$. ρ_ε can be estimated by making ten cycle energy production calculations with CORCOST. These calculations should be made using two arbitrarily chosen reload enrichments ε_1 and ε_2 and five different initial reactor conditions. For each initial reactor condition, then, ρ_ε can be calculated as:

$$\rho_\varepsilon = \frac{\varepsilon_1 - \varepsilon_2}{E_1 - E_2} \tag{6.2}$$

The average value of the ρ_ε's for each of the five different initial coniditions is accurate enough to use in the calculation of N_ε in Equation (6.1).

It was found for the Zion-I reactor that in order to maintain an error of less than 1% in cycle energy the number of CELL enrichment data, N_ε, available to the D.P. optimization had to be 50 for the range of enrichments previously mentioned.

Once CELL has been used to generate N_ε different sets of enrichment data for the reactor in question, CELL need never be used again. From this point onward all of the cycle calculations performed by CORCOST both in developing correlations and in the D.P. algorithm use the data in these N_ε sets.

Using the CELL-calculated time-dependent cross section and nuclide density properties for reload enrichments, the CORCOST code (see Section 3.2.2) calculates the spatial flux and power distributions, the changes of these distributions with time and the energy produced by the reactor during each cycle. A description of the input information required by CORCOST for any pressurized water reactor is given in Appendix A.3. Of particular interest to the user of the CORCOST code for the optimization of nuclear fuel loading is the setting up of the radial mesh points. These mesh points must be arranged so that refueling with the desired batch fractions can be achieved. If a batch fraction f is one of the batch fractions to be surveyed by the optimization, then one of the radial mesh points must be located at the radial position, R, such that

$$R = \sqrt{(1-f)R_{MAX}^2} \qquad (6.3)$$

where R_{MAX} is the radius of the reactor core.

For example, the Zion-I reactor has a core radius of 168.53 cm. If a reload batch fraction of 0.25 is to be used by the optimization procedure then one of the radial mesh points must be positioned at R = 145.95 cm.

In this manner radial mesh points for all of the batch fractions which are to be surveyed by the optimization are positioned. The remainder of the radial mesh points can be positioned at reasonable intervals throughout the

rest of the core so as to achieve an adequate description of the neutron flux and power density distributions within the core. As was previously pointed out, a mesh point sensitivity study was performed on the CORCOST code (see Appendix G) which demonstrated that as few as ten radial mesh points could be used to adequately describe the reactor.

The cost information required as input to CORCOST to calculate the nuclear fuel cycle revenue requirements is also described in Appendix A.3.

6.2 Collecting Operating Data for the Reactor

The second task in the application of the in-core simulation and optimization model is the collection of operational and cost data on the reactor in question. The general nature of this data and its use was described in Sections 4.3.2 and 4.3.3. The data is to be used in the development of correlations (see Section 6.3) relating the cycle energy and nuclear fuel revenue requirements to the state of the reactor and the reload enrichment, ε_i, and batch size, f_i. The collection of this data is much simplified by the fact that the D.P. optimization deals only in discrete values of batch fraction. Furthermore, it has been found that the state of the reactor can be defined by the two average parameters, εII and BII. εII

is the average fissile enrichment, Equation (4.12), and BII the average burnup of the nuclear fuel in the inner, 1-f, region of the reactor core. The collection of data then reduces to making many CORCOST runs for each value of f_i over a wide range of the variables εII, BII and ε_i.

f_i and E_i are input parameters to CORCOST and can be varied at the operator's discretion (see Appendix A.3). εII and BII are implicit inputs to CORCOST since they are calculated on the basis of the spatial distribution of the accumulated flux-times of fuel in the reactor at the beginning of the cycle which is input as THETA (I,J,K) (see Appendix A.3) by the code operator. In collecting operational data the range of εII and BII must be similar to the range in these variables that is to be experienced during the optimization itself. For the cases studied in this report using the Zion-I reactor, the range of εII was between 2.10 and 2.85 w/o and BII was between 14,000 and 27,000 MWD/T. The cycle energy E_i, the cycle fuel burnup revenue requirements, BU$, and the cycle fuel fabrication and reprocessing revenue requirements, FAR$, are all calculated and printed by the CORCOST code.

The accuracy that can be achieved by correlations (see Section 6.3) to this operational data is dependent on the number of data points used, where each data point represents one cycle energy production calculation. Experience has shown that about 20 data points for each batch

fraction to be used by the optimization is sufficient. However, if the goodness of any correlation fit on the basis of the criteria outlined in Appendix D.1 is suspect more data points for that fit might help.

The cycle length, TSCED in years (see Appendix A.3), is taken as constant for all of the cycle calculations used to collect these data points. This simplification introduces little error in the dynamic programs end of cycle evaluation where the correlations based on these data are used. This is due to the fact that the end of cycle evaluator is always comparing fuel costs for producing energy for one cycle at a time and as a result never compares costs incurred in producing energy over different time periods (see Section 4.3.2.1). The cycle length used in the data collection for the Zion reactor was 1.05 years.

The procedure for collecting this information for each batch fraction, f, which is subsequently to be surveyed by the optimization algorithm for the reactor in question is as follows:

1. Select a set of reload enrichments, ε_i, that covers the range of enrichments which are to be used by the optimization procedure. As was described, that range for the Zion reactor was between 1.8 and 5.0 w/o. For the purpose of data collection all N_ε , Equation (6.1), enrichments need not be used in the data collection procedure. Eight or

nine different enrichments with the above range are adequate to produce data points that span the entire region of interest.

2. Select various sets of input THETA values that span the range of interest of εII and BII for the reactor.

3. Perform the necessary, about 20, cycle energy calculations with the CORCOST code for a variety of combinations of ε_i, EII and BII and tabulate the resulting energy productions, E_i, and revenue requirements, BU$ add FAR$.

These three steps are repeated for each batch fraction f. For the sample optimization problem discussed in Chapter 5 four different batch fractions varying from 0.25 to 0.37 were used. For a more extensive optimization the batch fractions which are surveyed by the optimization should cover a broader range, e.g. 0.20 to 0.40, as described in Section 7.6.

6.3 Preparation of the Required Correlations

All of these data must be reduced to equation form for use in the optimization procedure. This is accomplished by using least squares polynomial fitting procedures (see Appendix D.1) to determine the terms and their respective coefficients that best describe the relationship among all of the variables of interest. For each batch fraction, f, equations expressing the following relationships must be

produced:

$$\epsilon_i = \epsilon_i(E_i, \epsilon II, BII) \tag{6.4}$$

$$BU\$ = BU\$(\epsilon_i, E_i, \epsilon II, BII) \tag{6.5}$$

$$FAR\$ = FAR\$(\epsilon_i, E_i, \epsilon II, BII) \tag{6.6}$$

A fourth relationship for each f must also be derived. The incremental cost, MC_i, of changing E_i in a cycle must be derived. This is accomplished by differentiating Equation (6.5)

$$MC_i = \frac{\partial BU\$}{\partial E_i} = MC_i(\epsilon_i, E_i, \epsilon II, BII) \tag{6.7}$$

For an example of the form of a typical set of Equations (6.4) through (6.7) see Table 4.1.

Once these Equations (6.4) through (6.7) are derived for each f, they are incorporated in the form of FORTRAN statements into the ESTMAT subroutine (see Appendix D.3) of CORCOST.

6.4 The Dynamic Programming Procedure

With the coding of Equations (6.4) through (6.7) into the ESTMAT subroutine the CORCOST code is ready for use as the in-core simulator in the optimizer of the nuclear fuel reload strategy for the reactor which these equations

describe. The objective of the optimizations is to minimize the discounted total revenue required to produce a specified amount of energy E_i in each fuel cycle i over a planning horizon of many cycles for the reactor in question. The dynamic programming procedure for doing this is discussed at length in Chapter 4. This procedure has not as yet been incorporated into the program. Consequently, the operator must perform all of the evaluating procedures described in Chapter 4. Since the operation of the CORCOST code as the in-core simulator is described in detail in Appendix A, this section shall be devoted to describing how the operator of this code uses the information from CORCOST and performs the evaluation required at the end of every cycle by the D.P. algorithm.

The objective of the End of Cycle Evaluation is to select the n-best paths for which a full CORCOST calculation is to be performed for the subsequent cycle. This evaluation procedure will be described for the End of Cycle i, which is any cycle in the planning horizon with the exception of the last cycle, which will be dealt with later. The evaluation is based upon the total discounted revenue requirements, $\overline{TC}$, through the end of cycle i and the estimated revenue required to produce E_{i+1} in cycle i + 1. The explanation of this evaluation procedure is best presented by an example evaluation. The example chosen is an evaluation performed at the end of the third cycle for the optimization sample problem referred to as Case II in Chapter 6. The end-of-cycle evaluation pro-

cedure is as follows:

1. For the n paths for which CORCOST calculations were performed tabulate the cycle energy produced, E_i, the nuclear fuel revenue requirement for the cycle, C_i, and the fuel value V_i (see Equation 4.22) at the end of Cycle i. For example, at the end of Cycle 3 of the Case II sample optimization (see Chapter 5) there were five paths for which CORCOST calculations were performed. These paths were $\bar{F}$(D-D-C), $\bar{F}$(D-C-B), $\bar{F}$(C-B-D), $\bar{F}$(C-B-C), and $\bar{F}$(C-A-C). In Table 6.1 the tabulation of E_3, C_3 and V_3 for these five paths is displayed.

The possibility exists that the calculated cycle energy E_i does not agree with the cycle energy demanded by the utility system. If E_i is not within a prescribed error band (2% was used in the optimization problem in Chapter 5), then ε_i for this path must be adjusted and the CORCOST calculation performed again. This adjusting is done on the basis of the sensitivity of reload enrichment to cycle energy demanded, PEI, which is calculated and printed for this purpose by CORCOST.

$$PEI = \frac{\partial \varepsilon_i}{\partial E_i} \tag{6.8}$$

The new value of enrichment, ε_i, to be used in the new CORCOST run for the path that failed to produce the cycle energy demanded, E_i^d, is

Table 6.1

Sample End-of-Cycle Calculation. Performed at the End of Cycle 3 with Predictions for Cycle 4, Case II Initial Conditions for the Sample Problem of Chapter 6

	Cycle 3 Calculations				Cycle 4 Estimates		
Path Designation	E_3 GWD/cycle	C_{3_6} ($\$x10^6$)	$\sum C_i$ $10^6\$$	V_{3_6} $10^6\$$	$PVCE_4$ $10^6\$$	TCE_4 $10^6\$$	TVE_4 $10^6\$$
D-C-C	305.0	9.159305	36.298309	11.613039			
D-C-C-A					7.571690	43.869999	32.256930
D-C-C-B					7.727530	44.025839	32.412769
D-C-C-C					7.287038	43.585347	31.972777
D-C-C-D					7.616919	43.915228	32.302158
D-C-B	305.8	9.219324	36.352249	11.142390			
D-C-B-A					7.587220	43.939470	32.797079
D-C-B-B					7.224068	43.576317	32.433927
D-C-B-C					7.561609	43.913853	32.771463
D-C-B-D					7.946045	44.298294	33.155904
C-B-D	298.6	9.253234	36.384739	12.123860			
C-B-D-A					7.216165	43.600904	31.477044
C-B-D-B					6.848357	43.233095	31.092355
C-B-D-C					7.216863	43.661602	31.477742
C-B-D-D					7.297624	43.682364	31.558504
C-B-C	301.7	9.304499	36.441019	11.30126			
C-B-C-A					7.892475	44.333494	33.032234
C-B-C-B					8.135838	44.576857	33.275597
C-B-C-C					7.579770	44.020789	32.719529
C-B-C-D					7.614294	44.055313	32.754053
C-A-C	299.8	9.452867	36.478679	11.373970			
C-A-C-A					7.850490	44.329169	32.955199
C-A-C-B					8.206640	44.685319	33.311349
C-A-C-C					7.414689	43.893368	32.519398
C-A-C-D					7.596977	44.075656	32.716860

$$\varepsilon'_i = \varepsilon_i - (E_i - E_i^d) \cdot PEI \qquad (6.9)$$

2. The total revenue requirement, $\overline{TC}$, incurred by each of the n paths over all i cycles, TC, already traversed

$$\overline{TC}_i = \sum_{j=1}^{i} C_j \qquad (6.10)$$

must also be calculated and tabulated. For the example shown in Table 6.1, $\overline{TC}_i$ for each path appears in the fourth column. $\overline{TC}_i$ is calculated by summing the nuclear fuel revenue requirements incurred by each path in the first three cycles of the planning horizon, i.e.,

$$\overline{TC}_3 = C_1 + C_2 + C_3 \qquad (6.11)$$

C_3 as calculated by CORCOST for each of the five paths also appears in Table 6.1. C_1 and C_2 would appear on the similar tabulations to that shown as Table 6.1 for cycles 1 and 2.

3. The second half of Table 6.1 requires estimates, CE, for the costs of traversing Cycle (i + 1) (in the case displayed in Table 6.1 cycle 4) by means of the progeny of all paths which traversed cycle i, Cycle 3. For example, the progeny of path $\overline{P}$(D-C-C) through cycle 4 are paths $\overline{P}$(D-C-C-A), $\overline{P}$(D-C-C-B), $\overline{P}$(D-C-C-C), and $\overline{P}$(D-C-C-D) as shown in Table 6.1. The estimate of the revenue requirement CE of producing E_4 is printed by CORCOST as TOT$ (see

Appendix F.3). These estimated costs printed by CORCOST are the only costs calculated by that code which are not present valued to time t = 0, the beginning of the planning horizon. Therefore, CE_4 must be present valued to the beginning of the planning horizon before it is tabulated as shown in Table 6.1 as $PV \cdot CE_4$. TCE_4 and TVE_4 are calculated using the following equations:

$$TCE_{i+1} = \sum_{j=1}^{i} C_j + PV \cdot CE_{i+1} \tag{6.12}$$

and

$$TVE_{i+1} = \sum_{j=1}^{i} C_j + PV \cdot CE_{i+1} - V_i \tag{6.13}$$

The interpretation and significance of TCE and TVE are explained in Section 4.

Table 6.2, the ranking of paths at the beginning of Cycle i + 1, Cycle 4 in this example, shows the ranking of TCE and TVE for all paths in order of ascending costs. From R_c and R_v a combined ranking R_s is calculated

$$R_s = W_c \cdot R_c + W_v \cdot R_v \tag{6.14}$$

where W_c and W_v are weighting functions which for the sample in Table 6.2 were 0.4 and 0.6 respectively. All paths are now ordered by ascending value of R_s and the first seven paths are listed in Table 6.2 as the combined

Table 6.2

THE RANKING OF PATHS AT THE BEGINNING OF CYCLE 4, FOR THE SAMPLE CALCULATION

Cycle 4 Estimates

R_c	Path	$TCE_p(10^6\$)$	Path	$TVE_p(10^6\$)$	R_v
1	C-B-D-B	43.233095	C-B-D-B	31.092355	1
2	D-C-B-B	43.576317	C-B-D-A	31.477044	2
3	D-C-C-C	43.585347	C-B-D-C	31.477742	3
4	C-B-D-A	43.600904	C-B-D-D	31.558504	4
5	C-B-D-C	43.661602	D-C-C-C	31.972277	5
6	C-B-D-D	43.682364	D-C-C-A	32.256930	6
7	P-C-C-A	43.869999	D-C-C-D	32.302158	7
8	C-A-C-C	43.893368	D-C-C-B	32.412769	8
9	D-C-B-C	43.913853	D-C-B-B	32.433927	9
10	D-C-C-D	43.915228	C-A-C-C	32.519398	10
11	D-C-B-A	43.939470	C-A-C-D	32.716860	11
12	C-B-C-C	44.020789	C-B-C-C	32.719529	12
13	D-C-C-B	44.025839	C-B-C-D	32.754053	13
14	C-B-C-D	44.055313	D-C-B-C	32.771463	14
15	C-A-C-D	44.075656	D-C-B-A	32.797079	15
16	D-C-B-D	44.298294	C-A-C-A	32.955199	16
17	C-A-C-A	44.329169	C-B-C-A	33.032234	17
18	C-B-C-A	44.333494	D-C-B-D	33.155904	18
19	C-B-C-B	44.576857	C-B-C-B	33.275547	19
20	C-A-C-B	44.685319	C-A-C-B	33.311349	20

Combined Order

	Path	R_s
1	C-B-D-B	1.0
2	C-B-D-A	2.8
3	C-B-D-C	3.8
4	D-C-C-C	4.2
5	C-B-D-D	4.8
6	D-C-B-B	6.2
7	D-C-C-A	6.4

order. The n-best paths for Cycle i + 1 are the first n paths of the combined order listing. For the example demonstrated in Table 6.2 the first five paths comprised the n-best set, $\overline{P}$(C-B-D-B), $\overline{P}$(C-B-D-A), $\overline{P}$(C-B-D-C), $\overline{P}$(D-C-C-C), $\overline{P}$(C-B-D-D).

The in-core simulator now simulates the refueling decision represented by these n-best paths traversing cycle i + 1 and calculates the energy produced and the total cycle discounted revenue required by each. At this juncture the end of cycle evaluating procedure for cycle i + 1 commences in the same manner as described above for cycle i.

When the end of the last cycle in the planning horizon is reached an end effect calculation must be performed in order to evaluate the fuel remaining in the reactor at the end of the planning period. End effect considerations are discussed in Section 5.2. In accord with the purposes of this chapter, however, only the mechanics of performing one such end effect calculation shall be presented. Recall that there are n-paths calculated through the last cycle in the planning period. The end effect calculation used in the sample problem of Chapter 5 requires each of these paths to produce energy over four more cycles for which the batch fraction is specified, i.e. no "optimization" of batch fractions beyond the planning horizon need to be carried out. This eliminates the end of cycle evaluation

for these cycles beyond the planning period. All that remains for the operator to do is to use the information calculated by CORCOST to decide what enrichment is to be used for each path to achieve the required energy with the required batch fraction in each cycle. In the Case II sample optimization the end effect consisted of refueling the reactor with a batch fraction of 0.25 and the enrichment required to produce a cycle energy of 285.4 GWD/cycle for each of four cycles after the planning period.

The optimal path is selected after an end-effect calculation is performed for each of the n-best paths traversing the last cycle in the planning period. The optimal path is the path with the minimum total discounted revenue requirements, $\overline{TC}^*$, over the planning horizon plus the four subsequent cycles.

7. CONCLUSIONS AND RECOMMENDATIONS

This chapter presents some general conclusions and recommendations for future work to which the development and operation of this in-core simulation and optimization model has led. The purpose is to point out where improvements to the models can be most effective, where the major economic gains to variable reloading strategies can be realized and where the physical constraints on reactor operation have the most impact.

7.1 The Dynamic Programming Optimization

The dynamic programming procedure as described in Chapter 4 is capable of finding an optimal solution to the nuclear refueling decision problem. Using an evaluation at the end of each stage based on the total path revenue requirements and the value of the fuel, V_i, see Equations (3.8) and (4.21), in the reactor and an estimation of the costs of producing energy in the next cycle, does decouple present decisions from future decisions permitting the straight forward use of Belman's Principle of Optimality and, consequently, a dynamic programming algorithm.

An n-best set of five paths was shown to contain the optimal solution at each stage. The n-best set represents the n paths which are to be simulated by CORCOST through

the next cycle. An n-best set of five paths was found to be necessary to find an optimal policy which was further shown not to be a narrow local optimum.

Case II described in Section 5.5.3 had a very large number, 10 out of 16, of paths eliminated during the second cycle of the five cycle sample problem due to violations of engineering constraints. This was caused by a lack of diversity in the state of the reactor for the paths entering a cycle that had a 25% increase in cycle energy demand. Consequently, the choice as to the number of sub-optimal paths carried from one cycle to the next cannot be based solely on that number's ability to contain the economic optimal policy up to that stage. The n-best set should contain enough diversity in reactor states so as to ensure the inclusion of paths which do not violate engineering constraints.

7.2 Satisfying a Schedule of Varying Energy Requirements

Optimization of the reload batch fraction, f, and enrichment, ε, at each cycle to meet a varying energy demand from cycle to cycle not only produces the economic optimum refueling strategy but also aides the reactor in avoiding constraints on power peaking and burnup.

Furthermore, planning two or three cycles in advance of any large variation in cycle energy demand is economically advantageous when the energy demands must be met within constraints on power peaking and burnup. This preplanning is

accomplished in the dynamic programming algorithm by carrying from cycle to cycle n paths with different previous refueling policies. By not permitting large variations in cycle energy, E_i, demands for the first two cycles of a planning period, the dynamic program is given the opportunity to preplan for large changes in E_i. This exclusion of large E_i variations from the first two cycles of a planning period results in the increase in the number of feasible paths through the cycles with large changes in E_i and consequently, improves the choice of an economic optimal path for the entire planning horizon. Likewise consideration of the importance of preplanning dictates that the end of the planning horizon must be dealt with carefully. The state of the reactor at the end of the planning horizon will dictate the feasible and economically advantageous energy demand from the first cycle following the planning horizon. It is desirable, therefore, to leave the reactor in a state which is commensurate with the energy that it might be expected to produce after the planning horizon. This implies carrying out the entire utility system optimization two or three years beyond the period for which strategies are actually being planned.

It was also found that the range of enrichments used in the optimizations of reload decisions to satisfy the

varying energy demand of this problem within the physical constraints was from 1.8 to 5.0 w/o. If, however, the constraint on average discharge burnup, B_{MAX}, were changed from 50,000 MWD/T the upper bound of 5.0 w/o would change proportionately with the change in B_{MAX}, see Equation (4.18).

Requirements for large variations, larger then 20%, in cycle energy close to the start of the planning period can result from a lack of planning. The recommendation, therefore, to avoid large variations in cycle energies implies a series of planning calculations made, say yearly, so as to adjust future reload designs gradually to changes in system performance and forecast demands. Also requirements for abrupt changes in system cycle energies in the time close to the beginning of the planning period should be shared among several reactors on the system so that no one of them will be expected to undergo severe short range changes in planned fuel strategies. If this planning were carried out on a yearly basis the planning horizon would be only one year but the system optimization and the in-core optimization should be performed for this year plus about four more years, three or four refueling cycles, into the future. This not only will leave the reactor at the end of the one year planning horizon in a state that is commensurate with expected future energy demands but also obviates the necessity of performing an end effect calculation after the fifth cycle. The reason for the latter

is that refueling decisions and energy production in the sixth cycle were found, as was expected, not to have any effect on decisions in the first cycle so evaluating future energy potential of fuel at that point is unnecessary.

7.3 The Use of CORCOST* as the In-Core Simulator and Cost Calculator

The severest limitation on the use of CORCOST as the In-Core Simulator in the Nuclear Power Management Model is the computation time that CORCOST uses. CORCOST's use as the In-Core Simulator for the Simulation and Optimization presented in this report has been adequate. Furthermore, the use of CORCOST in an on-line capacity as the In-Core Simulator in the Nuclear Power Management Model does not incur a large expense in computation costs, $5000 - $6000, compared with the savings reaped by the optimization, approximately $10 million. However, faster nuclear simulators of the 1-D variety (19) or the complete precalculated variety (34, 37) would be even less expensive. The drawback to the use of these faster in-core simulators and optimizers is the accuracy lost in the simplifications of the physical situation that they require. The method presented here, a dynamic programming optimization with the CORCOST in-core simulator, could very easily be used as a check on the accuracy of these simpler codes as they are being developed. Even more important, however, these

---

* The combination of the CORE and CYCOST codes, see Appendix A.

simpler methods can benefit from the results obtained from the "D-P with CORCOST" method.

For example, as shown in the Case II optimization presented in Section 5.5.3, the constraints on power peaking and burnup significantly affect the optimization of nuclear refueling decisions. Consequently, any In-Core Simulator and optimizer must have the capacity to calculate power peaking and burnup peaking in the reactor under varying refueling conditions. A one dimensional nuclear depletion code such as that developed by Henderson (19) would be capable of doing this to the degree of accuracy required and with a significant decrease in computational time over the 2-D Core model. Zero-dimensional codes would be incapable of calculating spatially dependent power and burnup peaks and consequently would not be adequate as In-Core Simulators. An alternative to these on-line nuclear calculational methods would be simulating all refueling decisions by means of precalculated correlations. Besides only having to relate the nuclear costs and the changes in reactor states to cycle energy produced for a broad variety of nuclear refueling decisions these correlations also must calculate the effects on power peaking and maximum burnup due to the refueling decisions. The calculation of these engineering constraints in all

of the methods mentioned above might well be accomplished by setting guidelines for refueling which would prevent excess power and burnup peaking. Some of these guidelines can be deduced from the results presented here. These guidelines could establish the range of feasibility for the decision variables, ε_i and f_i, that would not violate any engineering constraints given the state of the reactor.

For example, from the optimization calculations presented in Chapter 5 it is possible to set two very coarse guidelines on future optimizations of large pressurized water reactors.

1) The use of large reload enrichments leads to high batch discharge burnups. Experience has shown that a relationship similar to Equation (4.18) can be readily derived for a reactor which will indicate the maximum enrichment that the optimization procedure should consider. Equation (4.18) is rearranged and repeated here for example sake:

$$\varepsilon_{MAX} = 0.27057 + 9.2684 \times 10^{-5} B_{MAX} \qquad (7.1)$$

2) Large differences, $\Delta\varepsilon$, between the reload enrichment $\varepsilon_i(f)$ and the average fissile enrichment of the remaining fuel $\varepsilon_i(1-f)$ in the reactor result

in violation of power peaking constraints. For example, for the Zion-I reactor this $\Delta\varepsilon$ should be less than 2.2 w/o if a power peak greater than 3.3 is to be avoided. A similar guideline for other reactors can be derived prior to optimizing the refueling decisions for that reactor which will enhance the efficiency of the dynamic programming optimization.

7.4 Recommendations

The effectiveness of the dynamic programming optimization presented in this report is a function of the spacing between available batch fractions and the range of values covered by the available batch fractions. Decreasing the spacing between batch fraction values from the 0.04 level used in the examples of Chapter 5 will in all likelihood decrease the cost of the optimal path but may increase the number of n-best paths necessary to contain the optimal solution. This increase in the n-best set will increase the computation time required for the optimization but the decrease in the optimal path cost may warrant this reduction in the spacing of the available batch fractions.

Besides increasing the density of batch fractions available at each cycle the optimal strategy could be improved by using a different set of values of the batch fractions available in one cycle than in another, dependent on the

cycle energy demand. It was observed that large cycle energy demands were met with large batch fractions in the optimal policy. Therefore, the optimization should be given a range of batch fractions from which it is to select an optimal, f, that includes only the larger f's if the cycle energies are large. For example, for the Zion-I reactor the recommendation is made that the batch fractions available in the dynamic optimization be the function of cycle energy presented in Table 7.1.

Table 7.1

The Recommended Range of Batch Fractions, f, Available to the Optimization Model for the Zion-I Reactor

Range of E_i [GWD/cycle]	Range of f
<300	0.2 - 0.3
300-400	0.25 - 0.35
>400	0.3 - 0.4

APPENDIX A THE CORE CODE

A.1 History of the CORE Code

The version of the 2-D, one and a half group, depletion analysis and fuel cycle cost code which performs the in-core simulation discussed in Chapter 3 of this report is called CORCOST. CORCOST is the CORE code with the addition of the CYCOST, fuel cycle cost calculator, subroutine. Both CORE and CORCOST are available through the MIT Nuclear Engineering Department Computer Code Library. The CORE code description and input manual (21) is also available through the Nuclear Engineering Department Computer Code Library. The objective of this Appendix is to describe the development of CORE and CORCOST and to present an input manual for CORCOST.

The MOVE code (25) written originally in 1961 was selected as the in-core simulator for MIT's Nuclear Power Management Model. However, the computing speed of the MOVE code and the nuclear refueling options available in MOVE both had to be augmented before MOVE could be used by the Nuclear Power Management Model. The computing speed of the MOVE code was significantly increased by recoding the entire program.

The new program produced is CORE which solves the same equations as MOVE. The refueling options in CORE were then

increased to permit any batch in the reactor to have a different enrichment. Finally, the capacity to refuel a reactor with any size batch of fuel (see Section A.2) was added to CORE. The addition of the CYCOST subroutine to CORE permits the calculation of the nuclear fuel revenue requirements for any refueling strategy. This fuel cycle costing version of CORE is called CORCOST.

A.2 The CORCOST Nuclear Fuel Management and Fuel Cycle Costing Procedures

The neutron spatial behavior is described by a composite two-group diffusion equation in the CORCOST code. The solution of the equation as performed by CORCOST is presented by McLeod (25) pp. 68 to 84 and repeated by Kearney (21), Section 3B. However, the CORCOST nuclear refueling procedures shall be described in the next two sections and the fuel cycle costing subroutine in Appendix C.

A.2.1 Nuclear Refueling Procedures in CORCOST

The CORCOST code similar to its predecessor, CORE, automatically unloads irradiated fuel and loads fresh fuel into the reactor at the end of each cycle. All of this fuel handling in CORCOST is performed by the RESHFL subroutine. Previously, i.e., when using the MOVE code, all of the batches in the reactor were of the same size and the fresh fuel loaded into the reactor at each cycle likewise had to be that same size which is specified by the

parameter NSRB at the beginning of a calculation. NSRB (see Section A.3) is an integer which specifies the outermost radial mesh point of the inner scatter fueled zone. A different outermost radial mesh point would define a different reload batch fraction, f, where f is defined as

$$f \equiv 1 - [R(NSRB)^2 / R(IRL)^2] \qquad (A.1)$$

and IRL is the maximum number of radial mesh points describing the reactor core.

Equation (A.1) indicates that varying NSRB from cycle to cycle would permit reloadings with different batch fractions at each cycle. CORCOST does just that by reading in a new value for NSRB called NSRB1 for each cycle.

Having different size batches of fuel of different initial enrichments in the reactor requires the addition of two new parameters, other than batch number and spatial flux-time distributions, to describe each batch for fuel in the inner (1-f) region of the core. IPROP(k) designates the CELL data input to CORCOST that contains the time dependent properties for batch k fuel. The volume fraction for each batch k, VOLFRC(k), is defined as

$$VOLFRC(k) = \frac{VOL(k)}{\sum_{k=1}^{KK} VOL(k)} \qquad (A.2)$$

where

VOL(k) is the volume of batch k in the inner (1-f) region of the core and

KK is the total number of batches in the inner region.

The volume fractions of all batches of fuel are calculated at the beginning of each cycle. This calculation is necessitated by the fact that the unloading of portions of a batch or the changing of the size of the inner zone can alter the volume fractions of batches from one cycle to the next.

Any changes in the size of the inner zone also requires changes in the scattering of all the fuel in that zone. The CORCOST code places equal amounts of fuel from each batch of fuel be present at each inner region mesh point in order to simulate the scatter refueling procedure. For example, if an inner zone includes all mesh points out to and including the tenth mesh point, NSRB = 10, and if 30% of the fuel represented at mesh point 10 is batch No. 2 fuel then 30% of the fuel represented at mesh point 3 is batch No. 2 fuel. If the inner zone is expanded during the next cycle out to mesh point 11, NSRB1 = 11, this fuel in batch No. 2 must be redistributed in equal amounts over this new larger zone. This is accomplished by recalculating the volume fraction for batch No. 2, VOLFRC(2), as was previ-

ously mentioned and by recalculating the flux-time values at all of the mesh points, one through eleven for all batches. This expansion of the inner zone would reduce VOLFRC(2). The flux-time values are recalculated in the following manner for a change in NSRB to NSRB1.

$$\bar{\theta}(J,k) = \frac{\sum_{I=1}^{NSRB} \theta(I,J,k)\cdot V(I,J)}{\sum_{I=1}^{NSRB} V(I,J)} \qquad (A.3)$$

for each J and for each k.

In Equation (A.3) I and J are the radial and axial mesh point notations respectively, V(I,J) is the volume at mesh position I, J and $\bar{\theta}$ (J,k) is the average flux-time exposure of batch k fuel in a radial plane at axial position J. θ for all mesh points in the inner region is given by:

$$\theta\ (I,J,k) = \bar{\theta}\ (J,k) \quad \begin{array}{l}\text{for I=1 to NSRB1}\\ \text{for all J}\\ \text{for all k}\end{array} \qquad (A.4)$$

Fresh fuel is loaded into the outer region, I = NSRB1 to IRL, of the core. Since there is only one batch of fresh fuel, i.e. not yet irradiated, the volume fraction of this fuel is unity, θ(I,J,k) for the entire outer region is zero and the initial enrichment of this fuel is designated by the interger IPPROP. (See Section A.3).

A detailed explanation of the flow of logic in the RESHFL subroutine is presented in the next section. However, a brief explanation of RESHFL's use might be advantageous prior to discussing its logic. In general, the flux-time values for each mesh point at the end of a previously calculated cycle, referred to as EOC's, are read into CORCOST. Likewise, the volume fractions and enrichment specifications for this fuel are read into the code. RESHFL is immediately called to prepare the fuel in the reactor for the first cycle of the present calculation. Using the specified reload batch fractions and enrichments RESHFL discharges all the fuel needed, scatters all of the remaining fuel in the inner region and then loads the core with the correct fuel in the outer region. The first cycle depletion is then performed and RESHFL is again called at the end of that cycle. It performs the same refueling procedures as mentioned above but also calls subroutine BATCH and CYCOST which calculate the nuclear fuel revenue requirements during this first cycle. This entire procedure is performed for each subsequent cycle of this calculation with the exception of the last cycle.

At the end of the last cycle in a given calculation RESHFL also simulates refueling the core with all feasible batch fractions f. The number of feasible f's are designated by two parameters included in the DATA statement in the

RESHFL routine. They are MAXF, the maximum number of f's to be surveyed, and MINF the number of the radial mesh points associated with the smallest feasible reload batch fraction. This simulation uses the estimating subroutine ESTMAT, Appendix D.4, to predict for each feasible f the reload enrichment and costs of producing a specified amount of energy.

It should also be noted that CORCOST is not limited to commencing its calculations with EOC θ's. Beginning of cycle θ's can be used or the option also exists to use no θ input values at all.

A.2.2 The Flow of Logic in the RESHFL Subroutine

Figure A.1, The Flow of Logic in the RESHFL Subroutine, outlines the sequence of operations performed by the RESHFL subroutine. RESHFL is called by Subroutine MOVESC and CORCOST code at the beginning of the first cycle of the calculation and at the end of every cycle in the calculation. The numbers at the top of the operation boxes refer to the Fortran statement number in the RESHFL subroutine where this operation is performed. The parenthesis inside operation boxes specify the subroutine called by RESHFL to perform this operation. A "Case" as used in Table A.1 refers to one CORCOST calculation which may involve many consecutive cycle calculations. BOC and EOC refer to the beginning and end of a cycle respectively. E_{I+1} is the required energy from the first cycle after all cycles in the present case and ϵ_{I+1}, BU$, FAR$, and MC_{I+1}, are the required reload enrich-

Figure A.1 Flow of Logic in the RESHFL Subroutine

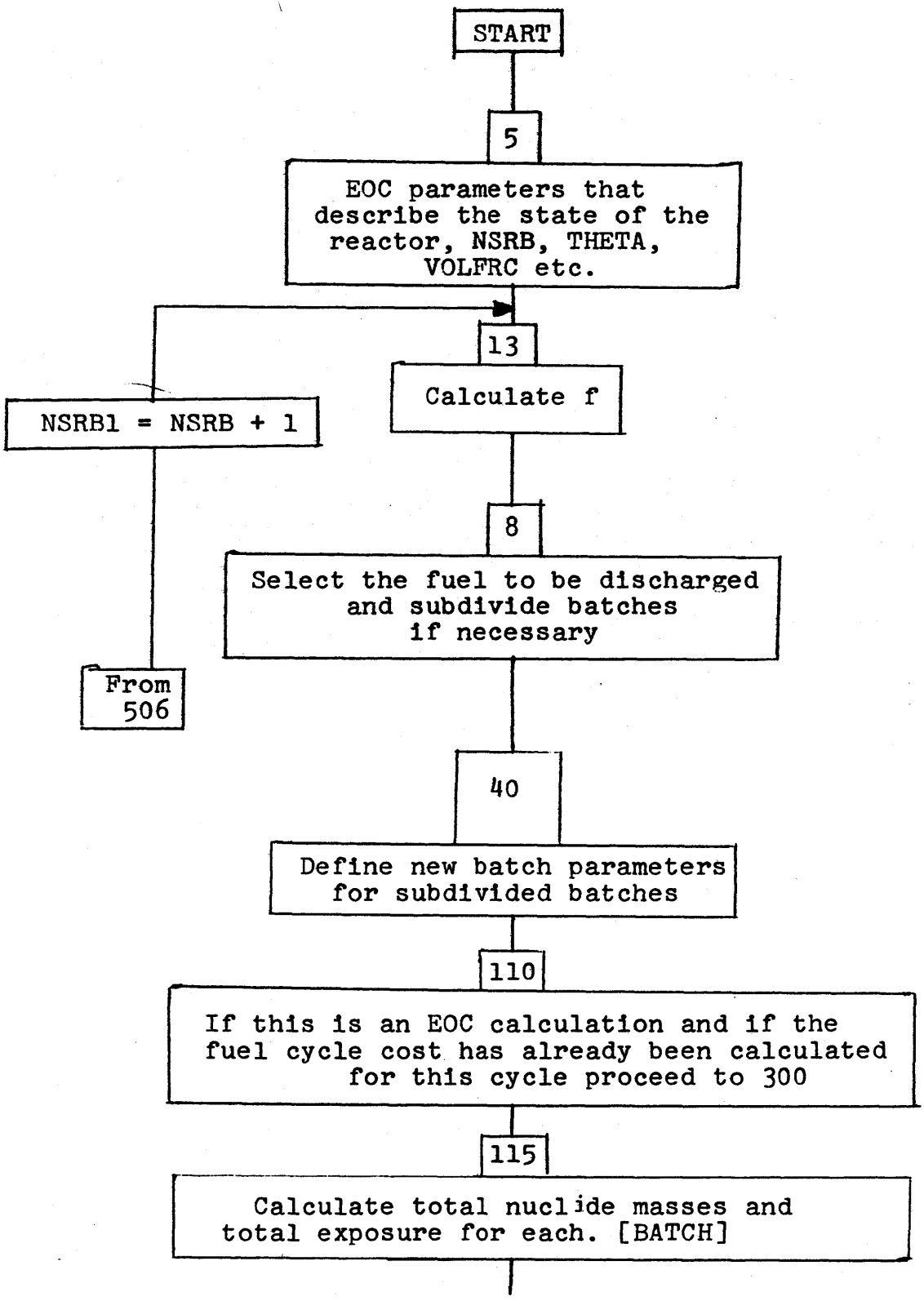

Figure A.1 (Cont'd)

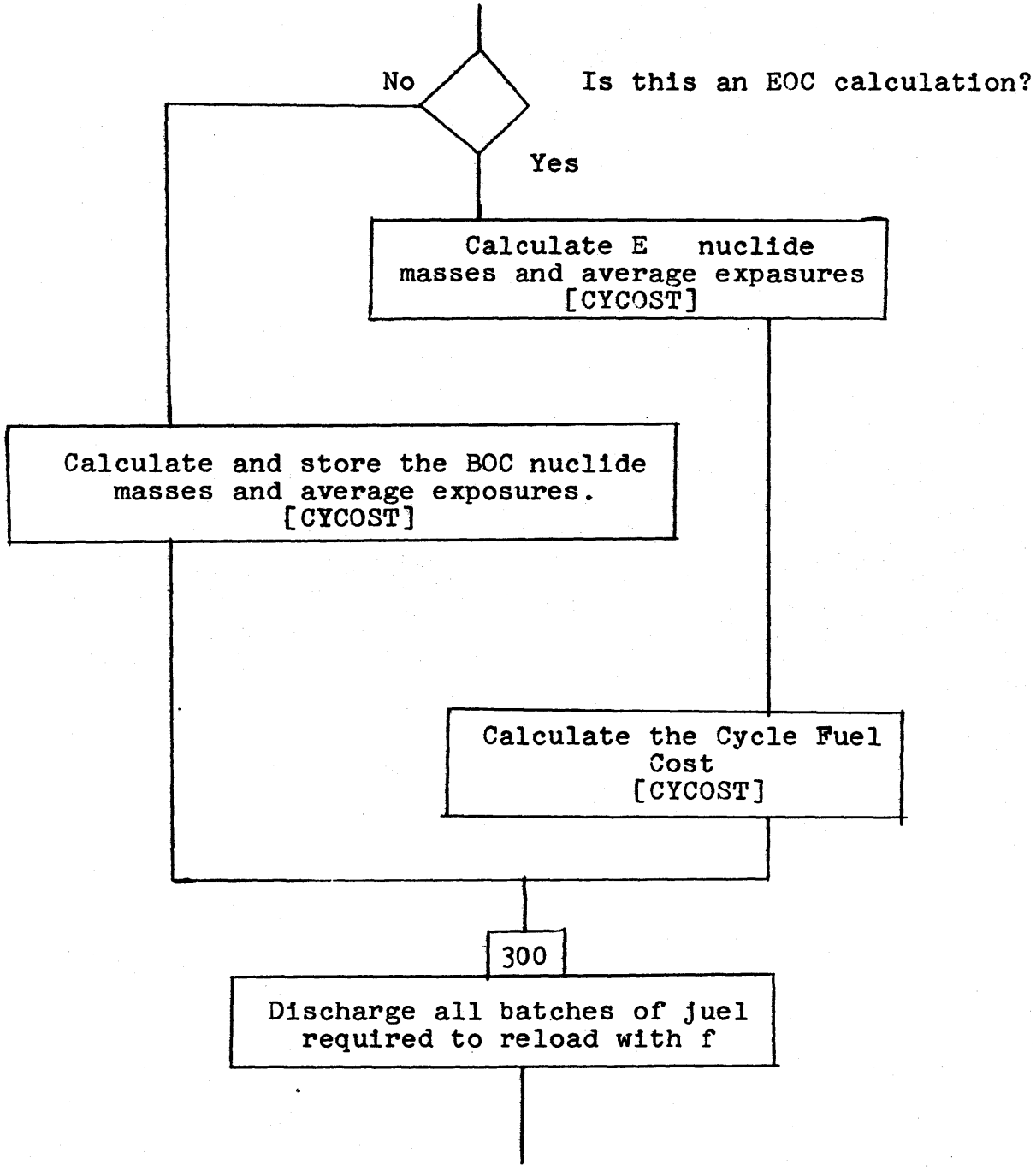

Figure A.1 (Cont'd)

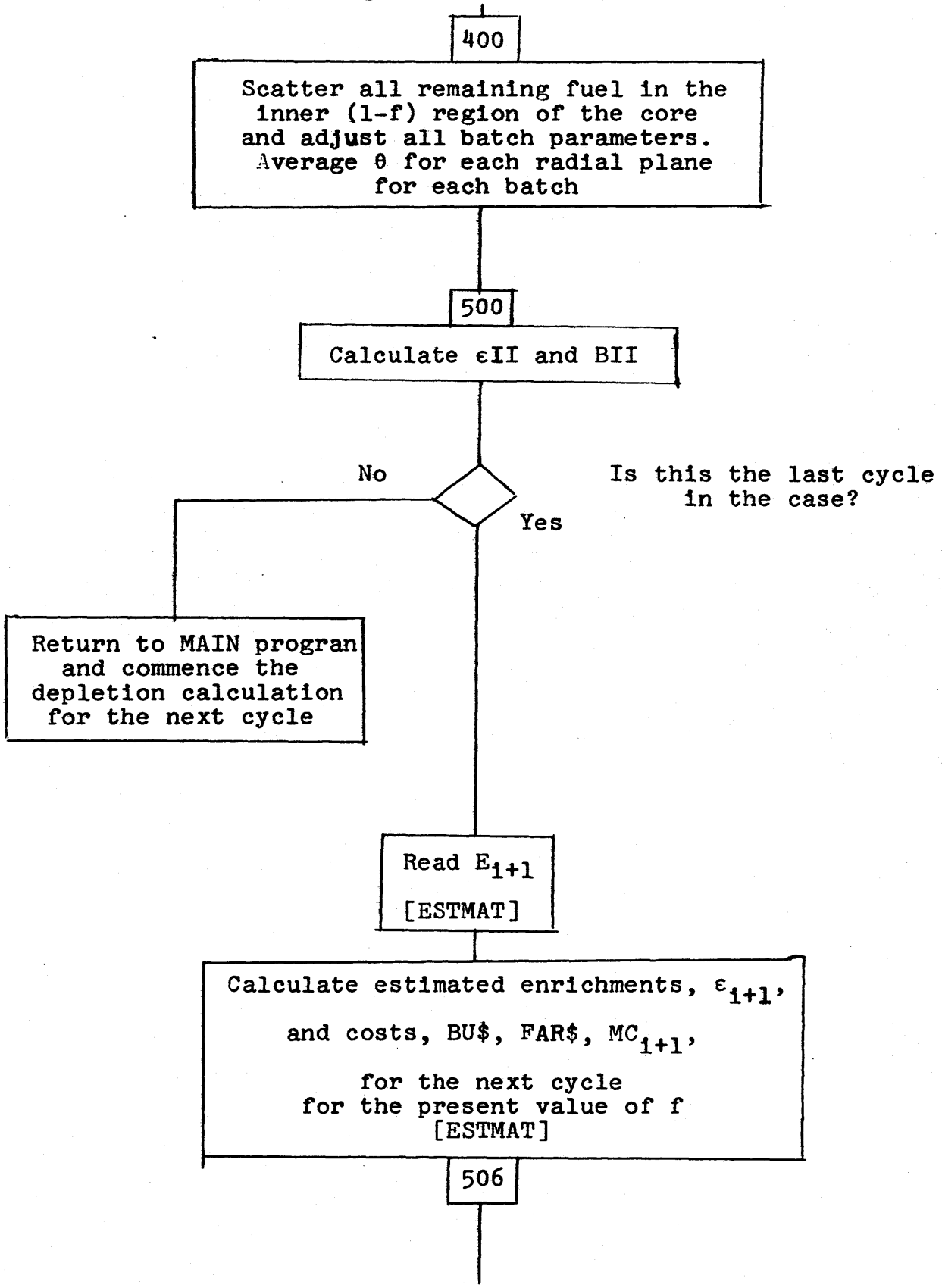

Figure A.1 (Cont'd)

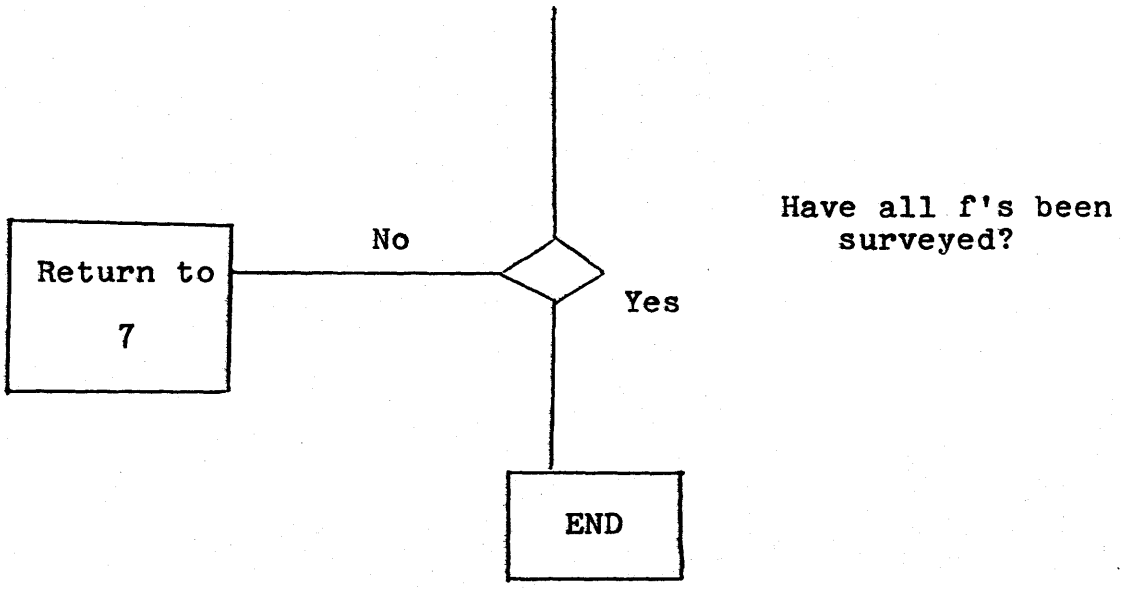

ment, burnup, fixed and marginal costs respectively incurred in the production of E_{I+1}, see Chapter 4.

A.3 CORCOST Input Description

There are nine basic types of input data used by the CORCOST code. They are:

I. Title Card
II. Floating Point Data
III. Fixed Point Data
IV. Reload Enrichment Specification
V. Radial Mesh Position Designation
VI. CELL Data
VII. Poison Data
VIII. Starting Flux-Time Data
IX. Fuel Batch Size and Economic Information

Definitions of all variables are given along with the limitations on their size and the format in which they are to be punched on cards. See Sections 2D and 4 of Summary Description of the Fuel Depletion Code CELLMOVE (21) for more elaborate definitions of the variables.

Some definitions refer to the variable ZETA, which is used in CELL as the size of the flux-time step, in neutrons/barn, for the step-wise solution of the nuclide concentration equations. The input data described below must be supplied exactly in the order given.

I. Title Card:

All 72 columns are available for use.

II. Floating Point Data:

This data is punched on three cards in 6E12.8 format.

H	active height of core, cm
DELR	radial reflector savings, cm
DELH	axial reflector savings, cm
ZSYM	axial symmetry control; if = 0.0, core is assumed to be axially symmetric around midplane; if ≠ 0, full core height calculation is performed
DBSQU	initial thermal leakage estimate, cm^{-1}
PFAST	initial fast non-leakage probability estimate
PDENAV	core average power density, kW/l
ERROR	flux iteration convergence criterion; when $\|\Delta\phi\|/\phi <$ ERROR at all points, flux iteration has converged
DELCRT	end-of-life convergence criterion; when k_{eff} with no control poison is within CRIT $\pm$ DELCRT, the cycle is terminated and the reactor refueled (CRIT is defined next).
CRIT	the no control k_{eff} desired at the end of each cycle, normally 1.0
ZET2	the central flux-time step taken during the irradiation, neutrons/barn
F	over-relaxation parameter in extrapolated Liebmann method; must be between 1.0 and 2.0, with 1.5 generally a good choice

TIGG maximum number of iterations permitted for flux calculation; a number >50 is usually satisfactory

SSCVG convergence criterion for attainment of steady-state refueling; when $|\Delta\theta|/\theta$ <SSCVG for all points of two successive discharged fuel batches, steady-state is attained.

EIGMN1 specifies the error allowed in the eigenvalue as it converges on 1.0

FDAMP as the change in soluble poison content is made in an attempt to reach criticality FDAMP is the ratio of the new recommended poison content and the previous poison content. Suggest FDAMP = 0.96

DKNU DKNU is the error convergence criteria on the eigenvalue in the inner iterations. DKNU < EIGNM1

III. Fixed Point Data:

The following data is punched in 2613 format.

NLOAD=N this specifies that N sets of CELL data are to be read into the code. Each set corresponds to a different enrichment. In subsequent cases, see input data group IX, NLOAD = 0 and new cell data need not be read in. In this case the N sets of CELL data from the previous case are used by the code.

NSRB the number of the outermost radial meshpoint in the scatter region. If IVARFR = 1, NSRB must be

the outermost radial meshpoint in the scatter region for the cycle that generated the θ cards which are to be read, see Section VIII, into the code C. If no θ cards are read in NSRB = NSRB1) and NSRB1 will be the outermost radial meshpoint in the scatter region for the cycle to beccalculated.

IRL — total number of radial mesh points. IRL can be any number, but it must be greater than NSRB

JZL — total number of axial mesh points, any number

NCYCM — maximum number of cycles to be run for this case

NTHETP=0 — print out flux-time distribution at start and end of each cycle; ≠0, bypass printout

NCP — >0, and IVARFR ≠ 1, punch starting flux-time distribution for (NCP+1)st cycle at end of NCPth cycle and foreevery subsequent cycle in increments of NCP; = 0, bypass punching of cards. If NCP > 0, and IVARFR = 1, punch out end of cycle flux-time distribution for the NCPth cycle and for every subsequent cycle in increments of NCP. If = 0, bypass punching of cards.

IPHBAT>0 — punch BATCH output data of nuclide masses, total core mass, average burnup data etc.

IPOIS poison management control parameter;
= 1, uniform poison removal
= 2, radial zone poison removal
= 3, axial bank poison removal

NPOISR number of radial mesh points, starting at the outer edge of core, containing no control poison

ITRATE maximum number of iterations permitted in obtaining the correct amount of control poison to give a poisoned k_{eff} within 1.0 ± 0.005

IPRT1 $\neq 0$, print out flux, power and theta distributions at each flux-time step; = 0, bypass printout but see IPRT3 below

IPRT2 $\neq 0$, print out detailed results from all subroutines; = 0, bypass printout; generally = 0

IPRT3 $\neq 0$, print out flux and power distributions at start and end of each cycle; = 0, bypass printout

IPSPPR $\neq 0$, print out values of lattice properties at each mesh point whenever they are calculated; = 0, bypass print out; generally = 0

IPSGMW $\neq 0$, print out control poison macroscopic absorption cross section at each mesh point; = 0, bypass print out

INORMP >0, normalized control poison absorption cross section read in for each mesh point; = 0, set to 1.0 at each point; <0, current values go unaltered

IABSP >0, absolute (fixed) poison macroscopic absorption cross section read in for each mesh point; = 0, set equal to zero at each point;< 0, current values go unaltered.

ITHET >0, flux-times normalized to the CELL value for ZETA are read in at each point to start the calculation; = 0, flux times set equal to zero at each point; = -1, current values go unaltered; < -1 THETA is set equal to THETAL for all mesh points for each zone.

NEWTHP = 0, print out flux time distribution at start of steady state cycle and punch flux times on cards suitable for subsequent input to CORE; = 1, print only; = 2, bypass both printout and punching.

NOZONE the total number of zones in the first reactor cycle or if ITHET > 0 NOZONE must be the total number of zones for the reactor cycle from which the flux time, THETA, values are being used to start the present cycle.

IFUELS this integer specifies the number of refuelings of the reactor that are to be simulated by this case. The refuel enrichment, see IENRIC(I), and refuel fraction, see NEWR(I), data are read

into the code on the basis of IFUELS, i.e. from 1 to IFUELS. IFUELS must be > 0.

IVARFR = 1, initiates the use of the variable reload batch fraction option. This option requires the operator to specify the size of the refuel batch as well as its enrichment. The size is designated by the NEWR(I) parameter. NEWR(I) specifies the radial mesh point that is to be the outer mesh point of the inner zone for the Ith refueling cycle. Therefore that fraction of the entire core that will be fresh fuel at the beginning of the Ith cycle, the reload fraction, FRAC, is

$$FRAC = \frac{R(IRL)^2 - R(NEWR(I))^2}{R(IRL)^2}$$

If IVARFR ≠ 1 the reactor is loaded with the same fraction at each refueling namely,

$$FRAC = \frac{R(IRL)^2 - R(NSRB)^2}{R(IRL)^2}$$

NSRB1 is the radial mesh designation of the outer-most radial mesh point for the inner zone for the first cycle of the present case.

IPRT4 =0 print out core average values of P1, QOPHI, SIGMA etc. and flux and power peaking factors at each depletion step

=1 no printing of these is done.

IV. Reload Enrichment Specification:

A) IPPROP specifies the initial enrichment of the outer zone of the reactor. It is specified by an integer from one to NLOAD. Each integer corresponds to a respective CELL data set read into CORE. e.g., IPPROP = 3 signifies that the third set of CELL data read into CORE contains the depletion information for the fuel enrichment desired in the outer zone. For obvious reasons:

$$IPPROP \leq NLOAD$$

IPROP(I) I = 1, KKZONE

these specify the initial enrichments in each of the zones (I) in the scatter region of the reactor. KKZONE = NOZONE - 1. The restriction that applies to IPPROP also applies to IPROP (I).

If IVARFR = 1 then IPPROP and IPROP(I) specify the initial enrichments for the batches represented by the flux time data, THETA

cards, which is to be read into the code. IPPROP and IPROP(I) are read in on the same card in 24I3 format.

B) IENRIC(I) I=1, IFUELS

these specify the refuel batch enrichment, the batch inserted in the outer zone, at each refueling I. If IVARFR ≠ 1 the enrichment designated for the first refueling, I=1, represents the fuel in the outer zone during the second cycle. If IVARFR = 1 IENRIC(I) represents the fuel in the outer zone during the first cycle. This is due to the fact that the values for IPPROP and IPPROP(I) read into the code were the reactor enrichment values for the end of the cycle which generated the flux time, theta, values which are to be reshuffled before the first cycle of the present case is calculated.

V. Radial Mesh Position Designation:

R(I),I=1,IRL outer radii for each radial mesh area, cm; in 6E 12.8 format

VI. CELL Data:

Read in block of cards containing CELL punched output, including the heading card punched by CELL.

VII. Poison Data:

A) Normalized Control Poison Data:

If INORMP>0, read in pointwise control poison macroscaopic absorption cross section arbitrarily normalized, i.e., in relative units. These are read in as ((SIGMWN (I,J),I=1,40), J-1, JZL) in 6E12.8 format.

B) Absolute Poison Data:

If IABSP>0, read in pointwise values for the fixed poison macroscopic absorption cross section as ((SIGMWA(I,J), I=1,40), J=1,JZL) in 6E12.8 format.

If IABSP $\leq$ 0, skip this part and go on to VIII.

VIII. Starting Flux Time Data:

If ITHET > 0, THETA flux time cards are to be read into the code. The first card is the title card. The first 72 columns give the title for the case from which these theta cards were generated. Columns 72-78 contain IX, JX, KX in 3I2 format where:

IX is the number of radial mesh points for which THETA's are to be read in.

JX is the number of axial mesh points for which THETA's are to be read in, and KX is the number of zones for which THETA's are to be read in. The next cards are the THETA cards for each of the above designated meshpoints as (((THETA (I,J,KK), I=1, IX), J=1,JX), KK=1, KX) in 10F8.5 format. These flux times are normalized to the CELL value for ZETA.

IX. Fuel Reload Batch Size Specification:

If IVARFR = 1 the following cards are read in if IVARFR ≠ 1 the input is completed for this case. Any number of cases can be run consecutively. If a second or subsequent case is to be run, merely repeat steps I through IX.

A) IBOC = 1, (I3 format)

The flux time, THETA, values read into the code are the desired beginning of cycle THETA's

= 2

The flux time, THETA, values read in were end o cycle values and must be adjusted, i.e out-in-scatter reshuffling is to be performed, automatically by the code. If no THETA cards are read in IBOC = 1.

B) VOLFRC(KK), KK = 1, KKZONE: (8F10.5 format)

The fractions of the inner zone occupied by each KK batch in the inner zone. If THETA cards are read in these fractions are for the cycle from which those cards were punched. If no THETA's are read in they are first cycle volume fractions.

C) TSCED (L,M), 1 = 1, 9; M = 1, 2 (9F8.3 format)

The time schedule in years for energy production for NCYCM + 4 cycles. L is the cycle designation.

M = 1 and 2 designates the time at the beginning of cycle energy production and for the time at the end of cycle energy production respectively. In order to account for refuelings

$$TSCED(L,2) \neq TSCED(L+1,1) \text{ for all } L$$

Since CYCOST calculates the ultimate discharge time for each reload batch on the basis of the cycle time schedule TSCED for future cycles, A TSCED must be given for four cycles beyond the maximum number of cycles required for each case.

D) TEVEC (k,N), k = 1, KKZONE; N = 1,4 (4F10.4 format)
The batch information required by CYCOST for each batch of fuel for which THETA cards were read in.
TEVEC (k,1) = The time that payment was made for fabrication of batch k fuel.
TEVEC (k,2) = The time that payments for reprocessing and conversion of batch k fuel were made.
TEVEC (k,3) = The initial enrichment of batch k fuel.
TEVEC (k,4) = Estimated average discharge exposure in MWD/T for batch k.

E) NEWR(I), I = 1, IFUELS (26I3 format)
NEWR(I) is the radial mesh point that is to be the outer mesh point of the inner zone for the Ith refueling cycle.

F) E(I) (F10.3 format)

E is the cycle energy which will be demanded of the reactor in cycle I = NCYCM + 1, the cycle which follows the last cycle of the present calculation.

A.3.1 HALT Designations in CORCOST

The CORCOST code automatically terminates when certain errors occur. These terminations are performed by the Subroutine HALT which prints an error message and an integer indicating the specific error and the subroutine in which it occurred. The following describes what error each of these integers refers to:

Integer	Subroutine	Error
0	SETUP	SETUP does not have enough available storage in array A. for this case. Correct by re-compiling MAIN with larger A.
1	MOVESC	Differential control flux time step is <0.0001 n/kb. This may result in infinite Do loop due to round-off errors.
2	SPACFX	Fluxes converged to negative values.
3	SPACFX	"OMEGA", i.e. fluxes, not converged in TIGG iterations.

4	SPFUN	IPOIS 0, wrong loop, insufficient poison, wrong NPOISZ or NPOISR.
5	MOVESC	Criticality error C CRIT even with no xenon or samarium.
6	PTPROP NCGTHV	$\sum_{I=1}^{4}$ ALAGZZ(I) $\neq$ 1. $\pm$ .00002. May attempting a lagragian fit outside range of available CELL data.
7	NCGTHV	negative atom densities.
8	MOVESC or RESHFL	Extrapolation of THET to k_{eff} = CRIT does not converge an attempt was made to reshuffle fuel using beginning of cycle thetas and with NSRB1 NSRB.
9	INPUT	NOZONE or IFUELS greater than maximum allowed in this version.

APPENDIX B: UNIT CELL INFORMATION TRANSFERRED FROM CELL TO CORCOST

N_m	Number densities for all pertinent nuclides, 8, cm^{-3}
$\nu\Sigma_f$	Number of neutrons released by thermal fissions per unit of thermal flux, cm^{-1}
Σ_f	Homogenized macroscopic thermal fission cross sections, cm^{-1}
$\frac{1 - P}{1 + \alpha}$	Number of resonance fissions per unit of slowing down density entering the resonance region
$\eta(1-P)$	Number of neutrons released by resonance fissions
P	Overall resonance escape probability
Σ_x	Xe-135 macroscopic absorption cross section
Σ_a	Cell macroscopic absorption cross section, excluding Xe-135

APPENDIX C: THE CYCOST ROUTINE

The CYCOST subroutine of the CORCOST code calculates the revenue required to produce nuclear energy during one cycle of operation and also sums up the requirements of many cycles to calculate the nuclear fuel revenue requirements over a multi-year horizon. The inputs to the subroutine include:

1. The cycle energy production and the uranium and plutonium nuclide masses at the beginning and end of each cycle as calculated by the CORCOST code
2. The time, TSCED, at the beginning and end of each cycle which is input by the code operator.
3. The time for purchase payments and credits received for all of the fuel in the reactor which is also an operator input.

The unit cost information used by CYCOST, see Table C.1, are included in a DATA statement at the beginning of the subroutine, see Section C.2.

TSCED (L,M) is the time schedule in years for the energy produced in Cycle L. The time at the beginning of energy production for the cycle is designated by M = 1 and at the end of energy production for the cycle by M = 2. The refueling shutdown time's $T_s(L)$, are not explicitly input to the code. However, they are calculated from TSCED,

Table C.1

Unit Cost and Fixed Time Parameters

Input to the Cycle Cost Routine CYCOST

CUF6	Unit cost of UF_6, \$kg U
CSEP	Charge for enrichment services, \$/kg Sep. Work
CFAB	Unit cost of fabrication services, \$/kg U
CRESH	Unit cost of fuel reprocessing and shipping, \$/kg U
CCONV	Unit cost of conversion of UNH to UF_6, \$/kg U
CP	Price of plutonium, \$/kg
XRATE	Effective cost of money
XF	Enrichment of the uranium input to the diffusion process
XW	Enrichment of the uranium tails from the diffusion process
TAUT	Income tax rate
TAPRE	Time prior to insertion of nuclear fuel when payments for uranium enrichment and fabrication is paid for
TPOST	Time after fuel discharge from the reactor when credit is received for spent fuel and reprocessing, conversion and shipment is paid for

$$T_s(L) = TSCED\ (L + 1,1) - TSCED\ (L,2) \qquad (C.1)$$

TEVEC(k,N) is the batch information required by CYCOST for each batch, k, of fuel in the reactor during the cycle being calculated. N = 1 designates the time that payments were made for the fabricating of the batch. k = 2 designates the estimated time that payments for processing and conversion of batch k fuel were made. N = 3 designates the initial enrichment of batch k. N = 4 designates the estimated average discharge exposure in MWD/T for batch k.

C.1 The Sequence of Calculations in CYCOST

The calculation of the nuclear fuel revenue requirement to produce cycle energy E_i procedes in the CYCOST code as described in Figure C.1.

C.2 CYCOST Fortran Listing

The following is the fortran source listing of the CYCOST subroutine. [All fortran listings are available through Prof. E.A. Mason's office or in the Nuclear Engineering Department's Library]

Figure C.1 The Flow of Logic in the CYCOST Subroutine

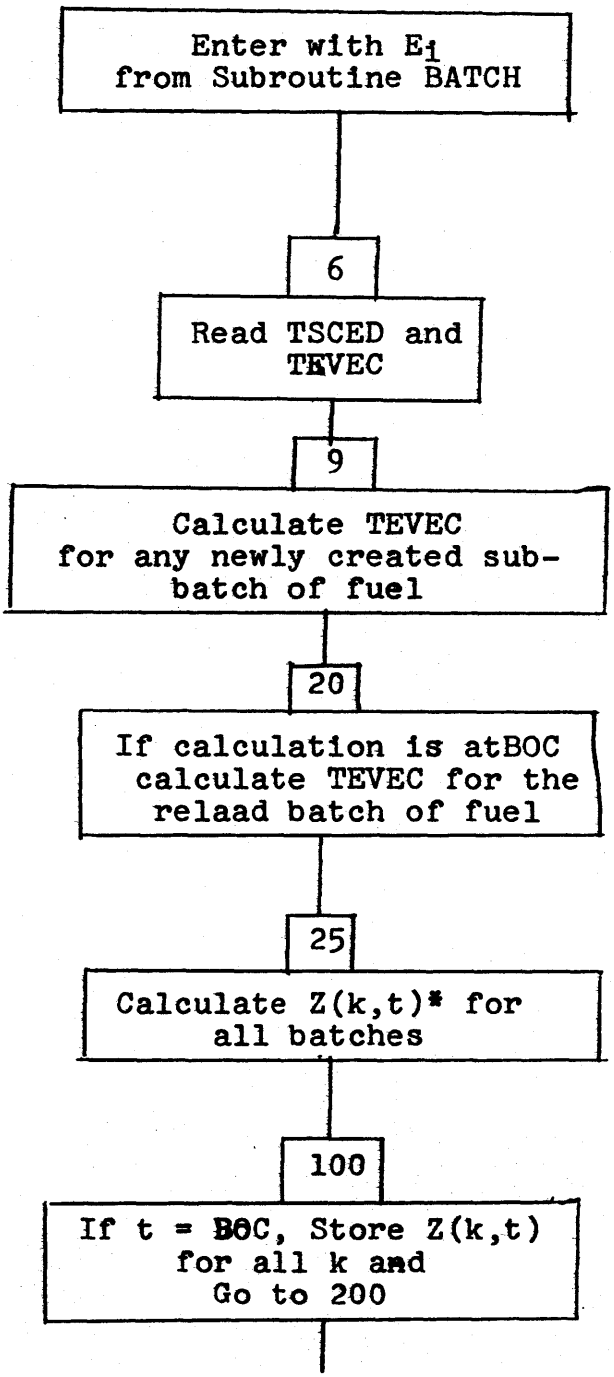

* See Equation (3.8)

Figure C.1 (Cont'd)

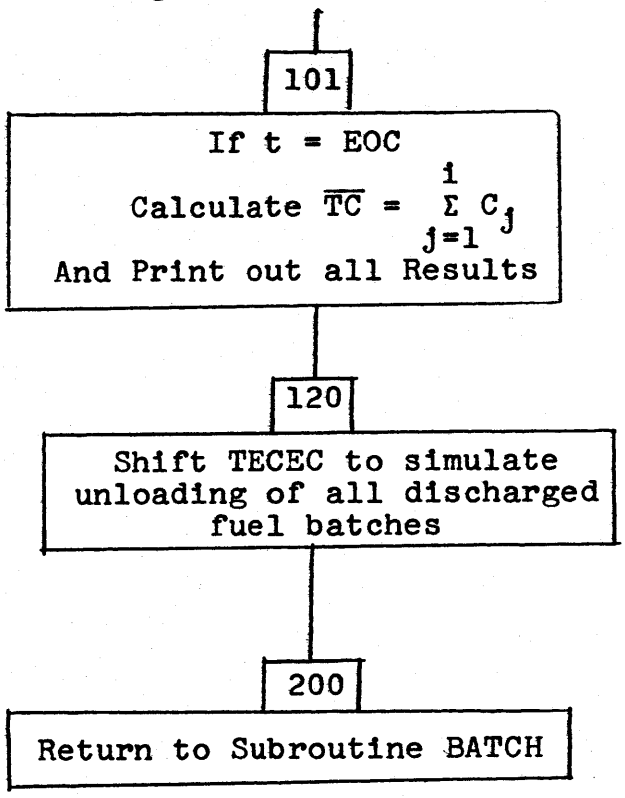

APPENDIX D: THE ZION REACTOR DATA CORRELATIONS

The end of cycle evaluation performed by the Dynamic program, (see Section 4.3.2.1) depends upon correlations to previously accumulated data on costs and energy production for the reactor being optimized. The first section, D.1, of this appendix describes the method for developing these correlations, the second section, D.2, lists all of the correlations used by the dynamic program for the Zion-I reactor and the third section, D.3 is a source listing of the ESTMAT subroutine of the CORCOST code into which these correlations are coded.

D.1 Least Squares Curve Fitting Procedures

The least squares curve fitting procedure and the best fit evaluation criteria described here are a paraphrasing of selected sections of Bevington's Data Reduction and Error Analysis for the Physical Sciences (4). The least squares fit calculations were performed using the computer code MULTIFIT written by P.F. Deaton (11) based on Bevington's work. The MULTIFIT code has the option of using any combination of eleven different terms in the fitting equation and can relate one dependent variable to a maximum of three independent variables. The function which is used by MULTIFIT contains the following terms:

$$Y(X,U,V) = A_o + A_1X + A_2X^2 + A_3U$$
$$+ A_4 \cdot U^2 + A_5 \cdot X \cdot U + A_6 \cdot U \cdot X^2 + A_7 \cdot U^2 \cdot X$$
$$+ A_8 \cdot X^2 \cdot U^2 + A_9 \cdot V + A_{10} \cdot V^2 + A_{11} \cdot X^3 \qquad (D.1)$$

The selection of the best set of terms in the correlation function and the variables which best describe the physical situation are based on the following correlation evaluating parameters.

1. The Multiple-Linear Correlation Coefficient, R.

R characterizes the correlation between a multitude of variables and is defined as

$$R^2 \equiv \sum_{j=1}^{n} \left(b_j \cdot \frac{S_j}{S_y} \cdot r_{jy}\right) \qquad (D.2)$$

where:

r_{jy} is the linear correlation coefficient between variables j and y

S_j^2 is the sample variance in j

S_y^2 is the sample variance in y

b is the slope of the straight line fit between j and y.

For a good fit R should be 1.

2. Reduced chi Squared, χ^2

χ^2 is a measure of the variance in the fitting function and the data base,

$$S^2/\overline{\sigma_i^2} \qquad (D.3)$$

where:

S^2 is the variance of the fit, a weighted average of the variances of the estimated function to the data and

σ_i^2 is the weighted average of the individual variances, σ_i^2, of each data point i.

If χ^2 is close to 1 the fit is good.

The χ^2 test is somewhat ambiguous in most instances unless the form of the parent function is known because tha statistics χ^2 measures not only the discrepancy between the estimated function, S^2, and the parent function but also the deviations between the data and the parent function simultaneously. F tests separate these two types of information and concentrates on the former permitting the evaluation of the estimated function vis a vis the data.

3. F-test of the Multiple Correlation Coefficient, F_R

Performing an F-test in terms of the multiple correlation coefficient can evaluate the goodness of an entire fit. Define:

$$F_r = \frac{R^2(N-n-1)}{(1-r^2)\ n}$$

where:

N is the number of data points,

(n+1) is the number of terms being fit

R is the multiple correlation coefficient, Equation (D.2) and

n is the number of variables being fit.

A large F_r corresponds to a good fit where the multiple correlation is good, i.e. $R \doteq 1$. A methodology for evaluation how large an F_r corresponds to what degree of accuracy of the fit is presented in Bevington (4), Section 10.2. F_r is essentially a test of the validity of the coefficients of a fitting function being non-zero.

An additional check on the correct inclusion of a term in the fit equation can be performed by comparing the fits achieved with the term included and with the term excluded. The comparison is usually based on the reduced chi squared, χ^2, values for each fit where F_χ is defined as

$$F_\chi = \frac{\Delta\chi^2}{\chi^2} \qquad (D.5)$$

If F_χ is small the additional term has not significantly improved the fit.

The fitting procedure used to derive the correlations relating nuclear reloading strategies and costs with cycle energy production used the above criteria in the following manner:

1. Select a set of variables which seem to describe the physical situation best.
2. Using the F test select the combination of terms that fits the data best for the variables selected in step 1. This is done by a trial and error approach where many combinations of terms are used to fit the data.
3. If the best fit does not reasonably satisfy the criteria

$$R = 1$$

$$\chi_V^2 = 1$$

F_R is large

return to step 1.

D.2 The Estimating Equations for the Zion-I Reactor

The following correlations, Table D.1, were derived to estimate the enrichment, ε_i, required to produce cycle energy E_i and the revenue required, BU$ and FAR$, to produce that energy. The state of the reactor to which these parameters are correlated are the average fissile enrichment, EII, and the average burnup, BII, of the inner (1-F) region of the reactor core.

D.3 The ESTMAT Subroutine Fortran Listing

The ESTMAT subroutine contains all of the Equations in Table D.2.1 as well as the equations for the sensitivity of reload enrichment to cycle energy, PEI, where

$$PEI = \frac{\partial \varepsilon}{\partial E_i} \qquad (D.3.1)$$

and for the incremental cost of energy in cycle i, MC_i,

$$MC_i = \frac{\partial BU\$}{\partial E_i} \qquad (D.3.2)$$

The Fortran listing for ESTMAT is given here to aid any future researchers who may wish to update the correlations given in Section D.2.

Table D.1

The Estimating Equations for Reload Enrichment and Revenue Requirements

$f = 0.37\dot{3}$

$$\varepsilon_i = 3.10761 - 1.49845 \cdot \varepsilon II - 0.237206 \cdot \varepsilon II^2 + 3.11489 \times 10^{-4} \cdot E_i + 4.74038 \times 10^{-10} \cdot \varepsilon II \cdot E_i^2 + 8.09742 \times 10^{-5} \cdot BII$$

$$BU\$ = -0.310964 \times 10^7 + 0.107712 \times 10^7 \cdot \varepsilon_i + 0.305585 \times 10^3 \cdot E_i + 4.43063 \cdot E_i \cdot \varepsilon_i + 9.55709 \times 10^{-4} \cdot \varepsilon_i \cdot E_i^2 + 0.15588 \times 10^7 \cdot \varepsilon II$$

$$FAR\$ = 6.28349 \times 10^6 - 2.80687 \times 10^6 \cdot \varepsilon II + 0.970468 \times 10^5 \cdot \varepsilon II^2 + 0.461963 \times 10^2 \cdot E_i + 0.917865 \times 10^{-1} \cdot E_i^2 + 0.164320 \times 10^3 \cdot E_i \cdot \varepsilon II + 0.245040 \times 10^2 \cdot E_i \cdot \varepsilon II^2 - 0.309479 \times 10^{-1} \cdot \varepsilon II \cdot E_i^2 - 0.190199 \times 10^7 \cdot E_i$$

$f = 0.33\dot{3}$

$$\varepsilon_i = 1.16345 + 2.30001 \cdot \varepsilon II - 1.18019 \cdot \varepsilon II^2 + 3.25073 \times 10^{-4} \cdot E_i + 1.57951 \times 10^{-9} \cdot \varepsilon II \cdot E_i^2 + 1.09669 \times 10^{-4} \cdot BII$$

$$BU\$ = -0.675096 \times 10^{7} + 0.284416 \times 10^{7} \cdot \varepsilon_i - 0.129942 \times 10^{6} \cdot \varepsilon_i^{2} + 0.514726 \times 10^{3} \cdot E_i - 0.119137 \times 10^{3} \cdot E_i \varepsilon_i + 0.34411 \times 10^{-2} \cdot \varepsilon_i \cdot E_i^{2} + 0.166193 \times 10^{7} \cdot \varepsilon II$$

$$FAR\$ = 0.54296 \times 10^{9} - 0.598666 \times 10^{9} \cdot \varepsilon II + 0.156672 \times 10^{9} \cdot \varepsilon II^{2} - 0.170841 \times 10^{5} \cdot E_i - 3.04801 \cdot E_i^{2} + 0.42431 \times 10^{5} \cdot E_i \cdot \varepsilon II - 0.148535 \times 10^{5} \cdot E_i \cdot \varepsilon II^{2} + 1.30725 \cdot \varepsilon II \cdot E_i^{2} - 0.211411 \times 10^{7} \cdot \varepsilon_i$$

$$f = 0.29\dot{3}$$

$$\varepsilon_i = 3.97173 - 2.35004 \cdot \varepsilon II - 0.438245 \cdot \varepsilon II^{2} + 0.506433 \times 10^{-3} \cdot E_i + 0.377401 \times 10^{-10} \cdot \varepsilon II \cdot E_i^{2} + 0.148358 \times 10^{-3} \cdot BII$$

$$BU\$ = -0.555231 \times 10^{7} + 0.194353 \times 10^{7} \cdot E_i - 0.595997 \times 10^{5} \cdot \varepsilon_i + 0.504668 \times 10^{3} \cdot E_i - 0.836234 \times 10^{2} \cdot E_i \cdot \varepsilon_i + 0.236018 \times 10^{-2} \cdot \varepsilon_i \cdot E_i^{2} + 0.168889 \times 10^{7} \cdot \varepsilon II$$

$$FAR\$ = 0.61109 \times 10^{7} + 0.279393 \times 10^{8} \cdot \varepsilon II - 0.15666 \times 10^{8} \cdot \varepsilon II^{2} - 0.882404 \times 10^{4} \cdot E_i + 0.52623 \times 10^{4} \cdot E_i \cdot \varepsilon II - 0.243165 \times 10^{-1} \cdot \varepsilon II^{2} \cdot E_i - 0.111516 \times 10^{7} \cdot \varepsilon_i$$

$$f = 0.25$$

$$\varepsilon_i = -48.1031 + 43.8328 \cdot \varepsilon II - 11.9952 \cdot \varepsilon II^{2} + 3.13902 \times 10^{-3} \cdot BII - 0.0.9.657 \times 10^{-6} \cdot BII^{2} - 2.31941 \times 10^{-3} \cdot \varepsilon II \cdot BII + 0.573766 \times 10^{-3} \cdot BII \cdot \varepsilon II^{2} + 0.637000 \times 10^{-3} \cdot E_i + 0.250357 \times 10^{-8} \cdot E_i^{2}$$

$$BU\$ = -2.01972 \times 10^{6} + 9.06899 \times 10^{4} \cdot E_i + 7.8172 \times 10^{4} \cdot E_i^{2} + 4.33242 \times 10^{2} \cdot E_i + 9.23784 \cdot \varepsilon_i \cdot E_i - 7.00328 \times 10^{-4} \cdot E_i \cdot E_i^{2} + 1.51838 \times 10^{6} \cdot \varepsilon II$$

$$FAR\$ = 2.068 \times 10^{8} - 2.19394 \times 10^{8} \cdot \varepsilon II + 5.58196 \times 10^{7} \cdot \varepsilon II^{2} - 1.05725 \times 10^{4} \cdot E_i - 1.30784 \cdot E_i^{2} + 1.96125 \times 10^{4} \cdot E_i \cdot EII - 6.33677 \times 10^{3} \cdot E_i \cdot \varepsilon II^{2} + 0.558702 \cdot \varepsilon II \cdot E_i^{2} - 4.78231 \times 10^{5} \cdot \varepsilon_i$$

APPENDIX E: ZION-I REACTOR DESIGN DATA

Table E.1

Zion-I Reactor Nuclear Design Data
First Cycle (9)

STRUCTURAL CHARACTERISTICS		
1.	Fuel Weight (UO_2), lbs.	216,600
2.	Zircaloy Weight, lbs.	44,547
3.	Core Diameter, inches	133.7
4.	Core Height, inches	143.4
	Reflector Thickness and Composition	
5.	Top - Water Plus Steel	10 in.
6.	Bottom - Water Plus Steel	10 in.
7.	Side - Water Plus Steel	15 in.
8.	H_2O/U, (cold) Core	4.09
9.	Number of Fuel Assemblies	193
10.	UO_2 Rods per Assembly	204
PERFORMANCE CHARACTERISTICS		
11.	Heat Output, MWt (initial rating)	3,250
12.	Average First Cycle Fuel Burnup, MWD/MT	14,040
	First Cycle Enrichments, weight %	
13.	Region 1	2.25
14.	Region 2	2.80
15.	Region 3	3.30
16.	Equilibrium Enrichment	3.2
17.	Nuclear Heat Flux Hot Channel Factor, F_q^N	2.71
18.	Nuclear Enthalpy Rise Hot Channel Factor, $F_{\Delta H}^N$	1.58

Table E.1

(Continued)

CONTROL CHARACTERISTICS		
	Effective Multiplication (Beginning of Life)	
	With Burnable Poison Rods in; no Boron	
19.	Cold, No Power, Clean	1.183
20.	Hot, No Power, Clean	1.154
21.	Hot, Full Power, Clean	1.132
22.	Hot, Full Power, Xe and Sm Equilibrium	1.092
23.	Absorber Material	5% Cd; 15% In; 80% Ag
24.	Full Length, Number	53
25.	Part Length, Number	8
26.	Number of Absorber Rods per RCC Assembly	20
27.	Total Rod Worth, BOL, %	See Table 3.2.1-3
	Boron Concentration for First Core Cycle Loading	
	With Burnable Poison Rods	
28.	Fuel Loading Shutdown; Rods in (k_{eff} = .83)	2000 ppm
	Rods in (k_{eff} = .90)	1428 ppm
29.	Shutdown (k_{eff} = .99) with Rods Inserted, Clean, Cold	653 ppm
30.	Shutdown (k_{eff} = .99) with Rods Inserted, Clean, Hot	503 ppm
31.	Shutdown (k_{eff} = .99)with No Rods Inserted, Clean, Cold	1408 ppm

Table E.1

(Continued)

32.	Shutdown (k_{eff} = .99) with No Rods Inserted, Clean, Hot	1265 ppm
	To Maintain k_{eff} = 1 at Hot Full Power, No Rods Inserted:	
33.	Clean	1168 ppm
34.	Xenon	880 ppm
35.	Xenon and Samarium	850 ppm
36.	Shutdown, All But One Rod Inserted, Clean, Cold (k_{eff} = .99)	831 ppm
37.	SHutdown, All But One Rod Inserted, Clean, Hot (k_{eff} = .99)	734 ppm
BURNABLE POISON RODS		
38.	Number and Material	1436, Borosilicate Glass
39.	Worth, Hot, Full Power, $\Delta\rho$	9.0%
40.	Worth, Cold, $\Delta\rho$	7.0%
KINETIC CHARACTERISTICS		
41.	Moderator Temperature Coefficient at Full Power ($^{\circ}F^{-1}$)	$-.3\times10^{-4}$ to -3.2×10^{-4}
42.	Moderator Pressure Coefficient (psi^{-1})	$+.3\times10^{-6}$ to 4.0×10^{-6}

Table E.1

(Continued)

43.	Moderator Density Coefficient, $\frac{\Delta k}{k}$/cm/cm^3	-1.0×10^{-5} to $+ .3 \times 10^{-5}$
44.	Doppler Coefficient ($°F^{-1}$)	$- 1.7 \times 10^{-5}$
45.	Delayed Neutron Fraction, %	.70 to .51
46.	Prompt Neutron Lifetime, sec	1.4×10^{-5} to 2.0×10^{-5}

Table E.2

Zion-I Reactor Thermal and Hydraulic Design Parameters

Total Heat Output, MWt	3250
Total Heat Output, Btu/hr	$11{,}090 \times 10^6$
Heat Generated in Fuel, %	97.4
Maximum Thermal Overpower Rating, %	112
Nominal System Pressure, psia	2250
Hot Channel Factors	
Heat Flux	
Nuclear, F_q^N	2.71
Engineering, F_q^E	1.03
Total	2.79
Enthalpy Rise	
Nuclear, $F_{\Delta H}^N$	1.58
Coolant Flow	
Total Flow Rate, lbs/hr	135.0×10^6
Average Velocity Along Fuel Rods, ft/sec	15.3
Average Mass Velocity, lb/hr-ft^2	2.52×10^6
Coolant Temperature, °F	
Design Nominal Inlet	530.2*
Average Rise in Vessel	64.1
Average Rise in Core	66.8
Average in Core	564.8
Average in Vessel	563.2
Nominal Outlet of Hot Channel	631.0
Heat Transfer	
Active Heat Transfer Surface Area, ft^2	52,200
Average Heat Flux, Btu/hr-ft^2	207,900
Maximum Heat Flux, Btu/hr-ft^2	579,600
Maximum Thermal Output, kw/ft	18.8
Maximum Clad Surface Temperature BOL at Nominal Pressure, °F	657
Maximum Average Clad Temperature BOL at Rated Power, °F	720
Fuel Central Temperatures (Region 3-BOL) for nominal fuel rod dimensions, °F	
Maximum at 100% Power	4250
Maximum at 112% Power	4500

*Best estimate Nominal Inlet Temperature is 524.9°F.

Table E.2

(Continued)

DNB Ratio	
Minimum DNB Ratio at nominal operating conditions	2.02
Pressure Drop, psi	
Across Core	31
Across Vessel, including nozzles	50

Table E.3

Zion-I Reactor Core Mechanical Design Parameters

Active Portion of the Core	
Equivalent Diameter, in.	132.7
Active Fuel Height, in.	144
Length-to-Daimeter Ratio	1.09
Total Cross Section Area, ft^2	96.06
Fuel Assemblies	
Number	193
Rod Array	15 x 15
Rods per Assembly	204(2)
Rod Pitch, in.	0.563
Overall Dimensions	8.426 x 8.426
Fuel Weight, (as UO_2), pounds	216,600
Total Weight, pounds	276,000
Number of Grids per Assembly	7
Number of Guide Thimbles	20
Diameter of Guide Thimbles (upper part), in.	0.545 O.D. x 0.515 I.D.
Diameter of Guide Thimbles (lower part), in.	0.484 O.D. x 0.454 I.D.
Fuel Rods	
Number	39,372
Outside Gap, in.	0.422
Diametral Gap, in.	
Regions 1 and 2	0.0075
Region 3	0.0085
Clad Thickness, in.	0.0243
Clad Material	Zircaloy
Overall Length	149.7
Length of End Cap, overall, in.	0.688
Length of End Cap, inserted in rod, in.	0.250

Table E.3

(Continued)

Fuel Pellets		
Material		UO_2 sintered
Density*(% of Theoretical)		
Region 1		94 (10.3g/cc)
Region 2		93 (10.19g/cc)
Region 3		92 (10.08g/cc)
Feed Enrichments w/o		
Region 1		2.25
Region 2		2.80
Region 3		3.30
Diameter, in.		
Regions 1 and 2		0.3659
Region 3		0.3649
Length, in.		0.600
Rod Cluster Control Assemblies		
Neutron Absorber		5% Cd, 15% In, 80% Ag
Cladding Material		Type 304 SS - Cold Worked
Clad Thickness, in.		0.019
Number of Clusters		
Full Length		53
Part Length		8
Number of Control Rods per Cluster		20
Length of Rod Control, in.		156.436 (overall) 149.136 (insertion length)
Length of Absorber Section, in.		142.00 (full length) 36.00 (part length)
Core Structure		
Core Barrel, in.	I.D.	148.0
	O.D.	152.5
Thermal Shield, in.	I.D.	158.5
	O.D.	164.0

*These densities are zion first core densities. All of the calculations performed for this study used the zion reactor at mid-life with a fuel density of 10.63 g/cc and a total uranium mass of 90,066 kg.

Table E.3

(Continued)

Burnable Poison Rods

Number	1436
Material	Borosilicate Glass
Outside Diameter, in.	0.4395
Inner Tube, O.D. in.	0.2365
Clad Material	S.S.
Inner Tube Material	S.S.
Boron Loading (natural) gm/cm of glass rod	.0603

(1) All dimensions are for cold conditions.

(2) Twenty-one rods are omitted: Twenty provide passage for control rods and one to contain in-core instrumentation.

APPENDIX F: INPUT TO THE CELL AND CORCOST CODES FOR ZION-I REACTOR

F.1 CELL Input for Zion-I Fuel of 1.9923 w/o Enrichment

The following is a list of the input parameters to the CELL Code for the Zion-I reactor with an enrichment of 1.9923 w/o.

Parameter	Value
ANIN(5)	4.5349E-04
ANIN(6)	0.0
ANIN(7)	0.0
ANIN(8)	2.2027E-02
ANIN(9)	0.0
ANIN(10)	0.0
ANIN(11)	0.0
ANIN(12)	0.0
ANIN(13)	0.0
ACLD	4.3116E-02
ACOL	2500E-02
RAD	4.7422E-01
R1	8.0680E-01
R2	5.3594E-01
TC	6.1722E-02

Parameter	Value
ZLAT	0.0
VFF	3.1168E-01
VFCOL	0.0
VFVD	8.6412E-02
VFCLD	5.0408E-01
VFEX	9.7825E-02
VEM(1)	2.9710E-02
VEM(2)	7.6705E-02
VEM(3)	8.4971E-01
VEM(4)	4.3868E-02
VEM(5)	0.0
ANN(1)	0.0
ANN(2)	8.4450E-02
ANN(3)	2.5000E-02
ANN(4)	8.5492E-02
ANN(5)	0.0
DIFAC(1)	1.0000E+00
DIFAC(2)	1.0300E+00
DIFAC(3)	1.0300E+00
DIFAC(4)	1.0000E+00
DIFAC(5)	1.0000E+00

Parameter	Value
SAO(1)	0.0
SAO(2)	1.8200E-01
SAO(3)	6.6800E-01
SAO(4)	0.0
SAO(5)	3.7490E+00
SAO(6)	6.6800E-01
SAO(7)	3.7490E+00
SAO(8)	0.0
STR(1)	1.7950E+01
STR(2)	8.0000E+00
STR(3)	4.4450E+01
STR(4)	0.0
STR(5)	1.1830E+01
STR(6)	4.4450E+01
STR(7)	1.1830E+01
STR(8)	0.0
SCOFA	7.6000E+00
SSRCL	8.0000E+00
SSRCO	4.4800E+01
ESSR(1)	9.7000E-01
ESSR(2)	1.3280E-01
ESSR(3)	4.1440E+01
ESSR(4)	0.0
ESSR(5)	4.1770E-01

Parameter	Value
ESSR(6)	4.1440E+01
ESSR(7)	4.1770E-01
ESSR(8)	0.0
RINT(1)	0.0
RINT(2)	3.0100E+00
RINT(3)	2.6760E-01
RINT(4)	2.0000E+00
RINT(5)	2.4450E+00
RINT(6)	2.6780E-01
RINT(7)	2.4450E+00
RINT(8)	0.0
RIUFP	1.8100E+02
RIPFP	2.6400E+02
TMOD	2.9600E+02
TEFF	1.3161E+03
TAU	5.4800E+01
PlIN	9.8500E-01
POWERD	9.8800E+00
PDNLIM	2.7400E+02
ENNFIS(1)	2.0290E+02
ENNFIS(2)	2.0160E+02
ENNFIS(3)	2.0650E+02
ENNFIS(4)	2.0720E+02
SFAC(1)	7.9808E-1
SFAC(2)	7.6846E-1

Parameter	Value
XEADJ	1.0000E+00
SMADJ	1.0000E+00
FDFCTR	1.0000E+00
ZETA	2.0000E-04
EVCUT	6.2500E-01
B22	2.7742E-04
EPSI	1.0476E+00
R18CHK	0.0
IL	63
NRES	68
NUMPOZ	30
NUMSPA	2
NWILK	1
NPOICK	0
NPT	7
NWT	0
ISKIP	0
INPUT	1
IPRNT	1
IPRT1	0
IPRT2	0
IPRWLK	0

F.2 CORCOST Input for the Zion-I Reactor

The following are the input parameters to the CORCOST code for the Zion-I Reactor for the first cycle of the Sample Problem as stated in Section 5.1.

Parameter	Value
H	3.6576E+02
DELR	5.6000E+00
DELH	5.6000E+00
ZSYM	0.0
DBSQU	7.7500E-05
PFAST	9.8500E-01
PDENAV	9.8800E+01
ERROR	0.0000E-03
DELCRT	5.0000E-05
CRIT	1.0000E+00
ZETZ	2.0000E-04
F	1.5500E+00
TIGG	7.5000E+01
SSCVG	2.5000E-04
EIGMWNI	1.0000E-03
FDAMP	9.6000E-01
DKNU	1.0000E-04
NLOAD	2
NSRB	10
IRL	15

Parameter	Value
JZL	5
NCYCM	1
NTHETP	0
NCP	1
IPHBAT	0
IPOIS	1
NPOISR	0
NPOISZ	0
ITRATE	10
IPRT1	0
IPRT2	0
IPRT3	1
IPSPPR	0
IPSGMW	0
INORMP	0
IABSD	0
ITHET	1
NEWTHP	1
NOZONE	3
IFUELS	1
IVARFA	1
NSRB1	9
IPRT4	1

Parameter	Value
IPPROD	2
IPROP(1)	2
IPROP(2)	2
IENRIC(1)	1
R(1)	8.430
R(2)	20.290
R 3)	42.100
R 4)	59.010
R(5)	75.870
R(6)	116.300
R(7)	124.600
R(8)	129.080
R(9)	133.410
R(10)	137.600
R(11)	141.670
R(12)	145.620
R(13)	149.470
R(14)	157.000
R(15)	168.530
IBOC	2
VOLFRC(1)	0.5
VOLFRC(2)	0.5
TSCED(1,1)	0.0

Parameter	Value
TSCED(2,1)	1.0588
TSCED(3,1)	2.5171
TSCED(4,1)	3.5587
TSCED(5,1)	4.4337
TSCED(6,1)	5.4555
TSCED(7,1)	6.4305
TSCED(8,1)	7.4523
TSCED(9,1)	8.4740
TSCED(1,2)	0.9338
TSCED(2,2)	2.3921
TSCED(3,2)	3.4337
TSCED(4,2)	4.3082
TSCED(5,2)	5.2837
TSCED(6,2)	6.3055
TSCED(7,2)	7.3272
TSCED(8,2)	8.3441
TSCED(9,2)	9.3708
TEVEC(1,1)	-1.5000
TEVEC(2,1)	-2.5000
TEVEC(3,1)	-3.5000
TEVEC(1,2)	4.0440
TEVEC(2,2)	3.0021
TEVEC(3,2)	1.5440

Parameter	Value
TEVEC(1,3)	0.0320
TEVEC(2,3)	0.0320
TEVEC(3,3)	0.0320
TEVEC(1,4)	31606.6
TEVEC(2,4)	31606.6
TEVEC(3,4)	31606.6
NEWR(1)	10
E	14,066.

F.3 Sample Output From CORCOST

The output from CORCOST is exactly similar to that from CORE with the exception of the nuclear fuel revenue requirement information. The variable outputs from the CORE code have all previously been defined (21, 25). The additional outputs from CORCOST are:

1. The TSCED and TEVEC input arrays as they were read into the code.
2. The beginning of cycle, BOC, uranium and plutonium value of the fuel and the BOC fabrication and reprocessing value of the fuel.
3. The end of cycle, EOC, uranium and plutonium fuel value and the EOC, fabrication and reprocessing value of the fuel,

4. The following discounted (to t=0), revenue requirements for each cycle:
   a. Total burnup of uranium and plutonium revenue requirement,
   b. The "Burnup" of uranium requirements
   c. The Plutonium Credits
   d. Total fabrication and reprocessing requirements,
   e. Fabrication requirements,
   f. Reprocessing requirements,
   g. Total Cycle, requirements, C_i, Equation (3.8).
5. The average cost of energy during each cycle, C_i, in mills/kwhre,
6. The sum of the discounted cycle revenue requirements, that have been calculated in this case, i.e. $\sum_{j=1}^{i} C_j$,
7. The average cost of energy from all the cycles calculated in this case in mills/kwhre,
8. The estimated information on energy production for the cycle following the last cycle of this case, including E_i, ε_i, BU$, FAR$, and MC_i as defined in Section (4.3.2.1) as well as the

total anticipated revenue requirements,

$$TOT\$ = BU\$ + FAR\$ \qquad (F.1)$$

and the required input parameters ANIN(5) and ANIN(8) for enrichment ε_i.

A sample output is available throughProf. E. A. Mason of the Nuclear Engineeering Department or through the Nuclear Engineering Department's Library.

APPENDIX G: MESH POINT SENSITIVITY OF THE CORE CODE

The following sensitivity analysis of the CORE code to the number of mesh points used to describe a reactor is excerpted from Progress Report No. 2., MITNE-140 (24) p. 32.

A mesh point sensitivity analysis was carried out using the CORE code (21) and the San Onofre reactor as a model. Table G.1 presents the results of this study. Assuming that the discharge burnup of 33,450 MWD/T given by Combustion Engineering (29) for the San Onofre reactor utilized a more accurate calculational technique than we have available to us, this value was used as a basis for comparison as the number of mesh points was varied. Note that there is no significant loss of accuracy as the number of mesh points decrease, but there is a large savings in computer time. This demonstrates that the CORCOST code satisfies the first two characteristics mentioned above, speed and sufficient accuracy. Therefore, the CORCOST code with a 15 x 5 mesh point arrangement will be used as the in-core simulator.

Table G.1

Sensitivity of CORE to Number of Mesh Points*

Steady State Cycle *(ε = 3.3 w/o)

($\bar{E}$ = 33,450)

Mesh Points	E [MWD/T]	$\bar{e}$† [mils/kwhr]	computing time [min/cycle]	Deviation in $\bar{E}$ [%]
270 [18x15]	33964	1.8531	1.20	1.56
144 [18x8]	34236	1.8432	0.83	2.28
100 [10x10]	33955	1.8492	0.55	1.51
80 [10x8]	34085	1.8446	0.44	1.90

*For the San Onofre Reactors 2 and 3 (32)

†$\bar{e}$ is the nuclear fuel cycle cost

Appendix H SUMMARY LISTING OF REACTOR CYCLE ENERGY AND COST CALCULATIONS

H.1 Calculations Performed to Develop the Predictive Correlations in the End-of-Cycle Evaluator f = 0.37

εII w/o	ε_1 w/o	BII MWD/T	E_1 MWD/T	BU\$ 10^6\$	FAR\$ 10^6\$
2.77024	3.5449	15.1253	15405	10.7656	4.5892
2.3284	3.5449	16.9834	11584	8.5074	4.4953
2.2620	3.5449	14.0156	11813	8.4971	4.0866
2.6788	3.5449	15.6049	14525	10.2792	4.3765
2.5123	3.2929	16.0781	12428	8.7829	4.9886
2.6777	3.2929	14.7374	14111	9.7756	4.9892
2.2230	3.2929	14.8779	10569	7.6535	3.8036
2.5320	3.2929	17.5572	12276	8.8322	4.2746
2.5673	3.0540	14.4103	12625	8.6662	4.3252
2.5564	3.0540	14.8500	12428	8.5721	4.1886
2.3730	3.0540	16.3365	10679	7.6189	4.3509
2.5168	3.0540	17.1802	11383	8.0872	3.5683
2.3346	2.8649	14.2095	10199	7.1356	3.8076
2.3122	2.8649	15.2063	9913	6.9963	4.4868
2.3632	2.8649	14.4542	10501	7.3340	4.6782
2.4950	2.8649	17.1802	10814	7.6417	3.4199

f = 0.29

ε_{II} w/o	ε_i w/o	BII MWD/T	E_i MWD/T	BU$ $10^6$$	FAR$ $10^6$$
2.3034	3.5449	17781	9266	7.0699	2.8847
2.2708	3.5449	15176	9279	7.0526	3.1615
2.4281	3.5449	17337	10363	7.7171	3.4160
2.2707	3.5449	16210	9455	7.0875	3.0962
2.6668	3.2929	15189	12684	8.8684	3.9201
2.6077	3.2929	16451	11808	8.4147	3.4561
2.5491	3.2929	17685	10944	7.9709	2.9590
2.4076	3.2929	19183	9208	7.0824	2.3435
2.1951	3.0540	15739	7916	5.9562	2.7995
2.2872	3.0540	15734	8696	6.4068	2.9266
2.5267	3.0540	15519	10871	7.6374	3.6146
2.5075	3.0540	16386	10457	7.4446	3.3106
2.2956	3.7734	15638	10239	7.6868	3.3530
2.2511	3.7734	14686	10096	7.5582	3.4245
2.5266	3.7734	15520	12316	8.8621	3.8932
2.4804	3.7734	18180	11055	8.3249	3.3426

f = 0.33

ε_{II} w/o	ε_i w/o	BII MWD/T	E_i MWD/T	BU\$ 10^6\$	FAR\$ 10^6\$
2.7067	3.5449	15.6969	14024	9.9163	4.2030
2.7515	3.5449	15.4782	14474	10.1663	4.3058
2.3377	3.5449	14.7172	11322	8.2076	3.7595
2.6209	3.5449	16.1483	13164	9.3253	4.0898
2.3260	3.2929	14.9682	10544	7.6121	3.5207
2.6404	3.2929	15.6395	12965	9.0480	3.8780
2.5774	3.2929	16.9768	12093	8.6492	3.4106
2.4657	3.2929	18.4198	10747	7.9603	2.8478
2.5502	3.054	14.7661	11874	8.2074	3.9791
2.2305	3.054	15.3778	9240	6.6862	3.2347
2.3780	3.054	14.9270	9990	7.1503	3.3507
2.4436	3.054	18.5047	9984	7.3314	2.9025
2.4493	2.8649	16.8960	9974	7.1009	3.2073
2.5654	2.8649	18.7626	10356	7.4422	2.9369
2.2851	2.8649	13.8140	9456	6.6904	3.3514
2.5502	2.8649	14.7661	11395	7.8271	3.8475

f = 0.25

ε_{II} w/o	ε_1 w/o	BII MWD/T	E_1 MWD/T	BU$ $10^6$$	FAR$ $10^6$$
2.2225	3.5449	17919	7568	6.0449	2.4206
2.3731	3.5449	16520	9167	6.9844	3.0171
2.4148	3.5449	19483	8830	6.8718	2.6327
2.1832	3.5449	16112	7720	6.0374	2.7417
2.2788	3.2929	16016	8220	6.2383	2.7082
2.3771	3.2929	18484	8342	6.4156	2.6460
2.5785	3.2929	17162	10662	7.7280	3.5436
2.1773	3.2929	16262	7207	5.6812	2.4529
2.2444	3.0540	17522	7124	5.5686	2.3553
2.3077	3.0540	18775	7372	5.7626	2.2076
2.1888	3.0540	15704	7123	5.4957	2.4305
2.5171	3.0540	20412	8633	6.6325	2.4065
2.2686	3.7734	16235	8786	6.7921	2.8764
2.2208	4.5714	15469	9683	7.6899	3.2099
2.5058	3.7734	16197	11029	8.0544	3.5895
2.4447	4.5714	18853	10689	8.4745	3.1786

H.2 Case I Calculations

Cy No.	Path	Ei MWD/T	fi	Ci 10^6\$	Vi 10^6\$
1	A	11122	.37	12.41032	12.4919
1	B	11115	.33	13.0164	12.8767
1	C	11109	.29	12.4204	13.8489
1	D	11022	.25	12.8644	15.4857
2	C-A	13896	.37	14.4466	11.2109
2	D-A	14224	.37	14.4468	11.71089
2	D-B	14056	.33	14.5546	12.0688
2	D-C	13973	.29	14.8106	12.6733
2	A-A	13991	.37	15.4537	12.2454
2	A-B	13896	.33	15.3503	11.9402
2	D-D	14084	.25	15.0417	12.9494
2	A-C	13744	.29	15.5218	12.9082
2	B-A	13917	.37	14.9806	12.8570
2	B-B	13959	.33	15.3236	12.3411
3	C-A-C	10425	.29	9.4041	11.1633
3	D-A-C	10244	.29	9.1881	11.7203
3	A-A-C	10136	.29	9.8251	10.3221
3	C-A-D	10187	.25	9.4721	12.1169
3	D-B-D	10410	.25	9.5179	12.4872
3	B-A-C	10207	.29	9.4298	10.3934
3	A-B-A	10465	.37	9.4327	10.5082
3	A-B-B	10291	.33	9.2715	10.7518
3	D-D-B	10544	.33	8.9672	11.6953
3	A-B-D	10238	.25	9.2540	11.8889

Cy No.	Path	Ei	fi	Ci	Vi
		MWD/T		10^6\$	10^6\$
4	C-A-C-D	8871	.25	7.4320	10.4922
4	C-A-D-D	9109	.25	7.4289	10.118908
4	C-A-D-B	8977	.33	7.1844	8.8084
4	D-B-C-C	9125	.29	7.6508	10.2029
4	D-B-A-C	8951	.29	7.9696	9.9909
4	A-B-D-C	8806	.29	7.0404	10.5959
4	A-B-D-D	8933	.25	7.1609	11.4010
4	A-B-D-B	9074	.25	7.2681	10.2023
4	A-B-B-C	8948	.29	7.6021	10.5661
4	A-B-D-B	9074	.33	7.2681	10.2023
5	C-A-C-D-A	9426	.37	7.4475	8.6383
5	C-A-C-D-C	9500	.29	7.6810	9.2465
5	D-B-A-C-C	9572	.29	7.9912	9.3090
5	C-A-D-D-C	9733	.29	7.5377	9.8451
5	C-A-D-B-B	9757	.33	7.6535	9.8268
5	A-B-D-D-A	9652	.37	7.7369	9.0223
5	A-B-D-D-C	9570	.29	7.5913	9.9359
5	A-B-D-D-D	9536	.25	7.5885	10.6875
5	A-B-D-C-B	9480	.33	7.8124	9.4270
5	A-B-D-C-A	9593	.37	7.9453	8.9396

H.3 Case II Calculations

Cy No.	Path	Ei	fi	Ci	Vi
		MWD/T		10^6\$	10^6\$
1	A	11022	.37	11.6550	12.3257
1	B	11026	.33	11.7650	12.6981
1	C	11108	.29	12.0327	13.3414
1	D	11254	.25	12.4880	14.5357
2	C-A	14097	.37	14.9930	12.5667
2	C-B	14134	.33	15.0988	13.4953
2	D-A	14048	.37	14.6335	12.4683
2	D-B	14206	.33	14.7879	13.2433
2	D-C	13941	.29	14.6510	14.1453
3	D-C-C	10426	.29	9.1593	11.6131
3	D-C-B	10447	.33	9.2193	11.1424
3	C-B-D	10202	.25	9.2532	12.1234
3	C-B-C	10306	.29	9.3095	11.3013
3	C-A-C	10244	.29	9.4528	11.3740
4	C-B-D-C	8796	.29	7.1408	10.3873
4	C-B-D-D	9000	.25	7.3018	11.1798
4	C-B-D-B	9060	.33	7.3807	10.0238
4	D-C-C-C	8907	.29	7.5494	10.5209
4	D-C-B-B	8870	.33	7.7327	9.8830
5	C-B-D-D-C	9561	.29	7.5460	9.9542
5	C-B-D-D-D	9651	.25	7.6558	10.8233
5	C-B-D-C-B	9576	.33	7.8280	9.4627
5	C-B-D-D-A	9614	.37	7.6555	9.0238
5	C-B-D-C-A	9550	.37	7.8624	8.8738

Appendix I. CELL Code Fortran Listing

A complete fortran listing of all computer codes used in this study resides with Professor E.A. Mason of the Nuclear Engineering Department and in the Nuclear Engineering Department Library.

Appendix J. CORCOST Code Fortran Listing

A complete fortran listing of all computer codes used in this study resides with Professor E.A. Mason of the Nuclear Engineering Department and in the Nuclear Engineering Department Library.

Appendix K

NOMENCLATURE*

B	Nuclear fuel burnup in MWD per metric tonne of U.
BII	The average burnup of the fuel in the inner, (1-f), portion of the reactor at the beginning of a cycle.
B.O.C.	Used to describe variables measured at the beginning of a cycle.
BU$	The total revenue requirements incurred by the burnup of nuclear fuel (U depletion less Pu production) during one cycle, discounted to B.O.C.
C	Total revenue required to produce energy during a cycle, discounted to t = 0.
c',c",c"'	Unit costs, $/kgU, for fabrication, reprocessing and conversion respectively.
c_P	Unit salvage value of Plutonium, $/kg.
c_U	Unit cost of uranium, $/kg.
CE	Estimate of the revenue required to produce energy during a cycle given the state of the reactor, discounted to B.O.C.

---

* For all the variables used in the CELL and CORCOST Codes, see Appendices A.3 and B.

E	The energy produced in one cycle by a reactor, in GWD or average core burnup MWD/T.
ε	Nuclear fuel reload enrichment, w/o.
εII	Average fissile, U-235 + Pu-239 + Pu-241, enrichment in the inner, (1-f), portion of the reactor core at B.O.C.
E.O.C.	Used to describe variables measured at the end of a cycle.
f	Nuclear fuel reload batch fraction.
F',F",F"'	The fractional yields of uranium and plutonium in fuel fabrication, reprocessing and conversion respectively.
FAR$	The revenue required during one cycle to pay the depreciation of all fuel service charges of fabrication, reprocessing, shipping and conversion, discounted to B.O.C.
g_i	The radial spacing in the CORCOST model of the reactor between mesh point i and i-1, in cm.
H	Active reactor core height, in cm.
i	Used as a subscript denoting a cycle.
IRL	Total number of radial mesh points used in the CORCOST model of the reactor.
JZL	Total number of axial mesh points used in the CORCOST model of the reactor.
k	Used as a subscript denoting a batch of nuclear fuel.
K	The <u>total</u> number of fuel batches in the reactor at any given time.

k_{eff} The ratio of the number of neutrons produced by a reactor in one generation to the number produced in the immediately preceding generation.

M(X) The mass of isotope X in a particular compound, kg.

MAXF The maximum number of batch fractions to be surveyed by the D.P. optimization.

MC The incremental cost, $\frac{\partial C}{\partial E}$, of producing one more unit of electricity during one cycle.

MINF The number of the radial mesh point, in the CORCOST model of the reactor, associated with the smallest feasible reload batch fraction.

N_ϵ The number of different enrichments for which CELL data must be available to the D.P. algorithm.

NF The factor normalizing the CORCOST calculation of power peaks to a more accurate calculation (in this study a CITATION calculation was used as a basis).

N(θ,k) Nuclide concentrations, cm^{-3}, calculated by CELL for use by CORCOST.

NOZONE Total number of batches and sub-batches in the reactor at one time.

NSRB The outermost radial mesh point of the inner, (1-f), scatter fuel region of the core.

NZ Total number of batches and sub-batches in the inner, (1-f), portion of the reactor.

Φ	Neutron flux in n/cm^2-sec.
ρ_ε	The sensitivity of cycle energy production to reload enrichment, w/o/MWD/T.
P	Nuclear refueling path notation, e.g., P(A-B-C) implies that the reactor was reloaded with batch fractions of 0.37 in the first cycle of the planning horizon, 0.33 in the second cycle and 0.29 in the third.
P(t)	The mass of the plutonium in a batch of fuel at time t.
P_{th}	Thermal power produced by the reactor, kW.
PDMXTA	The reactor core maximum to average power density ratio.
PV	Present value factor.
PVAUP	The present value factor which discounts a purchase of uranium to B.O.C. and a sale of uranium or plutonium to E.O.C.
PVE	The present value factor which discounts the revenues received for energy produced in cycle i to B.O.C.
PVEOC	The present value factor which discounts the value of fuel from the end of the cycle to the beginning of the cycle.
PVFAB	The present value factor which discounts payments for fabrication to the beginning or end of the cycle.

PVREP — The present value factor which discounts reprocessing, shipping and conversion payments to the beginning or end of the cycle.

PVTOT — The present value factor which discounts revenue requirements from the beginning of a cycle to the beginning of the planning horizon.

q"' — Reactor core power density, kw/l.

R — Radial mesh spacing location in CORCOST reactor model.

R_C — The ranking order of a path for its TCE_P at the beginning of a cycle.

R_{MAX} — Outer radius of the reactor core, cm.

R_S — The combined ranking ($W_C R_C + W_V R_V$) for a path at the beginning of a cycle.

R_V — The ranking order of a path for its TVE_P at the beginning of a cycle.

t_1 and t_2 — The time from the beginning of the planning horizon to beginning of a cycle, t_1, and the end of a cycle, t_2.

t_k^x — The time from the beginning of the planning horizon to when charges were paid for fuel, x, in batch k. If these charges occurred prior to the cycle y = 0 and if after, y = e.

$T_{1,i}$ and $T_{2,i}$ — The time at the beginning, $T_{1,i}$, and at the end, $T_{2,i}$, of a cycle i.

TAPRE — The time before insertion of fuel in a reactor when payment is made for the uranium in the

fuel batch, for the fabrication and for the enrichment of the uranium.

TC — The total revenue requirements for nuclear fuel over the planning period discounted to t = 0. TC_i are the total revenue requirements through cycle i discounted to t = 0.

$TCE_{P,i}$ — The sum of all revenue requirements for path P through cycle i plus the estimated revenue requirements CE_{i+1} for the (i+1) cycle.

TPOST — The time after the discharge of fuel from a reactor when reprocessing, conversion and shipping charges are paid and fuel credits are received.

TVE_P — The net cost of producing energy by path P as defined by Equation (4.20).

U(t) — The mass of uranium in a fuel batch at time t, in kg.

V_i — The book value of nuclear fuel at the end of cycle i.

Vol(k) — The volume of fuel batch k, cm^3.

W_C and W_V — The weighting functions for the ranking factors R_C and R_V respectively used in calculating the combined order of paths at the end of each cycle

x — The state of the reactor at the beginning of a cycle, defined as the spatial distribution of the uranium and plutonium nuclides and of the fission product poisons.

Z(k,t) — The value of the fuel in batch k at time t.

Appendix L. REFERENCES

1. Baleriaux H., Jamoulle, E. and Linaid de Guertechin, Simulation de l'Exploitation d'un Parc de Machines Themiques de Production d'Electriate Couple a des Stations de Pompage, Revue E (edition S.R.B.E.), Vol. V, No. 7, pp 3-24, 1967.

2. Baltimore Gas and Electric Co., "Calvert Cliffs Nuclear Power Plant, Units 1 and 2", Final Safety Analysis Report.

3. Belman, R.L. and Dreyfus, S., Applied Dynamic Programming, Princeton University Press, Princeton, New Jersey, 1962.

4. Bevington, Phillip R., Data Reduction and Error Analysis for the Physical Sciences, McGraw-Hill Book Company, New York, 1969.

5. Booth, R.R., "The ABC's of Probabalistic Simulation - A Simple Explanation of Principal Features and Uses, Production Co-ordination Dept., State Electricity Commission of Victoria, Australia, Feb. 1971.

6. Booth, R.R., A Power System Simulation Model Based on Probability Analysis.

7. Bukovsky, J., Martel, E., REFUEL - Nuclear Refueling Schedule Generator, Commonwealth Edison Co., unpublished internal report (1971).

8. Chayson, L., Yankee Core Evaluation, Quarterly Progress Report, WCAP-6060, Period ending Sept. 30, 1967.

9. Commonwealth Edison Co., Zion Station - Final Safety Analysis Report, Chicago, Illinois.

10. Conklin, James, Fuel Depletion and Cost During the Transient Period of a Large Pressurized Water Reactor, Chapter V, MITCOST, S.M. Thesis, Massachusetts Institute of Technology, Cambridge, Massachusetts (1971).

11. Deaton, Paul F., Utility System Integration and Optimization Models for Nuclear Power Management, Ph.D. Thesis, Massachusetts Institute of Technology, Cambridge, Massachusetts (1973).

12. Deaton, P.F. and E.A. Mason, A System Integration and Optimization Model for Nuclear Power Management Planning, Trans. Am. Nucl. Soc., 15, 373 (1972).

13. Dietrich, J.R. and J.M. West, Looking Ahead at the PWR, presentation at the American Nuclear Society, Power Division Meeting, August 1972.

14. El-Wakil, M.M., Nuclear Heat Transfer, International Text Book Co., Scranton, Pa., 1971.

15. Fagan, J.R. and Sesonske, A., Optimal Fuel Replacement in Reactivity Limited Systems, Journal of Nuclear Energy, 23, 1969.

16. Fowler, Vondy and Cunningham, Nuclear Reactor Core Analysis Code: CITATION, ORNL-TM-2496, Rev. 2, July 1971.

17. Goellner and Beaudreau, Summary Description of the Full Depletion Code, CELL, Department of Nuclear Engineering, Massachusetts Institute of Technology, Cambridge, Massachusetts, June 1968 (MITNE-89).

18. Hadley, G., Linear Programming, Addison Wesley Publishing Co., Inc., Reading, Massachusetts, 1962.

19. Henderson, R.R., A Reactor Performance and Fuel Management Simulator for Power Systems Planning Activities, Ph.D. thesis, Ohio State University (1971).

20. Hoskins, R.E., Kincel, E.F. and Strauch, S., Planning Through Simulation of Operating With Nuclear and Fossil Plants, American Power Conference, 1972.

21. Kearney, J.P., Ed., Summary Description of the Fuel Depletion Code CELL-MOVE, Unpublished Report, Department of Nuclear Engineering, Massachusetts Institute of Technology, Cambridge, Massachusetts, August 1971.

22. Martin, Richard J., (Commonwealth Edison Co.), Nuclear Fuel Purchasing and Contracts, lecture presented at MIT's Summer Course on Nuclear Fuel and Power Management, Cambridge, Massachusetts August 1971.

✓ 23. Mason, E.A., Deaton, P.F., Kearney, J.P., Development of Utility Simulation Model Progress Report No. 1, Department of Nuclear Engineering, Massachusetts Institute of Technology, Cambridge, Massachusetts, January 1971 (MITNE-124).

✓ 24. Mason, E.A., Deaton, P.F., Kearney, J.P., Rieck, F.A., Development of Utility Simulation Model Progress Report No. 2, Department of Nuclear Engineering, Massachusetts Institute of Technology, Cambridge Massachusetts, July 1971. (MITNE-140)

25. McLeod et al., The Effect of Fuel and Poison Management on Nuclear Power Systems, Department of Nuclear Engineering, Massachusetts Institute of Technology, Cambridge, Massachusetts, September 1961 (MINNE-10, NYO-9715).

26. Nuclear Industry Vol. 19, No. 8, August 1972, p. 19.

27. Rieck, Terrence, The Engineering Feasibility and Fuel Cost Analysis of Varying Nuclear Fuel Intervals Ph.D. Thesis, Massachusetts Institute of Technology, Cambridge, Massachusetts (in progress).

28. Rees, F.J. Maints - Optimal Maintenance Refueling Schedule Generator, unpublished internal report, Systems Control Inc., Palo Alto, California 1972.

29. Tees, F.J. and J.M. Goodrich, "Power Systems Approach to Optimal Nuclear Fuel Management," Prepared for Power Supply Planning Branch, Tennessee Valley Authority, Chattanooga, Tennessee SCI Project T279 June 1970.

30. Rothrack, R.B., unpublished work in progress, University of Washington.

31. Salmon, Royes, Two Computer Codes (REFCO and POW76) for Calculating the Fuel Cycle Costs of a Nuclear Power Reactor, ORNL-4695, Oak Ridge National Laboratory, May 1971, p. 9.

32. Southern California Edison Co. and San Diego Gas and Electric Co., San Onofre Nuclear Generating Station Units 2 & 3, Preliminary Safety Analysis Report.

33. Springsteen, D.F. (Chase Manhattan Bank), lecture to MIT's Summer Course on Nuclear Fuel and Power Management, Massachusetts Institute of Technology, Cambridge, Massachusetts, August 1971.

34. Specker, S.R. and Forkner, S.L., SCOPING - A Simulator with Cycling Optimization for Planning and Integrating Nuclear Generation into a Power System, Tennessee Valley Authority, unpublished internal report, FES-041 (1972).

35. Staver, R.L. and Sesonske, A., Optimization of BWR Fuel Management Using an Accelerated Exhaustive Search Algorithm, Journal of Nuclear Energy, 23, p. 673, 1969.

36. Wagner, Harvey M., Principles of Operations Research, Prentice Hall, Inc., New Jersey, 1969.

37. Watt, Hing Yan, Incremental Cost and Nuclear In-Core Optimization, Ph.D. thesis, Massachusetts Institute of Technology, Cambridge, Massachusetts (1973).

38. Westinghouse Atomic Power Department, High Burnup UO_2 Studies, Westinghouse Contribution Proceedings, 19th High Temperature Fuels Committee Meeting, 1964.

39. Benedict, Manson, "Economics of Nuclear Power", Class Notes, M.I.T., Nuclear Engineering Department, Cambridge, Mass., 1972.